ECOLE
POLYTECHNIQUE
DE BRUXELLES

ULB

UNIVERSITÉ LIBRE DE BRUXELLES

Multi-photon quantum interferences in multimode optics circuits

Mémoire présenté en vue de l'obtention du diplôme
d'Ingénieur Civil Physicien à finalité Photonique et Applications Quantiques

Philippe Neuville

Directeur
Professeur Nicolas J. Cerf

Superviseur
Zacharie Van Herstraeten

Service
Service QuIC

Année académique
2018 - 2019

Abstract

Multi-photon multimode quantum interferences have recently attracted an increasing attention because they lie at the heart of future quantum technologies with photonic integrated devices. The celebrated Hong-Ou-Mandel effect is the paradigm of such a quantum interferometric effect for two photons propagating in two modes, which originates from the indistinguishability of photons (being bosons, the trajectory where they are both reflected at a balanced beam splitter interferes destructively with the trajectory where they are both transmitted, which gives rise to the so-called bunching effect). In this Ms thesis, we explore the extension of quantum interferences to more than two photons in more than two modes. We focus on a Fourier interferometer, which is defined as the N-mode generalization of a balanced beam splitter (it is also sometimes called a N-splitter). We probe the probability of coincident detections of N photons impinging on this interferometer and connect it to the permanent of the matrix underlying the discrete Fourier transform. Although computing permanents is notoriously a very hard problem in comparison with determinants, we can infer a few implications of the indistinguishability of photons when compared to distinguishable classical particles. In particular, we exhibit the existence of a constructive interference effect for some odd values of N in a Fourier interferometer (while the interference is provably fully destructive for any even N). For example, the smallest nontrivial case (N=3) gives a coincidence probability of 1/3, which is 50% larger than for 3 classical particles. This leads us to investigate low-order quantum interferences by exploring a newly developed framework based on the generating function of the transition probabilities and associated recurrence relations. Using this, we are able to provide a precise interpretation of the constructive interference behind the coincidence probability in a 3-splitter, as well as the corresponding destructive interference in a 4-splitter. Further, we revisit the recurrence relations on transition probabilities by ascribing the minors appearing in the formulas to fermionic statistics. This results in an original decomposition of the transition probabilities that combines bosonic and fermionic interferometry. Our preliminary analysis of this decomposition for 2 and 3 modes seems to indicate that it is a promising path towards a better understanding of multimode quantum interferometers.

Keywords: Quantum optics, quantum multi-photon interferences, Hong-Ou-Mandel effect, multiport Fourier interferometer, quantum indistinguishability, matrix permanent.

Résumé

Les interférences quantiques multimodes multi-photons ont récemment attiré une attention grandissante puisqu'elles figurent au coeur des futures technologies quantiques intégrant des dispositifs photoniques. Le célèbre effet Hong-Ou-Mandel est le paradigme d'un tel effet de suppression quantique pour deux photons se propageant dans deux modes, provenant de l'indiscernabilité des photons (étant des bosons, la trajectoire où ils sont chacun réfléchi par un beam splitter équilibré interfère de manière destructive avec la trajectoire où ils sont chacun transmis, ce qui donne lieu au phénomène de bunching). A travers ce mémoire, nous explorons l'extension des interférences quantiques à plus de deux photons dans plus de deux modes. Nous nous concentrons sur un interféromètre dit de Fourier, qui est défini comme la généralisation à N modes d'un beam splitter équilibré (également connu sous l'appellation de N-splitter). Nous sondons la probabilité de détections coïncidentes de N photons frappant cet interféromètre et la connectons au permanent de la matrice sous-jacente à la transformée de Fourier discrète. Bien que le calcul de permanents soit notoirement un problème très difficile en comparaison avec les déterminants, nous pouvons déduire quelques implications de l'indiscernabilité des photons par rapport à des particules classiques distinguables. En particulier, nous montrons l'existence d'un effet d'interférence constructive pour certaines valeurs impaires de N dans un interféromètre de Fourier (alors qu'il est prouvé que l'interférence est totalement destructive pour n'importe quel N pair). A titre d'exemple, le plus petit cas non trivial ($N = 3$) donne une probabilité de coïncidence de $1/3$, soit 50% plus grand que pour 3 particules classiques. Ceci nous amène à étudier les interférences quantiques aux petits ordres en explorant un cadre nouvellement développé basé sur la fonction génératrice des probabilités de transition ainsi que les relations de récurrences qui y sont associées. Nous sommes ainsi capables de fournir une interprétation précise de l'interférence constructive se cachant derrière la probabilité de coïncidence dans un 3-splitter, ainsi que l'interférence destructive correspondante dans un 4-splitter. En outre, nous revisitons les relations de récurrences régissant les probabilités de transition en attribuant les mineurs apparaissant dans les formules à la statistique fermionique. Il en résulte une décomposition originale des probabilités de transition qui combine à la fois l'interférométrie bosonique et fermionique. Notre analyse préliminaire de cette décomposition pour les cas à 2 et 3 modes semble indiquer qu'il s'agit d'une voie prometteuse vers une meilleure compréhension des interféromètres quantiques multimodes.

Mots-clés: Optique quantique, interférences quantiques multi-photon, effet Hong-Ou-Mandel, interféromètre multiport de Fourier, indiscernabilité quantique, permanent matriciel.

Acknowledgments

First and most of all, I would like to thank my professor and thesis director Nicolas Cerf who gave me the opportunity to achieve this thesis and who dedicated time to guide and help me through my research. Working with him has proven to be very enriching and formative.

I also want to thank Zacharie Van Herstraeten, my supervisor and friend who always responded present in any situation to help me through difficulties, hard times and to have attended all the meetings concerning this work.

Thank you to all the members of the QuIC who kindly welcomed me during this year, especially Leonardo Novo and Michael Jabbour who have shown interest in my work and helped me several times.

To my thesis classmates, Célia Griffet and Timothée Hoffreumon, thank you for the good atmosphere during those many hours of work in the seminar room.

Of course, I want to thank my dear physicist friends, Casimir, Denis, Enea, Timothée, Eliott, Florian, and so many others without whom those years at university would not have been so amazing.

Finally, I would like to thank my parents who always supported me and cheered me up across my studies.

Contents

List of Figures

Introduction

Proving the superiority of quantum computation in solving problems that would be intractable on any classical computer has become a key goal in quantum information sciences, and is often called the quest for *quantum supremacy* [21]. In order to demonstrate the advantage of quantum devices over their classical counterparts, one needs to select a classically hard task. A promising candidate to this purpose resides in *boson sampling* [1]. Such a model consists in sampling from the probability distribution of detecting single bosons at the output of a linear interferometer [6]. It has long been known that quantum computation could in principle be implemented thanks to linear optics [12], and it was later confirmed that linear quantum optics constitutes a good candidate towards an efficient implementation of quantum computing [13]. Following this path, the photonic version of boson sampling is therefore considered as probably the most promising approach in order to demonstrate quantum supremacy. A (photonic) boson sampling device is based upon linear optics passive components (beam splitters and phase shifters forming an interferometer in which photon scattering takes place) followed by single-photon detectors. More generally, future quantum technologies are anticipated to rely on integrated photonic devices extending this boson sampling paradigm, hence a key to the implementation of quantum technologies stands in the comprehensive understanding of multiphoton quantum interferences in multimode interferometers.

Such interferometric quantum effects are precisely the topic of this Ms thesis. Especially, the thesis explores quantum interferences extended to setups involving more than two photons propagating in more than two modes within an interferometric setup. A famous example of such an interferometric (suppression) effect is the Hong-Ou-Mandel effect [9], which results from the indistinguishability of two photons sent simultaneously in two separate modes of a balanced beam splitter and states the impossibility of the coincident detection of the two photons. In this Ms thesis, we aim at gaining a better understanding and interpretation of such interferences. The interferometers considered here can be seen as the generalization of a balanced beam splitter to a number N of modes superior to two, so we named them *Fourier interferometers*. In analogy with a balanced beam splitter, they have the property that a single photon sent in any input port can be detected equiprobably at any output port. We study quantum interferences by building on a recent framework developed at QuIC, which is based on the generating function of the transition probabilities [10]. This function encapsulates the information related to all transition probabilities for any photon number. It can be used to derive a recurrence relation, which is the cornerstone of our study of quantum interferences. In particular, we observe that manipulating such a recurrence relation is a much more convenient path rather than directly computing transition probabilities in the Fock basis through cumbersome calculations. Using this framework, we then compare the behaviour of quantum interferences to a classical model (considering photons as distinguishable particles). Focusing on low-order interferometers, this enables us to provide a clear interpretation of the quantum interferometric phenomena at work.

This Ms thesis is divided in two parts: the first part is dedicated to the concepts

and theoretical background that we need to manipulate in order to deal with quantum interferences. In the second part, we present the results obtained in the course of this work. The background part is composed of two chapters, within which we overview all notions about quantum optics as well as the mathematical tools used to study quantum interferences. In the first chapter, we present the quantum optics concepts that will allow us to describe the physics of our setup. Among these, we find second quantization, the set of passive optical components, as well as the celebrated Hong-Ou-Mandel effect representing the initial motivation of this Ms thesis. The second chapter then focuses on the mathematical framework previously developed at QuIC that we will use to describe quantum interferences from a mathematical perspective. The key concepts presented in this chapter are the generating functions, the recurrence relations and the permanent of a matrix. The latter itself represents a mathematical object of interest as it is at the heart of our work. The second part of the thesis is dedicated to our results, and is organized in three chapters (Chapters 3-5). Chapter 3 compares the transition probabilities of photons through an interferometer in classical and quantum cases as a function of the number of modes N. This highlights a fundamental difference of behaviour between even and odd values of N. This also leads us to focus on the underlying problem of computing the permanent of Fourier matrices. In Chapter 4, we focus on the study of low-order interferometers (especially three and four modes), which are the simplest interesting — yet unstudied — cases. By working with the recurrence relations, we propose some conjectures that would simplify computations for higher orders. Finally, in Chapter 5, we go deeper in the study of the three-mode interferometer by introducing fermionic statistics in the formalism, allowing us to fully describe quantum interferences in this case. We then provide a conclusion on the obtained results.

Part I

Background

Chapter 1

Linear quantum optics

1.1 Outline

In this first chapter, we introduce concepts inherent to quantum optics that will be used across this thesis. Roughly speaking, quantum optics can be considered as the application of quantum mechanics to quanta of the electromagnetic field, namely photons, rather than considering light as electromagnetic waves.

We start this chapter by an overview presentation of the second quantization in order to introduce the mode operators and the Fock states along with their properties. We apply it to the case of bosonic systems as we will focus on situations where photons are involved. The following section will then be devoted to the passive optical components that are the beam splitters and the phase shifters. Their physics will be presented as well as the generalization of the beam splitter to the N-dimensional case to treat the N-splitters i.e. interferometers, involving a higher number of modes than traditional beam splitters, and the discrete Fourier transform matrices will be presented as well. Finally to end this chapter, we will present the celebrated effect in quantum interferometry that is the Hong-Ou-Mandel effect [9], which represents the initial motivation for this work.

Across this chapter we will mainly refer to [7] and [24] for the concepts specific to second quantization and various sources across the rest of this chapter.

1.2 Second quantization

1.2.1 Different quantizations

The first quantization can be denoted as the original form of quantum mechanics [19]. In such a formalism, the state of the system is usually described by state vectors or wave functions while observables are described by operators. A system of several identical particles, so characterized by the same physical parameters, is described by its Hamiltonian $\hat{H}$ which takes the general form [19]:

$$\hat{H} = \sum_i \hat{h}(\mathbf{r}_i) + \frac{1}{2}\sum_{i\neq j} V(\mathbf{r}_i - \mathbf{r}_j), \tag{1.2.1}$$

that includes two contributions, the first term is the summation of the single-particle Hamiltonians $\hat{h}$ and the second involves the interaction potential V between pairs of particles. Each observable depends on the coordinates $\mathbf{r}_i$ of the i^{th} particle. In general, this interaction potential term makes the Hamiltonian complicated to solve because of the interaction between particles.

The problem is described by the many-particle Schrödinger equation:

$$i\hbar\frac{\partial}{\partial t}\psi(\mathbf{r}_1,\ldots,\mathbf{r}_\mathcal{N},t)=\hat{H}\psi(\mathbf{r}_1,\ldots,\mathbf{r}_\mathcal{N},t), \tag{1.2.2}$$

where $\psi(\mathbf{r}_1,\ldots,\mathbf{r}_\mathcal{N},t)$ is the wave function of the many-particle system. Bosonic wave functions are symmetric while fermionic wave functions are anti-symmetric. We will only consider symmetric wave functions as we will next consider systems involving photons and thus bosons, which are integer spin particles. This results from the indistinguishability of identical particles, which means that the permutation of two particles does not affect any changes on the system when bosons are involved. This writes:

$$\psi(\mathbf{r}_1,\ldots,\mathbf{r}_i,\ldots,\mathbf{r}_j,\ldots,\mathbf{r}_\mathcal{N},t)=+\psi(\mathbf{r}_1,\ldots,\mathbf{r}_j,\ldots,\mathbf{r}_i,\ldots,\mathbf{r}_\mathcal{N},t), \tag{1.2.3}$$

where we have interchanged coordinates i and j. This result states that for a system of $\mathcal{N}$ bosons, the permutation between particles does not change the state of the system because of the indistinguishability of the particles. After the permutation, we would not be able to distinguish between the current state and the initial one.

For many-particle systems, the direct solution of Schrodinger equation (1.2.1) might be impractical and rather cumbersome. So for the cases where a lot of particles are parts of a system, it is necessary to make use of another formalism. This is where second quantization rises.

Second quantization is a formalism that is thus introduced in order to treat non-relativistic systems involving a large number of identical particles [24]. We could also see it as the reverse procedure of first quantization, i.e. attributing particle-like properties to wave electromagnetic fields [7]. Such a formalism has several advantages like automatically accounting for the symmetry of the wave function, it can be used the same way regardless of wether we work with bosons or fermions but also makes possible to vary the number of particles which becomes an observable $\hat{\mathcal{N}}$. We are now about to discuss several concepts that play an important role in the second quantization, that is : Fock states and mode operators.

1.2.2 Fock states

Also named number states, *Fock states* are quantum states that have a fixed number of particles (which are photons here). For a multimode case, we define them:

$$|n_1,n_2,\ldots\rangle\,, \tag{1.2.4}$$

this state indicates that there is n_i quanta in the i^{th} mode. This allows as well to define the state devoid of particles, namely the *vacuum state* or *ground state*:

$$|0\rangle\equiv|0,0,\ldots\rangle\,. \tag{1.2.5}$$

We can also define them from a mathematical perspective as being the eigenstates of the *number operator* $\hat{n}$, that will be defined in following section, associated to the eigenvalues n also named *occupation number*:

$$\hat{n_i}\,|n_1,\ldots,n_i,\ldots\rangle=n_i\,|n_1,\ldots,n_i,\ldots\rangle\,, \tag{1.2.6}$$

with the imposed constraint that the sum of the occupation numbers must be equal to the total number of particles:

$$\sum_{i=1}^{\infty} n_i = \mathcal{N}, \tag{1.2.7}$$

as the system counts exactly $\mathcal{N}$ particles.

Fock states form a complete set of $\mathcal{N}$-particle states that are completely symmetric and thus form the Fock space. This basis is thus completely symmetric as well and such states are orthonormal, so that they satisfy the orthogonality relation:

$$\langle n_1, n_2, \ldots | n_1', n_2', \ldots \rangle = \delta_{n_1,n_1'} \delta_{n_2,n_2'} \ldots, \tag{1.2.8}$$

and also the completeness relation

$$\sum_{n_1,n_2,\ldots} |n_1, n_2, \ldots\rangle \langle n_1, n_2, \ldots| = \mathbb{1}, \tag{1.2.9}$$

with $\mathbb{1}$ being the identity operator.

1.2.3 Mode operators

We can now introduce the operators that act on states with a well-defined number of particles, so Fock states. These are called *creation* and *annihilation operators* and are usually denoted by $\hat{a}^\dagger$ and $\hat{a}$ respectively, one being the adjoint of the other:

$$\hat{a}_i^\dagger |\ldots, n_i, \ldots\rangle = \sqrt{n_i + 1}\, |\ldots, n_i + 1, \ldots\rangle\,, \tag{1.2.10}$$

$$\hat{a}_i |\ldots, n_i, \ldots\rangle = \begin{cases} \sqrt{n_i}\, |\ldots, n_i - 1, \ldots\rangle\,, & \text{for } n_i \geq 1, \\ 0, & \text{for } n_i = 0. \end{cases} \tag{1.2.11}$$

As stated by their name, $\hat{a}_i^\dagger$ does increase the occupation number of the i^{th} mode by one as it adds a photon in it whereas $\hat{a}_i$ reduces n_i by one due to the destruction of a photon in this mode. In other words, those operators allow to go from the $\mathcal{N}$-particles states space to the $\mathcal{N}\pm1$-particles states spaces [24]. As having a negative number of particles is physically irrelevant, applying annihilation operators to empty modes results in a null result as shown by equation (1.2.11).

Mode operators obey the following commutation relations:

$$[\hat{a}_i, \hat{a}_j] = 0, \tag{1.2.12a}$$

$$[\hat{a}_i^\dagger, \hat{a}_j^\dagger] = 0, \tag{1.2.12b}$$

$$[\hat{a}_i, \hat{a}_j^\dagger] = \delta_{ij}. \tag{1.2.12c}$$

We can easily provide a physical interpretation to it. The first two relations state that if we first annihilate or create a particle in the i^{th} mode and then in the j^{th} mode or vice-versa, we get the same state at the end. However we see from third relation (1.2.12c) that in the case where we act on the same mode, the fact of creating a particle and then annihilating it is not equivalent to the opposite situation. The order is not arbitrary, the mode operators must be normal ordered by placing creation operators at the left of annihilation operators.

The demonstrations of the commutation relations are proposed here after and comes from [24].

Proof

As $\hat{a}_i$ commutes with itself, for $i = j$ the commutation (1.2.12a) is trivial. When $i \neq j$, according to the definition of the annihilation operator:

$$\begin{aligned}\hat{a}_i\hat{a}_j \left|...,n_i,...,n_j,...\right\rangle &= \hat{a}_i\sqrt{n_j}\left|...,n_i,...,n_j-1,...\right\rangle \\ &= \sqrt{n_i}\sqrt{n_j}\left|...,n_i-1,...,n_j-1,...\right\rangle \\ &= \hat{a}_j\hat{a}_i\left|...,n_i,...,n_j,...\right\rangle .\end{aligned} \tag{1.2.13}$$

Taking the adjoint of previous demonstration immediately proves (1.2.12b), indeed:

$$[\hat{a}_i,\hat{a}_j]^\dagger = [\hat{a}_i^\dagger,\hat{a}_j^\dagger] = 0. \tag{1.2.14}$$

Finally, when both operators are applied for $i \neq j$ we get:

$$\begin{aligned}\hat{a}_i\hat{a}_j^\dagger \left|...,n_i,...,n_j,...\right\rangle &= \hat{a}_i\sqrt{n_j+1}\left|...,n_i,...,n_j+1,...\right\rangle \\ &= \sqrt{n_i}\sqrt{n_j+1}\left|...,n_i-1,...,n_j+1,...\right\rangle \\ &= \hat{a}_j^\dagger\hat{a}_i\left|...,n_i,...,n_j,...\right\rangle .\end{aligned} \tag{1.2.15}$$

While when $i = j$:

$$\begin{aligned}(\hat{a}_i\hat{a}_i^\dagger - \hat{a}_i^\dagger\hat{a}_i)\left|...,n_i,...\right\rangle &= \hat{a}_i\sqrt{n_i+1}\left|...,n_i+1,...\right\rangle - \hat{a}_i^\dagger\sqrt{n_i}\left|...,n_i-1,...\right\rangle \\ &= \sqrt{n_i+1}\sqrt{n_i+1}\left|...,n_i,...\right\rangle - \sqrt{n_i}\sqrt{n_i}\left|...,n_i,...\right\rangle \\ &= \left|...,n_i,...\right\rangle ,\end{aligned} \tag{1.2.16}$$

proving (1.2.12c).

In the previous section, we mentioned the particle-number operator without giving any definition to it. It is now time do so thanks to the creation and annihilation operators. This is defined as:

$$\hat{n}_i = \hat{a}_i{}^\dagger\hat{a}_i. \tag{1.2.17}$$

Measuring this observable does provide the number of particles occupying the i^{th} mode so giving its occupation number.

Proof

By the definitions of mode operators:

$$\begin{aligned}\hat{n}_i\left|\ldots,n_i,\ldots\right\rangle &= \hat{a}_i{}^\dagger\hat{a}_i\left|\ldots,n_i,\ldots\right\rangle \\ &= \hat{a}_i{}^\dagger\sqrt{n_i}\left|\ldots,n_i-1,\ldots\right\rangle \\ &= \sqrt{n_i}\sqrt{n_i}\left|\ldots,n_i,\ldots\right\rangle \\ &= n_i\left|\ldots,n_i,\ldots\right\rangle .\end{aligned} \tag{1.2.18}$$

In the same vein of thinking we also define the *total number operator* which in turn gives the total bosons number of the system. Similarly to equation (1.2.17), we can link the total number operator to the particle-number operator and so to the creation and annihilation operators:

$$\hat{\mathcal{N}} = \sum_i \hat{n}_i = \sum_i \hat{a}_i{}^\dagger\hat{a}_i. \tag{1.2.19}$$

With the concepts previously introduced, we finally are able to derive a general writing for any many-particle state. Starting from the vacuum state $|0\rangle$, containing no particles, we can construct any state with any number of particles by means of $\hat{a_i}^\dagger$:

$$|n_1, n_2, \ldots\rangle = \frac{1}{\sqrt{n_1! n_2! \ldots}} (\hat{a}_1^\dagger)^{n_1} (\hat{a}_2^\dagger)^{n_2} \ldots |0\rangle \,. \tag{1.2.20}$$

Thanks to second quantization formalism the number of particles does not need anymore to be initially fixed to solve the problem as it is the case in first quantization. Creation and annihilation operators allow to manipulate with ease the state of the system by varying the number of particles in its different modes making of $\hat{\mathcal{N}}$ an observable and this without having to repeat the calculations.

The different notions exposed here will be used afterwards for the description of the system under consideration.

1.3 Passive optical components

1.3.1 Energy conservation

The optical components exposed in this section are denominated to be passive in the sense that they respect the conservation of energy. Indeed, no loss, absorption or production of energy is undertaken, in contrast with active components such as two-mode squeezer. This energy conservation is a consequence from the fact that each component will be represented by a unitary transformation matrix linking the inputs and the outputs of the component.

Proof

A unitary matrix U satisfies:

$$\mathrm{U}^\dagger \mathrm{U} = \mathrm{U}\mathrm{U}^\dagger = \mathrm{I}. \tag{1.3.1}$$

where I is the identity matrix. The matrix U links the output mode operators $\hat{b}$ to the input ones $\hat{a}$:

$$\hat{\mathbf{b}} = \mathrm{U}\hat{\mathbf{a}}, \tag{1.3.2}$$

which can be rewritten as:

$$\hat{b}_j = \sum_i \mathrm{U}_{ji} \hat{a}_i. \tag{1.3.3}$$

Multiplying this last equation by its Hermitian conjugate and summing over all the outputs we get:

$$\begin{aligned} \sum_j \hat{b}_j^\dagger \hat{b}_j &= \sum_j \sum_{i,k} \mathrm{U}_{ji}^\dagger \hat{a}_i^\dagger \mathrm{U}_{jk} \hat{a}_k \\ &= \sum_{i,k} \hat{a}_i^\dagger \hat{a}_k \sum_j \mathrm{U}_{ji}^\dagger \mathrm{U}_{jk} \\ &= \sum_i \hat{a}_i^\dagger \hat{a}_i, \end{aligned} \tag{1.3.4}$$

where we find back, thanks to equation (1.2.19), the number of photons implied at inputs and outputs:

$$\mathcal{N}_{out} = \mathcal{N}_{in}. \tag{1.3.5}$$

No photon is lost, absorbed or produced across the component. The total number of photons at the entrance of such passive components is thus well conserved and so is energy.

1.3.2 Phase shifter

The first element we describe is the phase shifter. This component does modify the beam passing through it only by shifting its phase.

Figure 1.1: Action of a phase shifter φ on incoming beam.

From the operators perspective, the phase shifter acts on the input mode as:

$$\hat{b} = \hat{a}e^{i\varphi}. \tag{1.3.6}$$

In the case represented by figure 1.1 the unitary of the phase shifter is a simple complex exponential with the phase φ as factor. In a multimode format, this unitary is generalized to a diagonal square matrix of order N with elements of modulus one on its diagonal entries, each entry corresponding to a definite mode.

1.3.3 Beam splitter

The beam splitter is an important optical device concerned in this thesis. While the phase shifter does act exclusively on the phase, the beam splitter splits in two a beam of light incident to it. The particularity of the beam splitter is thus to reflect only a part of the light it receives and to transmit the other part.

In interferometry, several beams are involved in the experiment. A situation with two incident beams is represented by figure 1.2, each output port corresponds to the superposition of beams resulting from transmissions and reflections of input ports.

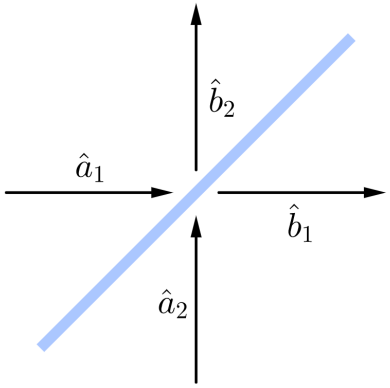

Figure 1.2: Action of a beam splitter on two incoming beams.

In order to determine the unitary matrix describing a beam splitter, we propose to analyze the relations between its outputs and inputs. Firstly, a beam splitter is characterized by its *transmittance* η which then allows to define the *reflection* and *transmission coefficients* [15], respectively $\mathcal{T}$ and $\mathcal{R}$:

$$\mathcal{T} = \sqrt{\eta} \quad \text{and} \quad \mathcal{R} = i\sqrt{1-\eta}, \tag{1.3.7}$$

where the complex factor i is due to the fact that a photon acquires an additional $\pi/2$ phase while it is reflected. Previous coefficients obey to:

$$|\mathcal{T}|^2 + |\mathcal{R}|^2 = 1, \tag{1.3.8}$$

as expected from energy conservation. The general form of the beam splitter matrix linking its output ports to input ports is thus:

$$\mathrm{U}_{BS} = \begin{pmatrix} \mathcal{T} & \mathcal{R} \\ \mathcal{R} & \mathcal{T} \end{pmatrix} = \begin{pmatrix} \sqrt{\eta} & i\sqrt{1-\eta} \\ i\sqrt{1-\eta} & \sqrt{\eta} \end{pmatrix}. \tag{1.3.9}$$

Proof

Using the representation of the beam splitter from figure 1.2, it is straightforward to determine the output port $\hat{b}_1$ in terms of inputs $\hat{a}_1$ and $\hat{a}_2$. Indeed, it consists in the transmission of $\hat{a}_1$ and reflection of $\hat{a}_2$, leading to:

$$\hat{b}_1 = \mathcal{T}\hat{a}_1 + \mathcal{R}\hat{a}_2. \tag{1.3.10}$$

Proceeding in a similar way for the other output ends with:

$$\hat{b}_2 = \mathcal{R}\hat{a}_1 + \mathcal{T}\hat{a}_2, \tag{1.3.11}$$

or in matrix writings:

$$\begin{pmatrix} \hat{b}_1 \\ \hat{b}_2 \end{pmatrix} = \begin{pmatrix} \mathcal{T} & \mathcal{R} \\ \mathcal{R} & \mathcal{T} \end{pmatrix} \begin{pmatrix} \hat{a}_1 \\ \hat{a}_2 \end{pmatrix}. \tag{1.3.12}$$

From now let us consider the beam splitter to be balanced ($\eta = 1/2$), also denoted as 50:50 beam splitter, meaning that it is equiprobable for a photon to be reflected or transmitted by the beam splitter. This makes reflection and transmission coefficients of equal magnitude:

$$|\mathcal{T}| = |\mathcal{R}| = \frac{1}{\sqrt{2}}. \tag{1.3.13}$$

Accounting for these considerations in equation (1.3.12) finally results in the input-output relation:

$$\begin{pmatrix} \hat{b}_1 \\ \hat{b}_2 \end{pmatrix} = \frac{1}{\sqrt{2}} \begin{pmatrix} 1 & i \\ i & 1 \end{pmatrix} \begin{pmatrix} \hat{a}_1 \\ \hat{a}_2 \end{pmatrix}. \tag{1.3.14}$$

The matrix of the balanced beam splitter is thus:

$$\mathrm{U}_{BS} = \frac{1}{\sqrt{2}} \begin{pmatrix} 1 & i \\ i & 1 \end{pmatrix}, \tag{1.3.15}$$

which is indeed a unitary matrix.

The balanced beam splitter is the component which led to the discovery of the celebrated *Hong-Ou-Mandel effect* [9] when one photon is simultaneously incident on each input port. The Hong-Ou-Mandel effect will be the subject of a following section.

By combining a balanced beam splitter with two $-\pi/2$ phase shifters, we obtain the Hadamard gate [5], as shown on figure 1.3. We will see that such a configuration corresponds to a second-order interferometer, i.e. accounting for two modes, and that gives rise to the Hong-Ou-Mandel effect.

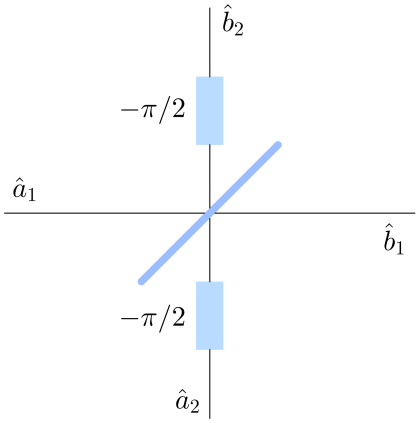

Figure 1.3: Hadamard gate constructed with balanced beam splitter and phase shifters.

Before constructing the unitary matrix of the Hadamard gate, it is a good opportunity to show the unitary of a phase shifter in a multimode system as mentioned in section 1.3.2. We already know that the phase shifter unitary is diagonal with elements of modulus one. Then, taking for example the phase shifter placed before the beam splitter and acting on the second input mode, we have:

$$\mathrm{U}_{-\pi/2} = \begin{pmatrix} 1 & 0 \\ 0 & e^{-i\pi/2} \end{pmatrix} = \begin{pmatrix} 1 & 0 \\ 0 & -i \end{pmatrix}, \tag{1.3.16}$$

note that it is similar for the second phase shifter placed after the beam splitter as they act on the same second mode.

Now that the matrices of the different components are known, it is then possible to determine the matrix of the Hadamard gate. By simple matrix multiplication, we get:

$$\begin{aligned} \begin{pmatrix} \hat{b}_1 \\ \hat{b}_2 \end{pmatrix} &= \mathrm{U}_{-\pi/2}\mathrm{U}_{BS}\mathrm{U}_{-\pi/2} \begin{pmatrix} \hat{a}_1 \\ \hat{a}_2 \end{pmatrix} \\ &= \frac{1}{\sqrt{2}} \begin{pmatrix} 1 & 0 \\ 0 & -i \end{pmatrix} \begin{pmatrix} 1 & i \\ i & 1 \end{pmatrix} \begin{pmatrix} 1 & 0 \\ 0 & -i \end{pmatrix} \begin{pmatrix} \hat{a}_1 \\ \hat{a}_2 \end{pmatrix} \\ &= \frac{1}{\sqrt{2}} \begin{pmatrix} 1 & 1 \\ 1 & -1 \end{pmatrix} \begin{pmatrix} \hat{a}_1 \\ \hat{a}_2 \end{pmatrix}. \end{aligned} \tag{1.3.17}$$

We thus find for the Hadamard gate the following unitary matrix:

$$\mathrm{H} = \frac{1}{\sqrt{2}} \begin{pmatrix} 1 & 1 \\ 1 & -1 \end{pmatrix}. \tag{1.3.18}$$

Later, we will define a set of N-dimensional interferometers whose second order reduces to the Hadamard gate. Such interferometers will be here considered as balanced and described by specific unitary that is the *discrete Fourier transform* matrices which will have a dedicated section.

1.3.4 N-order interferometers

Previously, we have presented the elementary component that is the beam splitter which includes two input and output modes. As we are not going to limit ourselves to the case of only two modes, it is appropriate to introduce setups of higher dimensions namely *N-order interferometers* or *N-mode interferometers*. Such of a setup is represented in figure 1.4 and has now N input modes and N output modes.

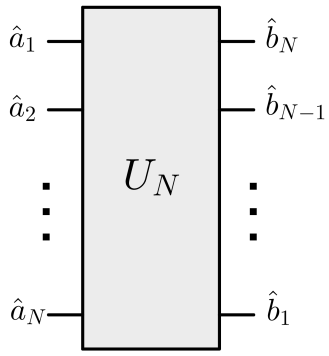

Figure 1.4: N-order interferometer.

As for the beam splitter, those devices are sites of interference phenomena. They are also described by a unitary, now of dimension N, that links its output ports to its input ports.

It is interesting to mention that such interferometers can be experimentally implemented thanks to simpler optical components. Indeed, based on [22], any $N \times N$ unitary operator can be factorized through a recursive algorithm that we are not explaining here. In that way any interferometer of N modes can be experimentally realized by using the passive components we have just described that are the phase shifters and the beam splitters.

To give an illustration of what has just been explained, we consider for simplicity a $N = 3$ interferometer. Such a device can be realized through an assembly of elementary optical components which is represented on figure 1.5 below inspired from [26].

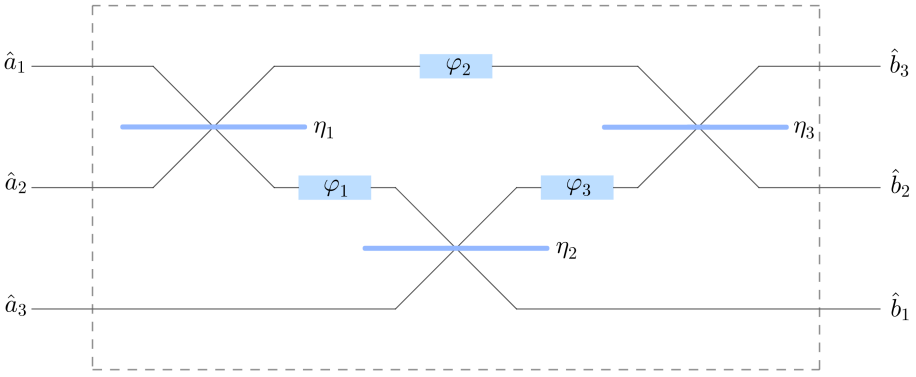

Figure 1.5: Tritter implementation with phase shifters and beam splitters.

Note that any of the components of the assembly is still characterized by its phase φ_i or by its transmission coefficient η_j. Acting on these allows to manipulate the behaviour of the device. For example, a particular choice of values makes it to be balanced and is then denominated as *tritter* [32]. For any given unitary to implement, the parameters of the components can be calculated by means of the algorithm [22].

1.3.5 Fourier interferometers

Now that the interferometers for any order have been presented in this section we introduce explicitly a unitary transformation representing a balanced interferometer. An example of unitaries representing suchlike devices correspond to the discrete Fourier transform (DFT) [14, 29].

Usually used in signal processing, the discrete Fourier transform can be expressed as a transformation matrix that is the *DFT matrix*. This matrix for a N-dimensional setup takes the following form:

$$\mathrm{F}_N = \frac{1}{\sqrt{N}} \begin{pmatrix} 1 & 1 & 1 & 1 & \cdots & 1 \\ 1 & \omega_N & \omega_N^2 & \omega_N^3 & \cdots & \omega_N^{N-1} \\ 1 & \omega_N^2 & \omega_N^4 & \omega_N^6 & \cdots & \omega_N^{2(N-1)} \\ 1 & \omega_N^3 & \omega_N^6 & \omega_N^9 & \cdots & \omega_N^{3(N-1)} \\ \vdots & \vdots & \vdots & \vdots & \ddots & \vdots \\ 1 & \omega_N^{N-1} & \omega_N^{2(N-1)} & \omega_N^{3(N-1)} & \cdots & \omega_N^{(N-1)(N-1)} \end{pmatrix}. \tag{1.3.19}$$

Where ω denotes the N^{th} root of unity and writes:

$$\omega_N = e^{-2\pi i/N}. \tag{1.3.20}$$

Note that the sign of the exponent is merely convention and might differ from one source to another. However this choice of convention is irrelevant in the way that it will not affect future computations. Given this definition, the DFT matrix elements are simply values disposed on the unit circle in the complex plane, rescaled by $1/\sqrt{N}$. Furthermore, the roots (1.3.20) satisfy:

$$\omega_N^N = 1, \tag{1.3.21a}$$
$$\omega_N^{-1} = \omega_N^*, \tag{1.3.21b}$$
$$\omega_N^{N-x} = (\omega_N^x)^*. \tag{1.3.21c}$$

This matrix being symmetric, it is straightforward to verify that it is a unitary transformation. As a reminder, it has to satisfy:

$$\mathrm{F}^\dagger \mathrm{F} = \mathrm{F}\mathrm{F}^\dagger = \mathrm{I} \Leftrightarrow \mathrm{F}^{-1} = \mathrm{F}^\dagger. \tag{1.3.22}$$

As we consider only balanced interferometers, the matrix states that a photon incoming on any of the input ports is going to be redirected towards any of the output ports with the same probability. In order to have a good comprehension of that through the DFT, we can express it by its matrix elements:

$$\mathrm{F}_{ji} = \frac{1}{\sqrt{N}} \omega_N^{(j-1)(i-1)}. \tag{1.3.23}$$

This represents the transition amplitude of a particle to go from input port i to output port j [14]. In order to obtain the transition probability, we take the squared modulus of the matrix element:

$$P_{ji} = |\mathrm{F}_{ji}|^2 = \frac{1}{N}, \tag{1.3.24}$$

as all matrix elements contain a complex exponential whose modulus is equal to one. Also, we have by summing over all the outputs:

$$\sum_j^N P_{ji} = 1. \tag{1.3.25}$$

Any photon entering this interferometer by any input port encounters thus the same probability to exit through any output port.

Finally, as the matrix insures the link between the input mode operators $\hat{a}_i$ and the output mode operators $\hat{b}_j$, we can write:

$$\hat{\mathbf{b}} = \mathrm{F}\hat{\mathbf{a}}, \tag{1.3.26}$$

$$\hat{b}_j = \frac{1}{\sqrt{N}} \sum_{i=1}^{N} \omega_N^{(j-1)(i-1)} \hat{a}_i. \tag{1.3.27}$$

We are now able to show that the Hadamard gate derived above at equation (1.3.18) corresponds to the second-order Fourier interferometer.

Proof

For $N = 2$, we have $\omega_2 = e^{-\pi i}$ and the DFT matrix then becomes:

$$\begin{aligned} \mathrm{F}_2 &= \frac{1}{\sqrt{2}} \begin{pmatrix} 1 & 1 \\ 1 & e^{-\pi i} \end{pmatrix} \\ &= \frac{1}{\sqrt{2}} \begin{pmatrix} 1 & 1 \\ 1 & -1 \end{pmatrix}, \end{aligned} \tag{1.3.28}$$

where we retrieve the Hadamard gate.

To sum up, DFT matrices correspond to an example of unitaries of any order balanced interferometers. It is the transition matrix that links the output ports and the input ports of the interferometer. We will use it in the rest especially for computing transition probabilities of photons across such interferometers. This will be achieved in the second part of this thesis.

1.4 Hong-Ou-Mandel effect

The Hong-Ou-Mandel effect has been first highlighted in 1987 [9] and is due to the indistinguishable character of the particles involved in the experiments. It is also known as the photon *coalescence* [8]. In order to provide a proper description of it, we first illustrate it from a physical point of view and then we complete this with a mathematical description in order to see that it can be explained by means of the different concepts that have been introduced so far.

1.4.1 Physical description

The experiment consists in sending simultaneously two photons in a 50:50 beam splitter separately through its input modes. As the beam splitter is balanced, each impinging particle has equal probability to be transmitted or to be reflected. Let us first consider that these two particles can be distinguished from each other. This can be the case when a difference between their physical properties, such as e.g. orthogonal polarization states, is existing.

Each of the photons can either be transmitted or reflected independently of each other. The beam splitter then gives rise to four possible outcomes for the two photons that are as follows:

(a) The descending photon is transmitted and the ascending photon is reflected

(b) The descending photon is reflected and the ascending photon is transmitted

(c) Both photons are reflected

(d) Both photons are transmitted

Those configurations are depicted in figure 1.6 here after:

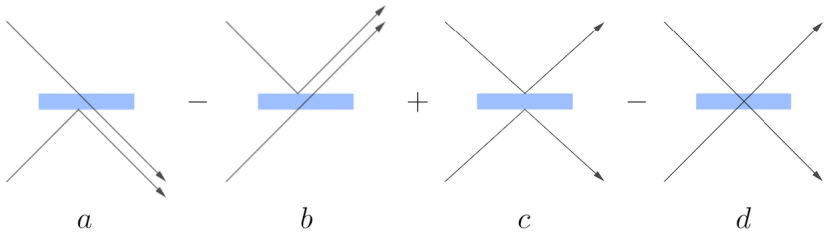

Figure 1.6: Possible configurations of two photons through a beam splitter with the respective sign of the amplitude of this event: one reflected and the other transmitted (a and b); both reflected (c); both transmitted (d).

To each of these configurations is associated a probability amplitude. Since all the outcomes are distinguishable, the probability of a given outcome is simply given by the squared modulus of the corresponding amplitude. The output state of the beam splitter then corresponds to a superposition with contributions from each of these configurations. The negative sign associated to some configurations originates from introduction of relative phase shifts π inducing a factor -1 in front of the corresponding terms.

Let us now consider the situation where both of the photons are exactly the same so that they can be considered as indistinguishable. In this case, it appears now that by observing the different output configurations we are not able to distinguish anymore between the one where each photon is reflected (Fig. 1.6c) and the one where both photons are transmitted (Fig. 1.6d). As the associated amplitudes have opposite signs, they cancel each other. We thus have a destructive interference between these latter configurations. This states that due to their indistinguishability, the two photons must exit the beam splitter by the same output port (Fig. 1.6a, b), they are *bunching*. This quantum interference phenomenon is known as the Hong-Ou-Mandel effect. It can be attributed to the bosonic character of photons. In contrast, when fermions are concerned they always leave the beam splitter separately due to Pauli's exclusion principle [14].

1.4.2 Mathematical description

This complementary description makes use of concepts of mode operators and vacuum state presented in the first sections and consists in a development that is presented in [14] but that we include here. Again, we consider two identical particles entering a balanced beam splitter by its separate output ports whose we remind that the transition matrix is the Hadamard gate (that is also the DFT matrix for $N = 2$). As there is one photon entering each input port, we write the input state of the system thanks to the creation operators:

$$|\phi_{in}\rangle = \prod_{i=1}^{N} \hat{a}_i^\dagger |0\rangle = \hat{a}_1^\dagger \hat{a}_2^\dagger |0\rangle \,, \tag{1.4.1}$$

with $|0\rangle$ being the vacuum state.

In order to know the output of the system, we need to express its output state by means of the creation operators for the output ports $\hat{b}_i^\dagger$. But first, let us establish the connection between the input state and the output state. To do so, we introduce a new matrix that is the unitary *scattering matrix* S:

$$|\phi_{out}\rangle = S\,|\phi_{in}\rangle\,. \tag{1.4.2}$$

Using the definition of the input state, the fact that S is unitary and that $S\,|0\rangle = |0\rangle$, we can rewrite the output state as:

$$|\phi_{out}\rangle = S\hat{a}_1^\dagger S^\dagger S\hat{a}_2^\dagger ... S^\dagger S\hat{a}_N^\dagger S^\dagger S\,|0\rangle = \prod_{i=1}^{N} S\hat{a}_1^\dagger S^\dagger\,|0\rangle\,, \tag{1.4.3}$$

implying

$$S\hat{a}_i^\dagger S^\dagger = \sum_j \mathrm{U}_{ji}\hat{b}_j^\dagger, \tag{1.4.4}$$

to be injected in (1.4.3),

$$|\phi_{out}\rangle = \prod_{i=1}^{N}\left(\sum_{j=1}^{N}\mathrm{U}_{ji}\hat{b}_j^\dagger\right)|0\rangle\,, \tag{1.4.5}$$

which allows to obtain:

$$\begin{aligned}|\phi_{out}\rangle &= \frac{1}{2}(\hat{b}_1^\dagger + \hat{b}_2^\dagger)(\hat{b}_1^\dagger - \hat{b}_2^\dagger)\,|0\rangle \\ &= \frac{1}{2}[(\hat{b}_1^\dagger)^2 - \hat{b}_1^\dagger\hat{b}_2^\dagger + \hat{b}_2^\dagger\hat{b}_1^\dagger - (\hat{b}_2^\dagger)^2]\,|0\rangle\,,\end{aligned} \tag{1.4.6}$$

where we retrieve the commutation law (1.2.12b) making the second and third terms to cancel each other. Finally, the output state becomes then:

$$|\phi_{out}\rangle = \frac{1}{2}[(\hat{b}_1^\dagger)^2 - (\hat{b}_2^\dagger)^2]\,|0\rangle\,. \tag{1.4.7}$$

The output state is then a superposition of the configurations where two photons exit together randomly through only one of the output ports, this is the so-called *bunching effect*. We can also mention that this effect has fundamental implications in quantum information processing as it allows to characterize indistinguishability of photons [8].

The Hong-Ou-Mandel effect is a key concept in this work as one of its motivations resides in the study of this effect generalized to interferometers of any dimension and to get a better comprehension of the interferometric phenomena occurring within it. Next, we will thus be interested in the transition of a pattern accounting for single photons per input towards a pattern of single photons per output. This will be discussed in the second part of this thesis.

1.5 Conclusion

In this first chapter, we have presented the fundamental notions of linear quantum optics that this thesis will use in purpose to study quantum interferences for more than two indistinguishable photons in more than two modes. We first introduced second quantization as well as some concepts inherent in it that are Fock states and mode operators acting on it. Then we have presented the passive optical components such as the phase shifter, the beam splitter and Fourier interferometers which will allow to represent the interferometric systems under study. Finally, their mathematical behaviour has been introduced through the DFT before ending this chapter with a section dedicated to the quantum interference effect that is the Hong-Ou-Mandel effect standing as the motivational cornerstone of this thesis.

Chapter 2

Mathematical framework

2.1 Outline

The mathematical description of the quantum interferences in which we are interested in might seem cumbersome or of great difficulty. Nevertheless, we will see that by exploiting the right tools such of a description reveals to be of a certain elegance for Gaussian unitaries (i.e generated by quadratic Hamiltonians in $\hat{a}$ and $\hat{a}^\dagger$ [11]) in the Fock basis. The theoretical framework presented in this chapter rests on the key concept of *generating function*. From this, we will be able to derive the principal objects we will work with in order to obtain results in the second half of the thesis, that is the *recurrence relations*. Through these equations we will have access to the *multi-photon transition probabilities* that will be computed in order to study, among others, the generalization of the Hong-Ou-Mandel effect previously presented. Such equations relate the transition probabilities to each other and constitute a convenient way to compute them. It is important to note that in this chapter, we will not demonstrate the mathematical developments leading to the formalism just mentioned as those have been the subject of previous works [10, 11] which this thesis calls upon.

We start this chapter with the introduction of the concept of generating function. Its definition, the motivation of its use as well as the general expression allowing it to be obtained for any N will be stated. Working with the generating function as starting point, we will then show how to derive the recurrence equations allowing to obtain the transition probabilities by simple calculations. This will be illustrated in the two-mode case to give a global vision of the formalism. We will finally focus on the transition probabilities themselves to link it to the permanent of a matrix, which will constitute a second manner to compute transition probabilities. Indeed, the permanent is not unknown to quantum interferometry [23] and has itself been a mathematical curiosity of particular interest for the recent past decades.

The main references that we use in this chapter are [10], some of whose notations are used here, and [11].

2.2 Generating functions

2.2.1 Definition

We define a generating function as a way to encapsulate a sequence of numbers $\{c_n\}$ by processing them as coefficients of a power series. It is mathematically expressed as [31]:

$$f(x) \equiv \mathcal{T}_n[c_n](x) = \sum_{n=0} c_n x^n, \tag{2.2.1}$$

where

$$c_n = \frac{1}{n!} \frac{d^n f}{dx^n}\bigg|_{x=0}. \tag{2.2.2}$$

This function encapsulates the whole sequence $\{c_n\}$ as well as all information about this sequence.

Of course, it can be generalized for a sequence $c_{\mathbf{n}}$ involving several indices that are arranged in a vector $\mathbf{n} \in \mathbb{N}_0^N$ [10]:

$$f(\mathbf{x}) \equiv \mathcal{T}_{\mathbf{n}}[c_{\mathbf{n}}](\mathbf{x}) = \sum_{\mathbf{n}} c_{\mathbf{n}} \prod_{r=1}^{N} x_r^{n_r}. \tag{2.2.3}$$

In order to define the concept of generating function with simple words, let us cite George Pólya [20]:

> *"A generating function is a device somewhat similar to a bag. Instead of carrying many little objects detachedly, which could be embarrassing, we put them all in a bag, and then we have only one object to carry, the bag."*

Therefore, instead of handling all terms of the sequence in a separate way, the generating function will allow us to have only one object to handle. Now that we have exposed it, we are going to show why such a tool is powerful and to motivate its use.

2.2.2 Motivation

In previous section, we gave a definition of the generating function and mentioned the concept of sequence that is linked to it. As we are dealing with Gaussian unitaries in the Fock basis and here interested in beam splitters, the beam splitter unitary of transmittance η expressed in state space [11] is:

$$U_\eta^{BS} = \exp\left[\theta\left(\hat{a}^\dagger \hat{b} - \hat{a}\hat{b}^\dagger\right)\right], \quad \text{where } \eta = \cos^2\theta. \tag{2.2.4}$$

We remind that the objective is to access, and then quantify, the transition probabilities in purpose to study quantum interferences phenomena. We use the following notation to define the transition amplitude between Fock states for the unitary (2.2.4):

$$b_n^{(i,k)} = \langle n, m| U_\eta^{BS} |i, k\rangle, \tag{2.2.5}$$

that we will not use much further in contrast with the transition probability which is as expected linked to the amplitude as follows:

$$B_n^{(i,k)} = \left|b_n^{(i,k)}\right|^2 = \left|\langle n, m| U_\eta^{BS} |i, k\rangle\right|^2. \tag{2.2.6}$$

From this definition, we see that the transition probabilities simply correspond to the matrix elements (or rather their squared moduli) of the unitary U_η^{BS} expressed in the Fock basis. Also, due to conservation of energy, index $m = i + k - n$ is redundant and thus not indicated. Equation (2.2.6) expresses then the probability of having n and m photons respectively exiting the beam splitter by first and second output modes when i and k photons have been sent respectively through first and second input modes. The corresponding situation is represented in figure 2.1.

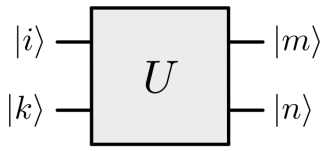

Figure 2.1: Two-mode network associated to the probability $B_n^{(i,k)}$.

Furthermore, conservation of energy imposes a condition on matrix elements. Indeed, all matrix elements are not permitted as:

$$\langle n,m|\, U_\eta^{BS}\, |i,k\rangle = 0 \text{ if } i+k \neq n+m. \tag{2.2.7}$$

Note that since the beginning, we have considered that the numbering of input and output modes is such that modes of corresponding number are linked by the path borrowed by a photon when this one is transmitted by the beam splitter. This is the reason why the i^{th} input and output modes are represented as diametrically opposed on figures 1.4, 1.5 and 2.1.

In order to show the usefulness of the generating function, let us show the analytical results expressing the transition amplitudes and probabilities between Fock states. As mentioned in the introduction, the derivation of these expressions is not included here but are available in the supplementary information section of [11]. Here we thus borrow the final results to expose it:

$$b_n^{(i,k)} = \sum_{m=\max(0,n-k)}^{\min(i,n)} (-1)^{i-m} \sqrt{\binom{i}{n}\binom{k}{m}\binom{n+m}{m}\binom{i-n+k-m}{i-n}}\, \eta^{2m+k-n}(1-\eta)^{i-2m+n}, \tag{2.2.8a}$$

$$B_n^{(i,k)} = \sum_{m,j=\max(0,n-k)}^{\min(i,n)} (-1)^{m+j} \binom{i}{m}\binom{k}{n-m}\binom{n}{j}\binom{i+k-n}{i-j}\, \eta^{k-n+m+j}(1-\eta)^{i+n-m-j}, \tag{2.2.8b}$$

where indices i, k, n and m still state the number of photons standing at the different input and output modes of the beam splitter.

Those two last equations are rather cumbersome. Working with these would not be convenient. This is the reason why we introduce the generating function as this one is much easier to manipulate and will also ensure to prove a relation that connects such probabilities i.e. the recurrence equations, that are the subject of an upcoming section.

When we presented the concept of generating function, we mentioned that it was associated to a sequence of numbers. Since we are concerned about the transition probabilities given by equation (2.2.6), the sequence to be considered here is nothing but the squared modulus of matrix elements of the unitary so the probabilities themselves. This way, we can adapt equation (2.2.3) in order to write the generating function of the transition probabilities of the beam splitter with transmittance η as:

$$f_\eta^{BS}(x,y,z,w) = \sum_{i,k,n,m} \overbrace{\left|\langle n,m|\, U_\eta^{BS}\, |i,k\rangle\right|^2}^{B_n^{(i,k)}} x^i y^k z^n w^m. \tag{2.2.9}$$

We end up with a four-variable generating function that encodes all of transition probabilities. The conventions used in the writing of equation (2.2.9) are depicted in figure 2.2.

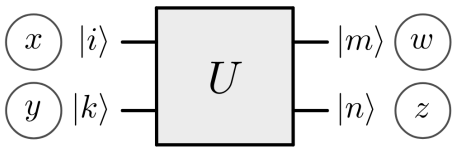

Figure 2.2: Definition conventions of $f_\eta^{BS}(x, y, z, w)$.

Finally, the obtained generating function of transition probabilities for a general (non-balanced) passive Gaussian unitary that is the beam splitter is:

$$f_\eta^{BS}(x, y, z, w) = \frac{1}{1 - \eta xz - (1-\eta)xw - \eta yw - (1-\eta)yz + xyzw}, \tag{2.2.10}$$

for a detailed derivation of how this follows from (2.2.9) we refer to [11].

It is from this function containing all the information about the transition probabilities that we are about to establish a relation that is easy to handle and that connects the probabilities to each other.

However, before establishing it let us have a look on the obtained generating function at equation (2.2.10). Among the terms included in the denominator let us especially observe each term from the second to the fifth included. Each term represents the different path possibilities of an incoming photon impinging on the beam splitter. For example, the term ηxz contains the transmittance coefficient as well as the indices linked to the first input and output modes. This first term thus stands for the situation where an incoming photon enters the beam splitter by its first input port (index x), is transmitted (η factor) and then goes out through the first output port (index z). The second term implies the same input but there the photon is reflected by the beam splitter ($1 - \eta$ factor) and exits by the second output (index w). The two next terms have similar interpretations but concern the second input of the beam splitter. The generating function thus accounts for the different scenarios that a photon can encounter when impinging on a beam splitter. But it also contains a last term that involves the scenario where two photons propagate through the beam splitter and leave it separately.

Until here, we focused exclusively on the situation where only two modes were involved. Next, we are going to see that the generating function formalism can of course be extended to an arbitrary number N of modes.

2.2.3 Generalization to N modes

In order to introduce the Hong-Ou-Mandel interferometric effect, we have worked with two modes. As we will work with a greater number of modes in the second part of this thesis, it is required to give the general formula allowing to obtain the generating function of the transition probabilities for a N-mode passive unitary. Those will be valuable to derive equations permitting the description of interferences phenomena in such N-mode passive unitaries.

Note that when N modes are considered, the transition probabilities (2.2.6) are now written:

$$B_{\mathbf{n}}^{(\mathbf{i})} = \left| \langle n_1, \ldots, n_N | \, U^{PI} \, | i_1, \ldots, i_N \rangle \right|^2, \tag{2.2.11}$$

with $\mathbf{i} = (i_1, \ldots, i_N) \in \mathbb{N}_0^N$, $\mathbf{n} = (n_1, \ldots, n_N) \in \mathbb{N}_0^N$ where $\mathbb{N}_0^N$ is the set of all natural numbers also including zero and U^{PI} is the N-mode passive interferometer unitary expressed in state space.

According to [10], the generating function extended to the N-mode case is written by means of the following formula (with PI standing for *passive interferometer*):

$$f^{PI}(\mathbf{x},\mathbf{z}) = \left(\sum_{m=0}^{N} (-1)^m \sum_{\alpha \in R_m^{(N)}} \sum_{\beta \in R_m^{(N)}} \left| \det\left[\mathrm{U}(\beta,\alpha) \right] \right|^2 \det\left[X(\alpha) \right] \det\left[Z(\beta) \right] \right)^{-1}, \quad (2.2.12)$$

where,

- X and Z are diagonal matrices with vectors $\mathbf{x}$ and $\mathbf{z}$ as diagonals respectively
- $\mathbf{x}$ and $\mathbf{z}$ are vectors standing for the variables associated respectively to inputs and outputs (e.g. see conventions in figure 2.2)
- $R_m^{(N)}$ is the set of all subsets of $\{1, 2, \ldots, N\}$ cardinality m
- $\mathrm{U}(\beta,\alpha)$ is the submatrix of U corresponding to the rows and columns whose indices belong to β and α respectively (furthermore, $\mathrm{U}(\alpha,\alpha)$ is written $\mathrm{U}(\alpha)$)

Notice that for each term, the sets α and β will always have the same cardinalities implying that the matrices $X(\alpha)$ and $Z(\beta)$ always have the same dimensions. In other words, there will always be as many variables characterizing the outputs z_j as there are variables characterizing the inputs x_i. Also, the matrix U governs the evolution of the mode operators in the phase space. In our case, this is none other than the N-order DFT matrix. The determinants of the square submatrices are denoted as *minors*.

The previous equation thus establishes the $2N$-variable generating function corresponding to order N. Naturally, the generating function derived at equation (2.2.10) for a beam splitter unitary can also be obtained using the general formula by setting $N = 2$.

Proof

For $N = 2$ we have $m \in \{0, 1, 2\}$, also

$$\mathbf{x} = (x, y), \quad \mathbf{z} = (z, w), \quad (2.2.13)$$

and

$$X = \begin{pmatrix} x & 0 \\ 0 & y \end{pmatrix}, \quad Z = \begin{pmatrix} z & 0 \\ 0 & w \end{pmatrix}. \quad (2.2.14)$$

Then from equation (2.2.12):

$$\begin{aligned} f^{PI}(x,y,z,w) = \Bigg[& \sum_{\alpha \in R_0^{(2)}} \sum_{\beta \in R_0^{(2)}} \left| \det\left[\mathrm{U}(\beta,\alpha) \right] \right|^2 \det\left[X(\alpha) \right] \det\left[Z(\beta) \right] \\ & - \sum_{\alpha \in R_1^{(2)}} \sum_{\beta \in R_1^{(2)}} \left| \det\left[\mathrm{U}(\beta,\alpha) \right] \right|^2 \det\left[X(\alpha) \right] \det\left[Z(\beta) \right] \\ & + \sum_{\alpha \in R_2^{(2)}} \sum_{\beta \in R_2^{(2)}} \left| \det\left[\mathrm{U}(\beta,\alpha) \right] \right|^2 \det\left[X(\alpha) \right] \det\left[Z(\beta) \right] \Bigg]^{-1}. \end{aligned} \quad (2.2.15)$$

Considering the values allocated to α and β:

$$\begin{aligned} f^{PI}(x,y,z,w) = \Big[1 \\ &- \left(\left|\det\left[\mathrm{U}(\beta,\alpha)\right]\right|^2 \det\left[X(\alpha)\right]\det\left[Z(\beta)\right]\right)\Big|_{\alpha=\{1\},\beta=\{1\}} \\ &- \left(\left|\det\left[\mathrm{U}(\beta,\alpha)\right]\right|^2 \det\left[X(\alpha)\right]\det\left[Z(\beta)\right]\right)\Big|_{\alpha=\{1\},\beta=\{2\}} \\ &- \left(\left|\det\left[\mathrm{U}(\beta,\alpha)\right]\right|^2 \det\left[X(\alpha)\right]\det\left[Z(\beta)\right]\right)\Big|_{\alpha=\{2\},\beta=\{1\}} \\ &- \left(\left|\det\left[\mathrm{U}(\beta,\alpha)\right]\right|^2 \det\left[X(\alpha)\right]\det\left[Z(\beta)\right]\right)\Big|_{\alpha=\{2\},\beta=\{2\}} \\ &+ \left(\left|\det\left[\mathrm{U}(\beta,\alpha)\right]\right|^2 \det\left[X(\alpha)\right]\det\left[Z(\beta)\right]\right)\Big|_{\alpha=\{1,2\},\beta=\{1,2\}}\Big]^{-1}. \end{aligned} \tag{2.2.16}$$

To go further, the matrix elements of U are written U_{ji} $(1 \leq j \leq N, 1 \leq i \leq N)$:

$$\begin{aligned} f^{PI}(x,y,z,w) = \big[1 &- \left|\mathrm{U}_{11}\right|^2 xz - \left|\mathrm{U}_{21}\right|^2 xw \\ &- \left|\mathrm{U}_{12}\right|^2 yz - \left|\mathrm{U}_{21}\right|^2 yw \\ &+ \left|\mathrm{U}_{11}\mathrm{U}_{22} - \mathrm{U}_{12}\mathrm{U}_{21}\right|^2 xyzw\big]^{-1}. \end{aligned} \tag{2.2.17}$$

By defining the unitary of a general beam splitter as:

$$\mathrm{U} = \begin{pmatrix} \sqrt{\eta} & \sqrt{1-\eta} \\ \sqrt{1-\eta} & -\sqrt{\eta} \end{pmatrix}. \tag{2.2.18}$$

Finally we obtain:

$$f^{PI}(x,y,z,w) = \left[1 - \eta xz - (1-\eta)xw - (1-\eta)yz - \eta yw + xyzw\right]^{-1}. \tag{2.2.19}$$

which, by reordering the terms, is exactly the generating function found in previous section at equation (2.2.10).

By proceeding the same way, we are able to construct the generating function for any number of modes N. Such higher order functions will be used in the second part of the thesis.

Now that the concept of generating function has been completely exposed, we can go forward towards the establishment of the relations linking the multiphoton transition probabilities among themselves in order to characterize quantum interferences. These are the recurrence relations that will reveal to be crucial in the rest of this work.

2.3 Recurrence relations

2.3.1 Shifting property

We are now about to derive the relations that will allow to access the multiphoton transition probabilities in a simple way with the generating function as a starting point. But before that, we still need to introduce a specific property of the latter that is the shifting property.

We express this shifting property as follows [10, 31]:

$$\mathcal{T}_n[c_{n+1}](x) = \frac{1}{x}(\mathcal{T}_n[c_n](x) - c_0), \tag{2.3.1}$$

whose proof is presented hereafter.

Proof

This proof comes from [10]. Let us consider a sequence $\{c_n\}$:

$$\begin{aligned}
\mathcal{T}_n[c_{n+1}](x) &= \sum_{n=0} c_{n+1}x^n \\
&= \frac{1}{x}\sum_{n=0} c_{n+1}x^{n+1} \\
&= \frac{1}{x}\sum_{n=1} c_n x^n \\
&= \frac{1}{x}\left(\sum_{n=0} c_n x^n - c_0\right) \\
&= \frac{1}{x}(\mathcal{T}[c_n](x) - c_0).
\end{aligned} \tag{2.3.2}$$

By use of the shift property, moving from the generating function to the corresponding recurrence relation will prove to be pretty simple.

2.3.2 Derivation from generating function

Now that all the pieces have fallen into position, we are finally ready to establish the announced relations. As for the generating function in previous section, we consider again the passive Gaussian unitary that is the beam splitter for illustrating the framework with ease.

To provide a clear reasoning, we take the liberty to remind the obtained expression of the generating function for such a unitary from equation (2.2.10):

$$f_\eta^{BS}(x,y,z,w) = \frac{1}{1-\eta xz-(1-\eta)xw-\eta yw-(1-\eta)yz+xyzw}. \tag{2.3.3}$$

From the shifting property just presented, we also synthesize:

$$\begin{aligned}
\{c_n\} &\longrightarrow f(x) = \sum_{n=0} c_n x^n, \\
\{c_{n-1}\} &\longrightarrow xf(x).
\end{aligned} \tag{2.3.4}$$

stating the association between a generating function $f(x)$ and a corresponding sequence $\{c_n\}$ [4]. The second line standing for the association of the generating function $xf(x)$ corresponding to the shifted sequence $\{c_{n-1}\}$.

Altogether, these elements allow us to derive the recurrence relation linking the transition probabilities for the beam splitter:

$$B_n^{(i,k)} = \eta B_{n-1}^{(i-1,k)} + (1-\eta)B_n^{(i-1,k)} + \eta B_n^{(i,k-1)} + (1-\eta)B_{n-1}^{(i,k-1)} - B_{n-1}^{(i-1,k-1)}. \tag{2.3.5}$$

Note that we are not considering a balanced beam splitter yet. This justifies the use of transmittance coefficient η in the expressions of this chapter until now.

Proof

Starting from the generating function for the transition probabilities of the beam splitter:

$$f_\eta^{BS}(x,y,z,w) = \frac{1}{1-\eta xz-(1-\eta)xw-\eta yw-(1-\eta)yz+xyzw}. \tag{2.3.6}$$

we then multiply the left side by the denominator and temporarily change the notation from $f_\eta^{BS}(x,y,z,w)$ to f_η^{BS} for the sake of clarity. By reorganizing terms:

$$f_\eta^{BS} = \eta xz f_\eta^{BS} + (1-\eta)xw f_\eta^{BS} + \eta yw f_\eta^{BS} + (1-\eta)yz f_\eta^{BS} - xyzw f_\eta^{BS} + 1. \tag{2.3.7}$$

We now see among the terms the same form as in equation (2.3.4) but for several variables. The shifting property can thus be applied, let us illustrate its use on the first term of the right-hand side. As previously we associate:

$$xz f_\eta^{BS}(x,y,z,w) \longrightarrow \{B_{n-1}^{(i-1,k)}\}. \tag{2.3.8}$$

The indices i and k associated respectively to variables x and z have been shifted. By applying the same process to the remaining terms, we end up with:

$$B_n^{(i,k)} = \eta B_{n-1}^{(i-1,k)} + (1-\eta)B_n^{(i-1,k)} + \eta B_n^{(i,k-1)} + (1-\eta)B_{n-1}^{(i,k-1)} - B_{n-1}^{(i-1,k-1)} + \delta_{i,0}\delta_{k,0}\delta_{n,0}\delta_{m,0}, \tag{2.3.9}$$

where we used the fact that we can also associate a generating function to the last term, indeed:

$$g(x,y,z,w) = \sum_{i,k,n,m} c_{i,k,n,m} x^i y^k z^n w^m = 1, \tag{2.3.10}$$

then the sequence $\{c_{i,k,n,m}\}$ associated to such a generating function is:

$$c_{i,k,n,m} = \delta_{i,0}\delta_{k,0}\delta_{n,0}\delta_{m,0}. \tag{2.3.11}$$

This latter term stands for defining some sort of an initial condition among transition probabilities. Indeed it imposes the condition $(i,k,n,m) = (0,0,0,0)$ to the whole equation (2.3.9), which makes the probability terms to account for a negative number of particles at some ports as some of their indices will be negative. As it is physically irrelevant, those probabilities then cancel. It then remains:

$$B_0^{(0,0)} = 1, \tag{2.3.12}$$

which is physically accurate since by sending no photons on the beam splitter we can only have vacuum coming out of it since the transformation is passive. In the future we will thus omit this last term as it is only significant when considering the vacuum transition.

Finally, the recurrence equation on transition proabilities is therefore:

$$B_n^{(i,k)} = \eta B_{n-1}^{(i-1,k)} + (1-\eta)B_n^{(i-1,k)} + \eta B_n^{(i,k-1)} + (1-\eta)B_{n-1}^{(i,k-1)} - B_{n-1}^{(i-1,k-1)}, \tag{2.3.13}$$

which is the result stated earlier.

2.3.3 Interpretation

Now that we have derived the recurrence relation for the beam splitter, we will take a closer look at it. At first glance it seems to be a fairly simple object, we will show that it is the case and that it is very convenient to manipulate in comparison with relations shown earlier in section 2.2.2. Also, this will allow to prove the Hang-Ou-Mandel effect in some other way. But before doing so, it seems adequate to interpret it.

The recurrence equation thus allows to compute the transition probability for an input pattern (i, k) of photons to a given output pattern (n, m). As it can be seen in the equation, this probability is expressed in terms of the beam splitter transmittance coefficient η and transition probabilities of situations involving reduced numbers of photons. We are about to see that such an equation gives rise to terms that should not appear in a classical description.

Once again, we rewrite the recurrence equation:

$$B_n^{(i,k)} = \underbrace{\eta B_{n-1}^{(i-1,k)} + (1-\eta) B_n^{(i-1,k)} + \eta B_n^{(i,k-1)} + (1-\eta) B_{n-1}^{(i,k-1)}}_{\text{classical behaviour}} - B_{n-1}^{(i-1,k-1)}. \tag{2.3.14}$$

By looking at the first four terms of the right-hand side, we notice that those depict the classical picture we would have of $B_n^{(i,k)}$ interpretation. Those components are represented below in figure 2.3, inspired from [10].

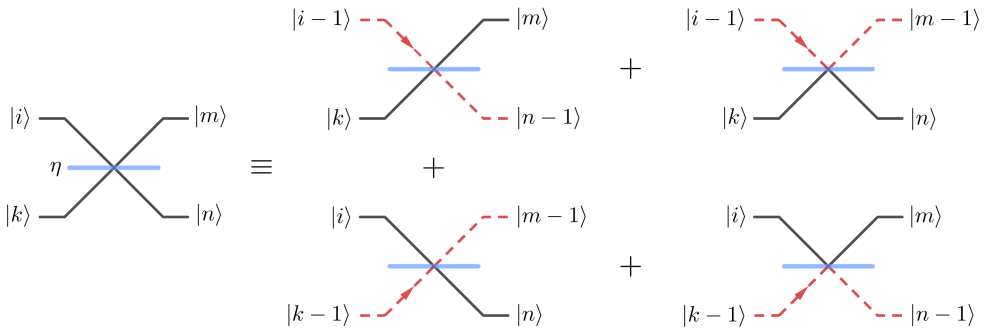

Figure 2.3: Classical components of recurrence equation for a beam splitter.

Indeed, these four terms do represent the different possible scenarios that a single photon could encounter when impinging on a beam splitter. These terms correspond to what we could obtain by performing a classical analysis of the beam splitter. In such an analysis, this would amount to consider the photons as being distinguishable and to be treated as balls of different colours that can end up in either exit with same probability. The classical picture would thus encourage to sum the probabilities of the different scenarios where the N^{th} photon has not yet reached the beam splitter [11], its trajectory being depicted by red dashed lines in figure 2.3, each multiplied by the corresponding transmission or reflection coefficient according to which path is undertaken by the photon. For instance, η must stand in front of $B_n^{(i,k-1)}$ as the photon is transmitted by the beam splitter. However we see that besides this classical component in the recurrence equation, there is also a fifth term.

We notice that unlike the other terms, this one has a negative coefficient. It therefore tends to decrease the transition probability under study and can then be associated to interferences that only occur in the quantum description. This last term may be considered like a *quantum interference suppression term* that is due to indistinguishability

of photons. Through the recurrence equation, the description then brings to light the quantum interferences effect.

Let us now consider again the specific case accounting for single photons at each input and output ports of the beam splitter so that $i = k = n = m = 1$. By replacing the corresponding values of the indices in the recurrence equation, this one becomes:

$$B_1^{(1,1)} = \eta B_0^{(0,1)} + (1-\eta)B_1^{(0,1)} + \eta B_1^{(1,0)} + (1-\eta)B_0^{(1,0)} - B_0^{(0,0)}, \tag{2.3.15}$$

where each of its classical component is represented in the figure 2.4 for this special case.

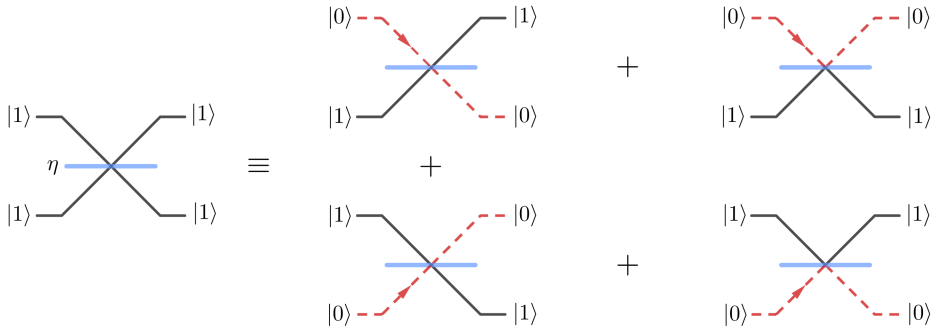

Figure 2.4: Classical specific case $i = k = n = m = 1$ for a beam splitter.

This situation gives rise to the standard Hong-Ou-Mandel effect presented at previous chapter. We recall that for a balanced beam splitter, this effect stated the impossibility of having any coincident detection of photons between the outputs as they both exit through the same output port. This effect can thus be exhibited thanks to the recurrence equation in terms of:

$$B_1^{(1,1)} = 0. \tag{2.3.16}$$

As stated earlier, it is impossible for single indistinguishable photons as inputs to exit the beam splitter separately.

Proof

Starting from the recurrence equation:

$$B_n^{(i,k)} = \eta B_{n-1}^{(i-1,k)} + (1-\eta)B_n^{(i-1,k)} + \eta B_n^{(i,k-1)} + (1-\eta)B_{n-1}^{(i,k-1)} - B_{n-1}^{(i-1,k-1)}. \tag{2.3.17}$$

And considering the specific case in which $i = k = n = m = 1$ we get:

$$B_1^{(1,1)} = \eta B_0^{(0,1)} + (1-\eta)B_1^{(0,1)} + \eta B_1^{(1,0)} + (1-\eta)B_0^{(1,0)} - B_0^{(0,0)}. \tag{2.3.18}$$

We can proceed to the identification of each term

$$B_0^{(0,1)} = \eta, \tag{2.3.19a}$$
$$B_1^{(0,1)} = 1-\eta, \tag{2.3.19b}$$
$$B_1^{(1,0)} = \eta, \tag{2.3.19c}$$
$$B_0^{(1,0)} = 1-\eta, \tag{2.3.19d}$$

to obtain:

$$B_1^{(1,1)} = \eta^2 + (1-\eta)^2 + \eta^2 + (1-\eta)^2 - 1, \tag{2.3.20}$$

where we have used equation (2.3.12). Then by considering a balanced beam splitter:

$$\begin{aligned} B_1^{(1,1)} &= \frac{1}{4} + \frac{1}{4} + \frac{1}{4} + \frac{1}{4} - 1 \\ &= 0. \end{aligned} \tag{2.3.21}$$

Note that there is another more general way to get this result. It invites us to exploit directly the recurrence rather than identifying its terms, which revealed to be simple specifically here but might become more challenging for a higher number N of modes.

A recurrence relation allows to express each term in terms of others. Provided an initial condition, it is then possible to determine the values of those terms. In our case, to find a certain transition probability associated to given input and output patterns, we have to inject its corresponding indices into equation (2.3.17). We illustrate this principle for the first right-handed term of (2.3.18), $B_0^{(0,1)}$.

$$\begin{aligned} B_0^{(0,1)} &= \eta B_{-1}^{(-1,1)} + (1-\eta) B_0^{(-1,1)} + \eta B_0^{(0,0)} + (1-\eta) B_{-1}^{(0,0)} - B_{-1}^{(-1,0)} \\ &= \eta B_0^{(0,0)} \\ &= \eta. \end{aligned} \tag{2.3.22}$$

Where we used equation (2.3.12) as initial condition and previous remark stating that negative number of particles has no physical meaning allowing us to drop concerned terms. By proceeding similarly for other terms, we find back results of equations (2.3.19) and finally end to the same result as previously found.

In the following we will study systems of order superior to two. In such cases, the complexity as well as the number of terms of such equations tend to rise rapidly. Although, thanks to the framework we presented here we will manage to exploit these equations.

2.3.4 Generalization to N modes

As for the generating function, it is possible to generalize the expression of recurrence relations to an arbitrary number of modes. The transition probabilities are still expressed by equation (2.2.11) and the following formula, also obtained in [10], allows to write the recurrence relation for N modes:

$$B_{\mathbf{n}}^{(\mathbf{i})} = \sum_{m=1}^{N} (-1)^{m-1} \sum_{\substack{\alpha \in R_m^{(N)} \\ \mathbf{i}_s \neq 0, s \in \alpha}} \sum_{\substack{\beta \in R_m^{(N)} \\ \mathbf{n}_r \neq 0, r \in \beta}} \left| \det \left[\mathrm{U}(\beta, \alpha) \right] \right|^2 B_{\mathbf{n}-\mathbf{1}_N^{(\beta)}}^{\left(\mathbf{i}-\mathbf{1}_N^{(\alpha)}\right)}, \tag{2.3.23}$$

where $\mathbf{1}_N^{(\alpha)}$ is defined as the vector of dimension N with ones at positions $j \in \alpha$ and zeros elsewhere, and $R_m^{(N)}$ has the same definition as in equation (2.2.12) for generalized generating function.

Thanks to this result we are able to write the recurrence relation of any order without the necessity of using the generating function. Also, let us mention that such a formalism enables to compute a probability by directly summing probabilities rather than amplitudes, which is usually the case.

Starting from the generating function we have introduced the recurrence equation allowing us to access the transition probabilities in a simple way and to realize that the concept of interferences is specific to the quantum case. Before concluding this chapter

we still need to introduce one last concept key concept we will need in the next part of this thesis and representative of a second way to compute transition probabilities. This is the permanent.

2.4 Permanent

2.4.1 Definition

The permanent [2, 18] of a square matrix is a matrix function that is similar to the determinant. The slight difference between the former and the latter is that the signatures associated to each permutation are all positive for the permanent while half of it are negative for the determinant. In other words, all negative terms appearing in the definition of the determinant are turned into positive terms. This formulation might sound simpler than for the determinant, however, computing the permanent turns out to be in general much more difficult.

Mathematically, the permanent of the $(n \times n)$-matrix $A = a_{ij}$ is defined as:

$$\operatorname{per} A = \sum_{\sigma \in S_n} \prod_{i=1}^{n} a_{i\sigma_i}, \tag{2.4.1}$$

where S_n is the group of permutations σ i.e. the permutations of $\{1, 2, \ldots, n\}$. For a given permutation σ, we call *diagonal* the product $\prod_{i=1}^{n} a_{i\sigma_i}$. The permanent can then also be defined as the sum of all diagonals of the matrix A [23].

As just said, such a seemingly simple difference between the determinant and the permanent makes this latter computationally harder. Indeed, no known algorithm can overcome this difference of complexity. In contrast to the determinant, that can be conveniently evaluated in polynomial time in the size of the matrix in question, no algorithm is able to compute the permanent in such time as such an object is characterized by exponential time complexity [30]. This is the reason why any discovery concerning evaluation or approximation of the permanent is thus interesting to complexity theory. But if the determinant is so easy to determine we could ask ourselves if there exists any transformation that would convert a permanent into it. Unfortunately, such a linear transformation on n-order matrices does not exist for $n \geq 3$ [16]. The simplification of the permanent is thus still an open problem.

2.4.2 Properties

Now that the concept of permanent has been introduced, it is adequate to present some of its properties [2] that we do not prove here. We consider the same matrix A as earlier.

1. Simultaneously left and right multiplying A by any n-order permutation matrices P and Q does not alter the permanent of A:

$$\operatorname{per} PAQ = \operatorname{per} A. \tag{2.4.2}$$

   The permanent of a matrix then does not change by permutation of its rows/columns in contrast with the determinant that alterns in sign at each permutation.

2. The permanent of A is invariant under transposition:

$$\operatorname{per} A^T = \operatorname{per} A. \tag{2.4.3}$$

3. If a whole n-order square matrix is multiplied by any factor c, its permanent is multiplied by this factor to the power of n:

$$\operatorname{per} cA = c^n \operatorname{per} A. \tag{2.4.4}$$

4. If A has a row/column filled with zeros, its permanent is zero.

5. If any row/column of A is multiplied by a factor c so is its permanent.

6. The permanent of a permutation matrix P of order n is equal to one:

$$\operatorname{per} P = 1. \tag{2.4.5}$$

   It is also the case for the identity matrix I.

7. If A results from the *direct sum* of matrices B and C then the permanent of A is equal to the product of the permanents of each matrix:

$$A = B \oplus C \Rightarrow \operatorname{per} A = \operatorname{per} B \times \operatorname{per} C. \tag{2.4.6}$$

   Note that the direct sum of an $(n \times m)$-matrix B and $(p \times q)$-matrix C results in a matrix of size $(n + p) \times (m + q)$:

$$B \oplus C = \begin{pmatrix} B & O \\ O & C \end{pmatrix}, \tag{2.4.7}$$

   where matrix O corresponds to the zero matrix with the appropriate dimension, as the top right matrix has a different dimension than the one in the bottom left.

8. The *Laplace expansion* for the permanent along a row/column is similar to the case of the determinant except that all terms are positive:

$$\operatorname{per} A = \sum_{j=1}^{N} a_{ij} \operatorname{per} A_{i,j} \quad \text{along a row,} \tag{2.4.8a}$$

$$\operatorname{per} A = \sum_{i=1}^{N} a_{ij} \operatorname{per} A_{i,j} \quad \text{along a column,} \tag{2.4.8b}$$

   where we defined $A_{i,j}$ as the matrix of order $N - 1$ acquired from matrix A by removing its i^{th} row and j^{th} column.

9. The permanent of the matrix that results from adding a multiple of a row/column of A to any other of its rows/columns can differ from the permanent of A. While the determinant is invariant to such operations the permanent is not, which is responsible of the difficulty of its evaluation [2].

Now that we have exposed different properties of the permanent, in the next section we are going to explain how it is related to interference phenomena that we are interested in for this thesis. In order to stay consistent with previous sections, we still work with the two-mode case. The generalization to a further number of modes does not represent any difficulty and is shown at the end of this section.

2.4.3 Relation with quantum interferences

In this work, we consider systems involving identical particles and more specifically bosons. The permanent is closely related to such systems. Indeed, we know from the first chapter that the quantum state of a system accounting for identical bosons must be symmetric with respect to permutation of particles. It turns out that the only combination of single particle functions that is completely symmetric corresponds to the permanent of these functions [30]. The permanent is thus a key element in the quantum statistical mechanics of identical bosons.

Previously, we stated that the transition probabilities for a beam splitter were given by the matrix elements of the unitary U_η^{BS} expressed in the Fock basis:

$$B_n^{(i,k)} = \left|\langle n,m|\, U_\eta^{BS}\, |i,k\rangle\right|^2. \tag{2.4.9}$$

From [23], the transition amplitudes can be linked to the permanent of a given matrix $\mathrm{M}[i,k|n,m]$ that we will define soon:

$$\langle n,m|\, U_\eta^{BS}\, |i,k\rangle = \frac{\operatorname{per}\mathrm{M}[i,k|n,m]}{\sqrt{i!k!n!m!}}, \tag{2.4.10}$$

we remind that U_η^{BS}, first given in equation (2.2.4), is expressed in state phase while $\mathrm{M}[i,k|n,m]$ is in phase space.

This last equation thus establishes the relation between the permanent associated to the matrix $\mathrm{M}[i,k|n,m]$ and the unitary transformation of multi-mode Fock states [23]. By taking the squared modulus of this expression, we find back the definition of the transition probabilities:

$$B_n^{(i,k)} = \frac{\left|\operatorname{per}\mathrm{M}[i,k|n,m]\right|^2}{i!k!n!m!}. \tag{2.4.11}$$

This proves that the transition probabilities can be computed in another way than with the recurrence equation thanks to the permanent of the matrix $\mathrm{M}[i,k|n,m]$.

Let us now define this matrix, which links the output modes to the input modes of the system according to their occupation. It is obtained by following this reasoning [25]:

- Start from the unitary transformation matrix linking input modes to output modes
- Repeat the first column i times and the second column k times (remove if zero index)
- Proceed identically for the rows based on indices n and m

As we consider passive components, the number of photons is conserved and the resulting matrix is thus square.

Then in the specific case of single photons at each port ($i = k = n = m = 1$) that interests us, we simply have to consider the DFT matrix and the equation (2.4.11) simplifies to the following expression for the transition probability:

$$B_1^{(1,1)} = \left|\operatorname{per}\mathrm{F}_2\right|^2, \tag{2.4.12}$$

as the denominator equals one.

Generalizing the writing of previous expressions for any order N is easy. By using the same notation as in equation (2.2.11) we get:

$$\langle n_1,\ldots,n_N|\, U^{BS}\, |i_1,\ldots,i_N\rangle = \frac{\operatorname{per}\mathrm{M}[i_1,\ldots,i_N|n_1,\ldots,n_N]}{\sqrt{i_1!\ldots i_N!n_1!\ldots n_N!}}, \tag{2.4.13}$$

then

$$B_{\mathbf{n}}^{(\mathbf{i})} = \frac{\left|\mathrm{per}\,\mathrm{M}[i_1,\ldots,i_N|n_1,\ldots,n_N]\right|^2}{i_1!\ldots i_N! n_1!\ldots n_N!}, \tag{2.4.14}$$

where the matrix $\mathrm{M}[i_1,\ldots,i_N|n_1,\ldots,n_N]$ is obtained following the same steps as above.

According to the dimension N of the balanced interferometers that we study in this thesis, the transition probability of a pattern involving one photon per port towards an output pattern of one photon per port simply resumes to the squared modulus of the permanent of the corresponding DFT matrix:

$$B_{\mathbf{n}}^{(\mathbf{i})} = \left|\mathrm{per}\,\mathrm{F}_N\right|^2. \tag{2.4.15}$$

We will make use of such an equation for transition probability computations in the following part of this thesis.

2.5 Conclusion

This chapter completes the first one in the presentation of all the concepts that will be necessary in the second part of this thesis, dedicated to the results, and therefore achieves this first part. While the first chapter focused on theoretical notions of quantum optics, this chapter dealt with the mathematical background that will be exploited next. We started by introducing the notion of generating function consisting in the starting point of the exposed formalism which then led to the establishment of recurrence equations. Those have allowed us to access the transition probabilities and to highlight the quantum character of interference effect by the presence of terms absent from a classical description. Finally, we have presented the matrix function that is the permanent and shown how it can be related to the domain of quantum interferences. This has shown that the transition probabilities can be computed in two different ways, thanks to the recurrence relations as well as the permanent. Also, let us insist on the fact that such a formalism allows to deal directly with probability sums rather than with amplitudes.

Part II

Results

Chapter 3

Comparison between classical and quantum transition probabilities

3.1 Motivation

In this chapter, we start the study of multi-photon quantum interferences. More specifically, we first focus on the transition probabilities associated to the generalization of the Hong-Ou-Mandel setup for more than two photons and more than two modes. This, in order to confront the classical case with the quantum case from a numerical perspective and to witness significant difference between them. Based on results from other work, such as for example the formulation of a *suppression law* stating which output patterns are not possible given an input pattern of one photon per mode [27, 28], we will go further in the description in the hope to have a better comprehensive understanding of such results. As previously shown, the quantum probabilities are intimately related to the permanent of the matrix linking occupied input modes to output modes. Then the difficulty of computing such probabilities comes down to the computation complexity of the permanent itself. To our knowledge, such a problem applied to the case of Fourier matrices has barely been addressed by the literature until now.

The chapter is divided in three parts. The first section of this chapter shows how classical transition probabilities can be computed considering one photon per input, we then remind the same computation method but for the quantum case thanks to the permanent. Thereafter we present a brief digression that is considering the permanent when it is applied to Fourier matrices. Thanks to some theorem [17], we manage to upper bound this permanent by one which supports its definition as transition probability when we take its square modulus. Also, we mention our attempt to facilitate the computation of this permanent by presenting a description available in appendix C. We then present the suppression law, and its derivation from [27], previously mentioned which corroborates the generalization of the Hong-Ou-Mandel effect in the even cases. In the following section, we present calculations of transition probabilities for both descriptions to the highest order that we are allowed to reach which will allow us to witness the evolution of those probabilities in function of the order N. We also present the code used to perform these calculations and some observations about the permanent we noticed during computations.

In this chapter, we refer to [17] and [27], from which we quote some results mentioned above that are respectively the theorem and the suppression law.

3.2 Probability computation

3.2.1 Classical case

Working in the classical situation is equivalent to consider particles that are distinguishable and noninterfering, and allows to apply simple combinatorics [27]. Having an input pattern of one particle per port, the probability to obtain any output pattern $\mathbf{n} = (n_1, \ldots, n_N)$ reads:

$$P_{cl}(\mathbf{n}) = \frac{1}{N^N} \frac{N!}{\prod_{j=1}^{N} n_j!}, \tag{3.2.1}$$

where we divide by the possible permutations within a same port.

Considering an output pattern of one photon per output, i.e. *coincident events*, then leads to the transition probability:

$$P_{cl} = \frac{N!}{N^N}, \tag{3.2.2}$$

this last result can easily be understood from figure 3.1, illustrating such configuration example for $N = 3$:

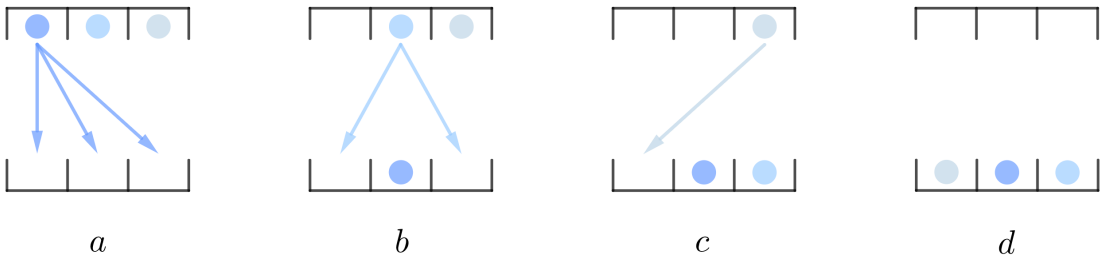

Figure 3.1: Steps of classical transition from one particle per input to one particle per output: initial state and possibilities of first particle (a); favorable possibilities of second particle (b); favorable possibility of last particle (c); final state (d).

Indeed starting from the initial state (Fig. 3.1a), the first particle has the liberty to go towards any available output port. Once it is fixed, the second particle has then two favorable possibilities (Fig. 3.1b) among the three ports. The last particle finally has only one remaining favorable possibility (Fig. 3.1c) to lead to the final state of one particle per port (Fig. 3.1d).

Classically, the transition probability towards coincident events for a third order system is thus:

$$P_{cl} = \frac{3}{3} \times \frac{2}{3} \times \frac{1}{3} = \frac{3!}{3^3} = \frac{2}{9} \tag{3.2.3}$$

This way of proceeding will be used in a next section to compute the classical probabilities to be faced with the quantum probabilities, whose calculation methods are recalled in the following.

3.2.2 Quantum case

This part constitutes a reminder of the results obtained in the last section of previous chapter concerning the transition probabilities computed in the quantum formalism. For the purpose of the section to be consistent with the writing used above for the classical

case, we will denote quantum probability by P_{qm}. Which implies to following equivalence between the writings:

$$P_{qm}(\mathbf{i}, \mathbf{n}) \equiv B_{\mathbf{n}}^{(\mathbf{i})}. \tag{3.2.4}$$

In previous chapter, we have obtained for the quantum transition probability the expression at equation (2.4.14):

$$B_{\mathbf{n}}^{(\mathbf{i})} = \frac{\left|\mathrm{per\,M}[i_1, \ldots, i_N | n_1, \ldots, n_N]\right|^2}{i_1! \ldots i_N! n_1! \ldots n_N!}. \tag{3.2.5}$$

In contrast with the classical case, the quantum probabilities do not have a calculation expression as simple as the former since the computation of those probabilities are related to the computation of a permanent.

Again, in the upcoming computations, we consider balanced interferometers described by the Fourier matrices of order N along with transitions from one photon per input port towards coincident events pattern. In this way, the quantum probabilities resume to the following expression:

$$P_{qm}(\mathbf{1}_N, \mathbf{1}_N) = \left|\mathrm{per\,F}_N\right|^2. \tag{3.2.6}$$

where $\mathbf{1}_N$ is defined as the vector of dimension N with ones at each position.

Since the complexity of the permanent computation scales unfavorably with the order N in the case of Fourier matrices, although mandatory to quantify the probabilities, we would rather try avoiding such calculation to determine which transitions are possible and which are not. This motivation has lead to the derivation of a law presented below that would make it easy to determine.

3.2.3 Permanent applied to Fourier matrices

We deviate here a little from the main topic of this thesis that are quantum interferences but we approach a problem that is closely related to it. In this section, we focus on the permanent of unitaries that are the discrete Fourier transform matrices. We have already stated that computing the permanent of such matrices is a difficult issue, though we know almost nothing about it when applied to the DFT. However, thanks to a theorem from [17], it is possible to show that the permanent of a Fourier matrix is upper bounded by one. We start from the theorem:

$$\left|\mathrm{per}\,(AB)\right|^2 \leq \mathrm{per}(AA^\dagger).\,\mathrm{per}(B^\dagger B), \tag{3.2.7}$$

then by taking the matrices A and B respectively as Fourier matrix F_N and identity matrix I in previous equation, we get:

$$\left|\mathrm{per}\,(\mathrm{F}_N\mathrm{I})\right|^2 \leq \mathrm{per}(\underbrace{\mathrm{F}_N\mathrm{F}_N^\dagger}_{=\mathrm{I}})\,\mathrm{per}(\underbrace{\mathrm{I}^\dagger\mathrm{I}}_{=\mathrm{I}}), \tag{3.2.8}$$

due to the fact that Fourier matrices are unitary matrices, to the properties of identity matrix and thanks to properties 1 and 6 from section 2.4.2. We finally get:

$$\left|\mathrm{per\,F}_N\right|^2 \leq 1, \tag{3.2.9}$$

which proves that the permanent of a Fourier matrix of order N is upper bounded. Furthermore, this last equation shows that the squared modulus of such a permanent is bounded by one. We thus retrieve the definition of a probability which can not be higher than one.

In the hope to facilitate the computation of the permanent when applied to the DFT, we also have attempted to simplify it. This has led to the establishment of a mathematical description based on the approximation of limited expansion and that is presented in appendix C. Unfortunately, such an attempt revealed to be unsuccessful.

3.2.4 Suppression law

As we mentioned in the introduction of this chapter, we are going to use some results previously obtained in other works. This law is one of them and is originally derived and proved in [27] for DFT matrices. In order to establish it, the vector $\mathbf{d}$ associated to a given output pattern $\mathbf{n}$ is introduced. This vector has N components specifying the output ports occupied by each particle. To build it we concatenate n_j times the j^{th} port number:

$$\mathbf{d} = \oplus_{j=1}^{N} \oplus_{k=1}^{n_j} (j). \tag{3.2.10}$$

Let us illustrate its use by an example over the output of coincident events for $N = 5$. In such a case, we have $\mathbf{n} = (1, 1, 1, 1, 1)$ and thanks to (3.2.10) the corresponding vector is thus $\mathbf{d} = (1, 2, 3, 4, 5)$. This vector can then be used in order to define a suppression law allowing to determine which events are possible without having to calculate any permanent. Such of a law establishes the impossibility of transition towards output patterns $\mathbf{n}$ whose sum of components of the associated vector $\mathbf{d}$ is not dividable by N:

$$Q(\mathbf{n}) := \mathrm{mod}\left(\sum_{l=1}^{N} d_l(\mathbf{n}), N\right) \neq 0 \Longrightarrow P_{qm}(\mathbf{i}, \mathbf{n}) = 0. \tag{3.2.11}$$

From this suppression law, we notice some important results by focusing on coincident events. Indeed, a significant difference arises according to the parity of the order N considered. The suppression law is effective for coincident events in cases where the order N is even. This can be easily shown mathematically as for such cases:

$$\mathbf{d} = (1, 2, \ldots, N) \text{ involves that } \sum_{l=1}^{N} d_l(\mathbf{n}) = \frac{N(N+1)}{2}, \tag{3.2.12}$$

which is not dividable by N when N is even, and then makes that $Q(\mathbf{n})$ differs from zero, implying a zero transition probability.

This then proves the generalization of the Hong-Ou-Mandel to any even dimension. According to the definition of quantum transition probabilities and following from this suppression law, we can interpret this conclusion from a mathematical point of view in terms of the permanent. From this result, the fact that the probability is zero comes from the fact that the permanent of Fourier transform matrix of even dimension vanishes. Such a remarkable result was already proved in [14] and the suppression law developed in [27] supports this outcome.

As this represents an important result for this thesis, we present its demonstration.

Proof

This proof comes from [14]. It consists in deriving the condition of cancellation for transition probability from one photon per input towards coincident events when we consider even-order Fourier interferometers.

The condition to prove the impossibility of coincident events resides in proving that the transition probability equals zero:

$$P_{qm}(\mathbf{1}_N, \mathbf{1}_N) = |\mathrm{per}\, \mathrm{F}_N|^2 = 0, \tag{3.2.13}$$

which boils down to prove that the permanent of the Fourier matrix vanishes (for clarity, we omit the dimensional index N in the following of this proof). To do so, we

have to show that F has certain symmetry causing it in some cases. For this purpose, we multiply the matrix F by the diagonal matrix Λ whose elements are:

$$\Lambda_{jk} \equiv \omega_N^{j-1}\delta_{jk}. \tag{3.2.14}$$

We thus obtain the matrix ΛF with:

$$\begin{aligned}(\Lambda\mathrm{F})_{ji} &= \sum_{k=1}^{N}\Lambda_{jk}\mathrm{F}_{ki} \\ &= \Lambda_{jj}\mathrm{F}_{ji} \\ &= \frac{1}{\sqrt{N}}\omega_N^{(j-1)i}.\end{aligned} \tag{3.2.15}$$

Thanks to the modulus function $\mathrm{mod}_N(x)$, matrix elements of ΛF can be expressed:

$$(\Lambda\mathrm{F})_{ji} = \frac{1}{\sqrt{N}}\omega_N^{(j-1)(\mathrm{mod}_N(i)+1-1)}, \tag{3.2.16}$$

since $\omega_N^N = \omega_N^0 = 1$.

We can then simplify the exponent by means of function $\tilde{\sigma}(i) = \mathrm{mod}_N(i) + 1$ which maps the elements of $\{1, 2, \ldots, N-1, N\}$ respectively to the list $\{2, 3, \ldots, N, 1\}$. Comparing this with equation (1.3.23) allows to write:

$$(\Lambda\mathrm{F})_{ji} = \mathrm{F}_{j\tilde{\sigma}(i)} \tag{3.2.17}$$

Multiplying the matrix F by matrix Λ therefore results in a cyclic permutation of the columns of F. Such a permutation does not affect the permanent of a matrix as it is symmetric to cyclic permutations, we thus obtain:

$$\mathrm{per}\,\mathrm{F} = \mathrm{per}(\Lambda\mathrm{F}), \tag{3.2.18}$$

where the right-handed term can also be written:

$$\mathrm{per}(\Lambda\mathrm{F}) = \mathrm{per}\,\Lambda\,\mathrm{per}\,\mathrm{F}, \tag{3.2.19}$$

since Λ is a diagonal matrix, whose permanent is given by:

$$\begin{aligned}\mathrm{per}\,\Lambda &= \prod_{k=1}^{N}\omega_N^{k-1} \\ &= \omega_N^{\sum_{k=1}^{N}k} \\ &= \omega_N^{N(N+1)/2} \\ &= e^{-i\pi(N+1)},\end{aligned} \tag{3.2.20}$$

following the definition (1.3.20).

Finally, we obtain for the permanent of Λ:

$$\mathrm{per}\,\Lambda = \begin{cases} 1, & \text{for } N \text{ odd}\ , \\ -1, & \text{for } N \text{ even}\ . \end{cases} \tag{3.2.21}$$

By comparing the equations (3.2.18) and (3.2.21) for the case of N being even:

$$\operatorname{per} \mathrm{F} = -\operatorname{per} \mathrm{F}, \tag{3.2.22}$$

which finally sets that:

$$\operatorname{per} \mathrm{F} = 0. \tag{3.2.23}$$

It is then impossible to observe coincident events in the case of an even number of photons and modes.

The Hong-Ou-Mandel effect can thus be generalized to any Fourier interferometer provided that it accounts for an even number of particles sent separately through the same number of modes. This is not the case for setups under the same conditions but with N odd, indeed, we will see through calculations of transition probabilities that the realization of coincident events is not impossible for such situations. However, note that reaching the manifestation of the Hong-Ou-Mandel effect in the odd case is achievable, at least for three modes, by considering a different setup. Indeed, what we have described here applied to the specific case of balanced interferometers corresponding to specific unitaries that are represented by the Fourier transform matrices presented in the first chapter. As an example we cite [3] stating that the Hong-Ou-Mandel effect could be observed for a biased interferometer in the case of $N = 3$.

Next, we compute numerical values of transition probabilities in classical and quantum cases as far as possible. The limit of this calculations being imposed by the complexity of the Fourier permanent. We will then be able to compare classical and quantum transition probabilities towards coincident events and witness the quantum behaviour with N.

3.3 Numerical computation

3.3.1 Behaviour related to number of modes

We then know how to calculate the transition probabilities whether in the classical case or in the quantum case. In this section, we evaluate such probabilities. While computing the classical probabilities does not lead to any limitation, this is not the case for the computation of the permanent. Thanks to Mathematica, we managed to reach the 23^{rd} order. The results obtained numerically are displayed at table A.1 while table A.2 shows the exact values in form of fractions. These table are available in appendix A.

Numerically the obtained results match with what we explained above, that is probabilities are zero when we consider the transition between one photon per input towards one photon per output in any case where N is even:

$$P_{qm}(\mathbf{1}_N, \mathbf{1}_N) \equiv B_{\mathbf{1}_N}^{(\mathbf{1}_N)} = 0, \quad \text{for } N \text{ even.} \tag{3.3.1}$$

The interferometric suppression effect encountered in the traditional Hong-Ou-Mandel effect due to the quantum indistinguishability of photons is thus well generalized to any even dimension. This does not apply for odd cases as the corresponding transition probabilities do not vanish. The nature of quantum interferences is then determined by the parity of the order N. This results in the emergence of an *even-odd* effect stating that the quantum interferences in the even cases are of a fully destructive nature tending to cancel the transition probability while the odd cases shows interferences constructive or destructive depending on the order. We will come back to this last point very soon. If the interferometric effect of the second order is perfectly known through the Hong-Ou-Mandel

effect we do not however have such a comprehension of interferences occurring for higher orders. We would like to have a comprehension of such destructive and constructive effects to be as clear as for the Hong-Ou-Mandel effect, that is the purpose of the following chapters.

Let us now focus our attention on the behaviour of the transition probabilities as a function of the dimension N as depicted in figure 3.2 where we plotted until order 10 due to the smallness of further values. The dashed lines stands for eye-guiding only. The classical probabilities are governed by $N!/N^N$ whose asymptotic behaviour is known to decrease exponentially. This implies the probability of having one particle per output port to highly decreases as the number of output arrangements rises sharply. On the other hand quantum evolution reveals itself to be more interesting about odd cases. As for the classical behaviour we might have expected that the probabilities keep evolving in a decreasing way. However, we first see that by comparing the transition probabilities corresponding to the 5^{th} and 7^{th} order this assumption does not hold. Indeed, quantum transition probability of the 7^{th} order reveals to be higher than the one corresponding to order 5. Such an event occurs again between orders 9 and 11 and between orders 15 and 17. It thus happens that the transition towards coincident events can be enhanced by passing from an odd order to the next one, which sounds counterintuitive. Given the behaviour of the first odd quantum probabilities depicted in figure 3.2, we first thought that such values would adopt an oscillation pattern around the classical behaviour. Nevertheless, computing further values revealed it to not be the case.

Since the smallness of quantum values from 8^{th} order does not permit any visibility on a graph, we should dispose of another way to witness the particularity of the quantum behaviour in a more visible way over a wider range of orders. For this purpose, we introduce the concept of *quantum enhancement* which is the ratio of quantum-to-classical transition probability [27], in following equation we omit port vectors $\mathbf{i}$ and $\mathbf{n}$ for clarity:

$$\mathcal{E} = \frac{P_{qm}}{P_{cl}}. \tag{3.3.2}$$

The behaviour of the latter is depicted for odd dimensions only in figure 3.3. There again, some observations exhibit the unexpected behaviour of the quantum probabilities. Above, we mentioned the fact that odd quantum probabilities might be destructive or constructive with respect to classical probabilities, this is expressed through the quantum enhancement as it is the ratio of occurrence probabilities. It allows to characterize the constructive or destructive character of the quantum probability in regard to the classical one. Stating an enhancement higher than one means that this transition is favored in the quantum case thus promoting the constructive nature of interferences. In contrast, an enhancement lower than one implies a less favored quantum transition. We see that $\mathcal{E}$ is constantly varying across the dimensions showing that for some of them, the classical realization of coincident events is more probable to occur than its quantum counterpart whereas the opposite situation is also possible for other dimensions. Especially, we see that the order 13 is the most favored of all while the following order is the least one. According to this figure, no periodic structure in its appearance is observable although it might be the case for higher orders. Being limited by the complexity of calculating permanents, we are currently not in measure to go further to verify this assumption.

The behaviour of quantum transition probabilities thus distinguishes from classical ones by those last particularities.

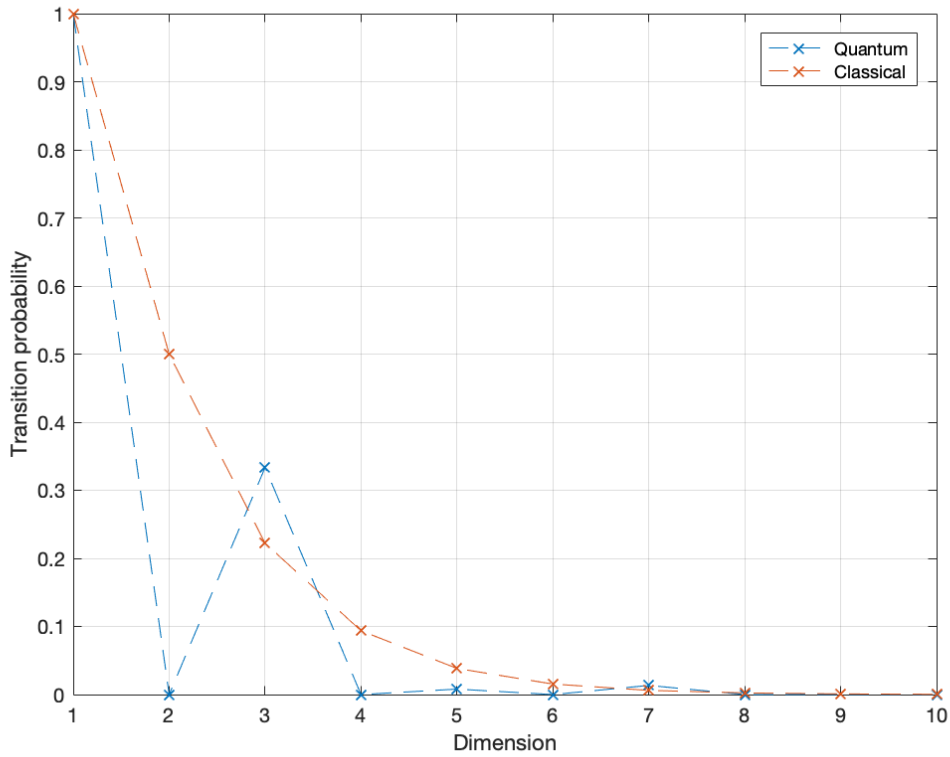

Figure 3.2: Classical (orange) and quantum (blue) transition probabilities behaviours with dimension (N).

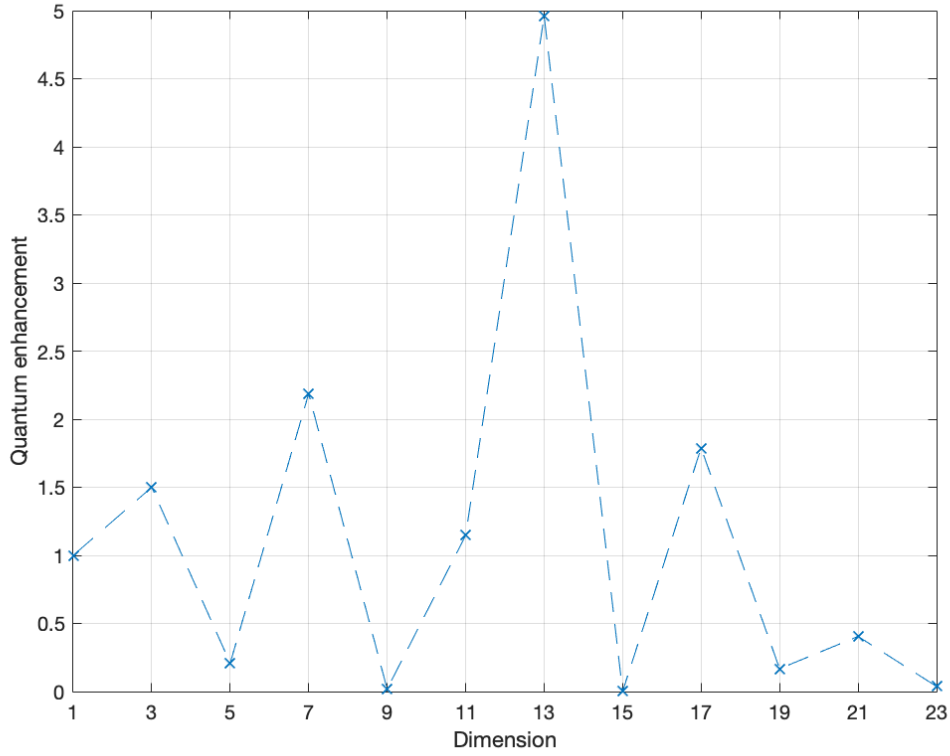

Figure 3.3: Quantum enhancement ($\mathcal{E}$) behaviour with dimension (N) for odd cases only.

3.3.2 Computation code

As already mentioned, the numerical results previously presented have been computed thanks to Mathematica. This computing system disposes of its own function allowing to compute the permanent. However, such a method revealed to become quickly inefficient while the order N rose. This motivated to establish a more effective way to compute the permanents. It could be achieved thanks to the code presented in appendix B.

The strategy behind this code is the following. As the computation complexity scales exponentially with the considered order, reducing the order of the matrix constituted then an advantage allowing to facilitate the computations. To reduce the order of the matrix, we apply the Laplace expansion along its first row following equation (2.4.8a). The permanent we want to calculate then resumes to the sum of permanents of order $N-1$ *submatrices* weighted by the elements of the first row of initial matrix that are all $1/\sqrt{N}$ as we consider Fourier matrices. The code then returns as a list the computed results of the N *subpermanents* from the submatrices arising from the Laplace expansion.

From the numerical values returned by the code, we observe interesting facts. Firstly, whatever the order N considered, every subpermanent is real implying then the permanent to be also real. Given the fact that the Fourier matrices are complex matrices, this is unexpected. Secondly and most importantly, we notice that subpermanents for a given order are all equal in absolute value whatever the parity of the order N. However in terms of signs, we observe a distinction between odd and even orders. Indeed, in the case of an odd order all the subpermanents have the same sign and as just said have the same value. In contrast, in the even cases they have the same absolute value but alternate in sign. From this outcome, we then understand why in the even case the permanent vanishes. The Laplace expansion allows to see that it is due to the fact of summing subpermanents of opposite signs that thus cancel each other. A particular case rises for the orders six and twelve as for those precise orders, all subpermanents are null. The statement about the values of the subpermanents in the odd and even cases can be easily demonstrated at low orders. Given that the demonstration for the general case at order N could not be achieved we however propose such a demonstration for the orders three and four.

Proof

We first consider $N=3$. For clarity, we next omit here the index N in the definition of ω_N as well as the square root factor appearing in the definition of the Fourier matrices. By applying the Laplace expansion to the first row of the DFT matrix it comes:

$$\begin{aligned}\operatorname{per}\begin{pmatrix}1 & 1 & 1\\ 1 & \omega & \omega^2\\ 1 & \omega^2 & \omega^4\end{pmatrix} &= 1.\operatorname{per}\begin{pmatrix}\omega & \omega^2\\ \omega^2 & \omega^4\end{pmatrix} + 1.\operatorname{per}\begin{pmatrix}1 & \omega^2\\ 1 & \omega^4\end{pmatrix} + 1.\operatorname{per}\begin{pmatrix}1 & \omega\\ 1 & \omega^2\end{pmatrix}\\ &= [\omega^5+\omega^4]+[\omega^4+\omega^2]+[\omega^2+\omega]\\ &= [\omega^2+\omega]+[\omega+\omega^2]+[\omega^2+\omega].\end{aligned} \tag{3.3.3}$$

Where we have used the property (1.3.21a) of ω. The obtained subpermanents are thus all equal.

Then, for $N=4$, by proceeding the same way than above we obtain:

$$\begin{aligned}\operatorname{per}\begin{pmatrix}1 & 1 & 1 & 1\\ 1 & \omega & \omega^2 & \omega^3\\ 1 & \omega^2 & \omega^4 & \omega^6\\ 1 & \omega^3 & \omega^6 & \omega^9\end{pmatrix} &= 1.\operatorname{per}\begin{pmatrix}\omega & \omega^2 & \omega^3\\ \omega^2 & \omega^4 & \omega^6\\ \omega^3 & \omega^6 & \omega^9\end{pmatrix} + 1.\operatorname{per}\begin{pmatrix}1 & \omega^2 & \omega^3\\ 1 & \omega^4 & \omega^6\\ 1 & \omega^6 & \omega^9\end{pmatrix}\\ &\quad + 1.\operatorname{per}\begin{pmatrix}1 & \omega & \omega^3\\ 1 & \omega^2 & \omega^6\\ 1 & \omega^3 & \omega^9\end{pmatrix} + 1.\operatorname{per}\begin{pmatrix}1 & \omega & \omega^2\\ 1 & \omega^2 & \omega^4\\ 1 & \omega^3 & \omega^6\end{pmatrix}\\ &= [\omega^2+\omega^3+\omega^3+\omega^2+\omega+\omega] + [\omega+1+\omega+\omega^3+1+\omega^3]\\ &\quad + [\omega^3+\omega^3+\omega^2+\omega+\omega+\omega^2] + [1+\omega+\omega+1+\omega^3+\omega^3].\end{aligned} \tag{3.3.4}$$

By looking closely at these four subpermanents, we notice that the first and the third ones are equal to the second and fourth multiplied by ω^2. Again, by use of (1.3.21a) it comes:

$$\begin{aligned}[\omega^2+\omega^3+\omega^3+\omega^2+\omega+\omega] &= [\omega^2+\omega^3+\omega^3+\omega^2+\omega^5+\omega^5]\\ &= \omega^2.[1+\omega+\omega+1+\omega^3+\omega^3]\\ &= -[1+\omega+\omega+1+\omega^3+\omega^3],\end{aligned} \tag{3.3.5}$$

because $\omega^2 = -1$ for $N = 4$, which leads these subpermanents to cancel each other resulting in a null permanent for the even case.

Once we noticed the behaviour of the values taken by the subpermanents, we can then speed up the code calculation by asking it to calculate and display only the first subpermanent. This way, we managed to obtain values until the order twenty-three. The permanent can then easily be computed from this subpermanent as:

$$\operatorname{per} \mathrm{F}_N = N\frac{1}{\sqrt{N}}\operatorname{per} \mathrm{F}_{1,1}, \quad \text{for } N \text{ odd}\ , \tag{3.3.6}$$

where we defined $\mathrm{F}_{1,1}$ as in equations (2.4.8).

3.4 Conclusion

We first reminded how to compute transition probabilities in the classical and then the quantum description. The former is based on simple combinatorics while the latter depends on a permanent computation. We then presented a digression about the permanent of Fourier matrices, there we showed an upper bound to it and also presented an attempt to facilitate its computation but which revealed to be unsuccessful. Also we exposed results which do not come from this work but were relevant to be mentioned, as the suppression law which supports the generalization of the Hong-Ou-Mandel effect for any even dimension. Especially, we have shown the proof for impossibility of having coincident events in the even cases that resulted from the vanishing permanent of Fourier matrices of corresponding even orders N. This allowed to witness the nature of quantum interferences according to the parity of the order under consideration to be fully destructive for even cases and destructive or constructive for odd cases. We have then explicitly calculated the numerical values for such probabilities to have a visual overview of their behavior with dimension N and to realize the apparently irregular character of quantum case. This has then lead to some discoveries about the subpermanents of the DFT matrix.

Chapter 4

Analysis for low-order interferometers through recurrence relations

4.1 Motivation

Although we have shown that there exist some significant differences between the behaviour of the classical and quantum transition probabilities, as the irregular behaviour of quantum probabilities and enhancement with the dimension, we still lack of a comprehensive understanding of quantum interferences. Nowadays, the paradigm of interferometric suppression effect due to the indistinguishability of the two photons that is the Hong-Ou-Mandel effect is well-known, whereas we do not have such a clear interpretation of its generalization to higher even orders resulting in the cancellation of transition probabilities nor for odd orders characterized by non-vanishing probabilities. Indeed, we still wonder what leads to such interferometric phenomena. Across this chapter, we make use of the formalism presented in the first part of this thesis based on notions of generating function and recurrence relation in order to enlighten and have a better understanding of constructive and destructive multi-photon quantum interferences. Especially, as the expressions will reveal to become quickly heavy to handle due to the rising number of terms when N grows, we will focus on low orders that are the third and fourth orders which represent the first interesting cases to not have been studied yet.

To begin this chapter we briefly remind the results proper to the Hong-Ou-Mandel effect, i.e. the generating function as well as the recurrence relation corresponding to the specific case of having one photon per output of a balanced beam-splitter. Afterwards, by applying the same reasoning that led to these latter we show the generating functions and the recurrence equations for Fourier interferometers having three and four modes. Thanks to the recurrences, we will check that they return the same probability values than those computed in previous chapter, proving once again the consistence of such a formalism. Also, we will present some observations made about the structure of such recurrence equations that we assume to be valid for any order N, as some could not be rigorously proved. Finally, we will propose some simplifications of the recurrences in order to be able to determine what is the *story* of the photons and to express the elements constituting the recurrence in terms of simpler *scenarios* to highlight the constructive or destructive nature of quantum interferences. This will facilitate their interpretations afterwards.

In this chapter, we refer to [10] as the covered results proper to the balanced beam splitter were first derived and obtained in it.

4.2 Hong-Ou-Mandel effect

4.2.1 General beam splitter

In the second chapter, we have presented the mathematical tools allowing us to describe and study passive interferometers. Especially, we illustrated such formalism by applying it to the case of the general two-mode interferometer [10]. We remind here these results previously established. For such a setup, the obtained generating function was:

$$f_{\eta}^{BS}(x,y,z,w) = \frac{1}{1-\eta xz-(1-\eta)xw-\eta yw-(1-\eta)yz+xyzw}, \tag{4.2.1}$$

which, by means of the shifting property, allowed to lead to the corresponding recurrence relation:

$$B_n^{(i,k)} = \eta B_{n-1}^{(i-1,k)} + (1-\eta)B_n^{(i-1,k)} + \eta B_n^{(i,k-1)} + (1-\eta)B_{n-1}^{(i,k-1)} - B_{n-1}^{(i-1,k-1)}, \tag{4.2.2}$$

4.2.2 Balanced beam splitter

As the Hong-Ou-Mandel effect arises for an unbiased beam splitter, the generating function becomes:

$$f_{1/2}^{BS}(x,y,z,w) = \left[1-\frac{1}{2}xz-\frac{1}{2}xw-\frac{1}{2}yw-\frac{1}{2}yz+xyzw\right]^{-1}. \tag{4.2.3}$$

In the study of the transition probability for an input pattern that consists in one photon per port towards an output pattern of one photon per port, the recurrence relation became:

$$B_1^{(1,1)} = \frac{1}{2}B_0^{(0,1)} + \frac{1}{2}B_1^{(0,1)} + \frac{1}{2}B_1^{(1,0)} + \frac{1}{2}B_0^{(1,0)} - B_0^{(0,0)}. \tag{4.2.4}$$

Such an equation enables to highlight the Hong-Ou-Mandel effect in terms of transition probabilities. Indeed, a balanced beam splitter makes equiprobable for a photon to undergo reflexion or transmission. By considering this and the definition of the last term as an initial condition implying vacuum at the input and the output:

$$B_0^{(0,1)} = B_1^{(0,1)} = B_0^{(1,0)} = B_1^{(1,0)} = \frac{1}{2}, \quad \text{and } B_0^{(0,0)} = 1, \tag{4.2.5}$$

this leads to the cancellation of the right-hand side:

$$B_1^{(1,1)} = 0, \tag{4.2.6}$$

stating the impossibility of having coincident events at outputs of the setup by sending one photon in each input.

The analysis of such relations in the case of the two-mode interferometer reveals to be quite simple as it only has a reduced number of terms. Especially, the quantum destructive nature of the interferences was brought to light through the last term, with a negative sign, whose scenario would not appear in a classical description as already seen in chapter 2. Such a term is due to the indistinguishability of the two photons involved in the experiments. We will see next that each recurrence contains such of a term standing for the vacuum propagation. Also, from the recurrence equation applied to the specific case of one photon per port, we notice that the recurrence can be decomposed in two blocks. Each containing transition probabilities involving a different number of photons, we will come back to it later.

Afterwards, we focus on interferometers involving first three then four modes in order to lead the same kind of analysis to acquire a better understanding of quantum interferometric effects in each case.

4.3 Study of low-order interferometers

4.3.1 Third order interferometer

In order to obtain the generating function for a greater number of modes, we can simply use equation (2.2.12) by setting, in this case, $N = 3$. The unitary to consider here is of course the third-order DFT matrix obtained from (1.3.19). Also, we adapt the vectors for labelling the input and output ports variables by writing:

$$\mathbf{x} = (x_1, x_2, x_3), \quad \mathbf{z} = (z_1, z_2, z_3), \tag{4.3.1}$$

such conventions used in the definition of the generating function of the tritter are depicted by figure 4.1.

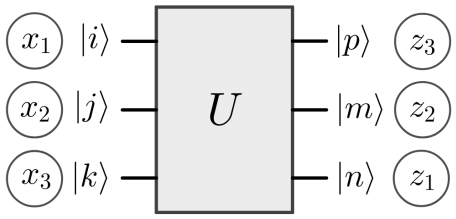

Figure 4.1: Conventions associated to the three-mode interferometer.

As the method to derive the generating function is strictly similar to the example in section 2.2.3 applied to two modes, we do not demonstrate its derivation. We then obtain:

$$\begin{aligned} f^{PI}(\mathbf{x}, \mathbf{z}) = \; & [1 - \frac{1}{3}(x_1z_1 + x_1z_2 + x_1z_3 + x_2z_1 + x_2z_2 + x_2z_3 + x_3z_1 + x_3z_2 + x_3z_3) \\ & + \frac{1}{3}(x_1x_2z_1z_2 + x_1x_2z_1z_3 + x_1x_2z_2z_3 \\ & + x_1x_3z_1z_2 + x_1x_3z_1z_3 + x_1x_3z_2z_3 \\ & + x_2x_3z_1z_2 + x_2x_3z_1z_3 + x_2x_3z_2z_3) \\ & - x_1x_2x_3z_1z_2z_3]^{-1}. \end{aligned} \tag{4.3.2}$$

As already said, the number of terms is significantly larger than in the two-mode case.

By using the shifting property applied to this generating function, it results in the following recurrence relation. Again, we do not prove such a result as it follows the same method as performed with two modes:

$$\begin{aligned} B_{n,m}^{(i,j,k)} = \; & \frac{1}{3}\Big[B_{n-1,m}^{(i-1,j,k)} + B_{n,m-1,}^{(i-1,j,k)} + B_{n,m}^{(i-1,j,k)} \\ & + B_{n-1,m}^{(i,j-1,k)} + B_{n,m-1}^{(i,j-1,k)} + B_{n,m}^{(i,j-1,k)} \\ & + B_{n-1,m}^{(i,j,k-1)} + B_{n,m-1}^{(i,j,k-1)} + B_{n,m}^{(i,j,k-1)}\Big] \\ & - \frac{1}{3}\Big[B_{n-1,m-1}^{(i-1,j-1,k)} + B_{n-1,m}^{(i-1,j-1,k)} + B_{n,m-1}^{(i-1,j-1,k)} \\ & + B_{n-1,m-1}^{(i-1,j,k-1)} + B_{n-1,m}^{(i-1,j,k-1)} + B_{n,m-1}^{(i-1,j,k-1)} \\ & + B_{n-1,m-1}^{(i,j-1,k-1)} + B_{n-1,m}^{(i,j-1,k-1)} + B_{n,m-1}^{(i,j-1,k-1)}\Big] \\ & + B_{n-1,m-1}^{(i-1,j-1,k-1)}. \end{aligned} \tag{4.3.3}$$

Such a recurrence expresses a transition probability in terms of other transition probabilities involving a lower number of photons. Thanks to this equation, we will be able to compute probabilities in another way than with the permanent and to interpret quantum interferences for three modes. As it stands, such a recurrence equation does not allow to perceive the nature of the quantum interferences yet. In an upcoming section, we will work towards making it apparent by simplifying this equation.

4.3.2 Fourth order interferometer

As in the preceding case, we adapt the vectors $\mathbf{x}$ and $\mathbf{z}$ to take into account here of the four inputs and outputs of the interferometer:

$$\mathbf{x} = (x_1, x_2, x_3, x_4), \quad \mathbf{z} = (z_1, z_2, z_3, z_4), \tag{4.3.4}$$

such an interferometer is now characterized by a unitary that is the fourth-order DFT matrix. The conventions corresponding to the case of $N = 4$ are represented in figure 4.2.

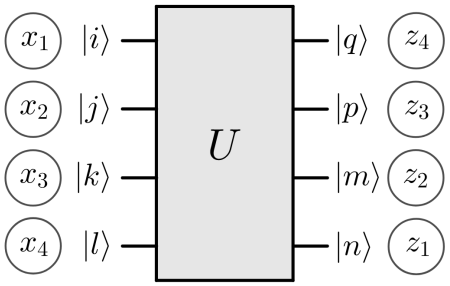

Figure 4.2: Conventions associated to the four-mode interferometer.

Again, we obtain the generating function from the general formula for $N = 4$ in this instance:

$$\begin{aligned}
f^{PI}(\mathbf{x},\mathbf{z}) = [1 &- \frac{1}{4}(x_1z_1 + x_1z_2 + x_1z_3 + x_1z_4 + x_2z_1 + x_2z_2 + x_2z_3 + x_2z_4 \\
&+ x_3z_1 + x_3z_2 + x_3z_3 + x_3z_4 + x_4z_1 + x_4z_2 + x_4z_3 + x_4z_4) \\
&+ \frac{1}{8}(x_1x_2z_1z_2 + 2.x_1x_2z_1z_3 + x_1x_2z_1z_4 + x_1x_2z_2z_3 + 2.x_1x_2z_2z_4 + x_1x_2z_3z_4 \\
&+ 2.x_1x_3z_1z_2 + 0.x_1x_3z_1z_3 + 2.x_1x_3z_1z_4 + 2.x_1x_3z_2z_3 + 0.x_1x_3z_2z_4 + 2.x_1x_3z_3z_4 \\
&+ x_1x_4z_1z_2 + 2.x_1x_4z_1z_3 + x_1x_4z_1z_4 + x_1x_4z_2z_3 + 2.x_1x_4z_2z_4 + x_1x_4z_3z_4 \\
&+ x_2x_3z_1z_2 + 2.x_2x_3z_1z_3 + x_2x_3z_1z_4 + x_2x_3z_2z_3 + 2.x_2x_3z_2z_4 + x_2x_3z_3z_4 \\
&+ 2.x_2x_4z_1z_2 + 0.x_2x_4z_1z_3 + 2.x_2x_4z_1z_4 + 2.x_2x_4z_2z_3 + 0.x_2x_4z_2z_4 + 2.x_2x_4z_3z_4 \\
&+ x_3x_4z_1z_2 + 2.x_3x_4z_1z_3 + x_3x_4z_1z_4 + x_3x_4z_2z_3 + 2.x_3x_4z_2z_4 + x_3x_4z_3z_4) \\
&- \frac{1}{4}(x_1x_2x_3z_1z_2z_3 + x_1x_2x_3z_1z_2z_4 + x_1x_2x_3z_1z_3z_4 + x_1x_2x_3z_2z_3z_4 \\
&+ x_1x_2x_4z_1z_2z_3 + x_1x_2x_4z_1z_2z_4 + x_1x_2x_4z_1z_3z_4 + x_1x_2x_4z_2z_3z_4 \\
&+ x_1x_3x_4z_1z_2z_3 + x_1x_3x_4z_1z_2z_4 + x_1x_3x_4z_1z_3z_4 + x_1x_3x_4z_2z_3z_4 \\
&+ x_2x_3x_4z_1z_2z_3 + x_2x_3x_4z_1z_2z_4 + x_2x_3x_4z_1z_3z_4 + x_2x_3x_4z_2z_3z_4) \\
&+ x_1x_2x_3x_4z_1z_2z_3z_4]^{-1}.
\end{aligned} \tag{4.3.5}$$

Once more, we find out that considering one more input and output ports results in a generating function containing a number of terms considerably higher than in the previous order. This could be expected as the generating function takes into consideration all of

the possible transition scenarios involving successively all number of photons from $N-1$ to zero. We denote as scenarios the different transition schemes that could be undergone by one or several photons.

Again by proceeding in the same way, we switch from the generating function to the recurrence equation proper to the four-mode interferometer:

$$
\begin{aligned}
B_{n,m,p}^{(i,j,k,l)} = \frac{1}{4}\Big[& B_{n-1,m,p}^{(i-1,j,k,l)} + B_{n,m-1,p}^{(i-1,j,k,l)} + B_{n,m,p-1}^{(i-1,j,k,l)} + B_{n,m,p}^{(i-1,j,k,l)} \\
& + B_{n-1,m,p}^{(i,j-1,k,l)} + B_{n,m-1,p}^{(i,j-1,k,l)} + B_{n,m,p-1}^{(i,j-1,k,l)} + B_{n,m,p}^{(i,j-1,k,l)} \\
& + B_{n-1,m,p}^{(i,j,k-1,l)} + B_{n,m-1,p}^{(i,j,k-1,l)} + B_{n,m,p-1}^{(i,j,k-1,l)} + B_{n,m,p}^{(i,j,k-1,l)} \\
& + B_{n-1,m,p}^{(i,j,k,l-1)} + B_{n,m-1,p}^{(i,j,k,l-1)} + B_{n,m,p-1}^{(i,j,k,l-1)} + B_{n,m,p}^{(i,j,k,l-1)}\Big] \\
& - \frac{1}{8}\Big[B_{n-1,m-1,p}^{(i-1,j-1,k,l)} + 2.B_{n-1,m,p-1}^{(i-1,j-1,k,l)} + B_{n-1,m,p}^{(i-1,j-1,k,l)} + B_{n,m-1,p-1}^{(i-1,j-1,k,l)} + 2.B_{n,m-1,p}^{(i-1,j-1,k,l)} + B_{n,m,p-1}^{(i-1,j-1,k,l)} \\
& + 2.B_{n-1,m-1,p}^{(i-1,j,k-1,l)} + 0.B_{n-1,m,p-1}^{(i-1,j,k-1,l)} + 2.B_{n-1,m,p}^{(i-1,j,k-1,l)} + 2.B_{n,m-1,p-1}^{(i-1,j,k-1,l)} + 0.B_{n,m-1,p}^{(i-1,j,k-1,l)} + 2.B_{n,m,p-1}^{(i-1,j,k-1,l)} \\
& + B_{n-1,m-1,p}^{(i-1,j,k,l-1)} + 2.B_{n-1,m,p-1}^{(i-1,j,k,l-1)} + B_{n-1,m,p}^{(i-1,j,k,l-1)} + B_{n,m-1,p-1}^{(i-1,j,k,l-1)} + 2.B_{n,m-1,p}^{(i-1,j,k,l-1)} + B_{n,m,p-1}^{(i-1,j,k,l-1)} \\
& + B_{n-1,m-1,p}^{(i,j-1,k-1,l)} + 2.B_{n-1,m,p-1}^{(i,j-1,k-1,l)} + B_{n-1,m,p}^{(i,j-1,k-1,l)} + B_{n,m-1,p-1}^{(i,j-1,k-1,l)} + 2.B_{n,m-1,p}^{(i,j-1,k-1,l)} + B_{n,m,p-1}^{(i,j-1,k-1,l)} \\
& + 2.B_{n-1,m-1,p}^{(i,j-1,k,l-1)} + 0.B_{n-1,m,p-1}^{(i,j-1,k,l-1)} + 2.B_{n-1,m,p}^{(i,j-1,k,l-1)} + 2.B_{n,m-1,p-1}^{(i,j-1,k,l-1)} + 0.B_{n,m-1,p}^{(i,j-1,k,l-1)} + 2.B_{n,m,p-1}^{(i,j-1,k,l-1)} \\
& + B_{n-1,m-1,p}^{(i,j,k-1,l-1)} + 2.B_{n-1,m,p-1}^{(i,j,k-1,l-1)} + B_{n-1,m,p}^{(i,j,k-1,l-1)} + B_{n,m-1,p-1}^{(i,j,k-1,l-1)} + 2.B_{n,m-1,p}^{(i,j,k-1,l-1)} + B_{n,m,p-1}^{(i,j,k-1,l-1)}\Big] \\
& + \frac{1}{4}\Big[B_{n-1,m-1,p-1}^{(i-1,j-1,k-1,l)} + B_{n-1,m-1,p}^{(i-1,j-1,k-1,l)} + B_{n-1,m,p-1}^{(i-1,j-1,k-1,l)} + B_{n,m-1,p-1}^{(i-1,j-1,k-1,l)} \\
& + B_{n-1,m-1,p-1}^{(i-1,j-1,k,l-1)} + B_{n-1,m-1,p}^{(i-1,j-1,k,l-1)} + B_{n-1,m,p-1}^{(i-1,j-1,k,l-1)} + B_{n,m-1,p-1}^{(i-1,j-1,k,l-1)} \\
& + B_{n-1,m-1,p-1}^{(i-1,j,k-1,l-1)} + B_{n-1,m-1,p}^{(i-1,j,k-1,l-1)} + B_{n-1,m,p-1}^{(i-1,j-1,k-1,l)} + B_{n,m-1,p-1}^{(i-1,j-1,k-1,l)} \\
& + B_{n-1,m-1,p-1}^{(i,j-1,k-1,l-1)} + B_{n-1,m-1,p}^{(i,j-1,k-1,l-1)} + B_{n-1,m,p-1}^{(i,j-1,k-1,l-1)} + B_{n,m-1,p-1}^{(i,j-1,k-1,l-1)}\Big] \\
& - B_{n-1,m-1,p-1}^{(i-1,j-1,k-1,l-1)}.
\end{aligned}
\tag{4.3.6}
$$

Note that in order to derive the recurrence relations just shown, we could have directly started from the formula generalizing the writing of recurrences for an arbitrary N at equation (2.3.23), rather than first obtaining the generating function and then applying to it the shifting property. But as both are important results, we started from the generating function. As we are interested in transition probabilities for the specific case where we consider one photon at each input and output port we next apply the recurrences in such situation. We will see that the recurrences are then organized in blocks as depicted at figure 4.3:

$$
B_{\mathbf{1}_N}^{(\mathbf{1}_N)} = \boxed{N-1 \text{ photons}} - \boxed{N-2 \text{ photons}} + \cdots + (-1)^{N-2}\boxed{1 \text{ photon}} + (-1)^{N-1}\boxed{\text{vacuum}}
$$

Figure 4.3: Block structure of a recurrence of order N for one photon per port.

Each block containing the transition probabilities involving a given number photons.

4.3.3 Recurrences for coincident events

The recurrence (4.3.3) expressed for the transition probability of a pattern involving one photon per input port towards an output pattern of one photon per port is obtained by setting the particular case:

$$
i = j = k = n = m = p = 1, \tag{4.3.7}
$$

by doing so, the recurrence equation becomes:

$$\begin{aligned} B_{1,1}^{(1,1,1)} = \quad & \frac{1}{3}\left[B_{0,1}^{(0,1,1)} + B_{1,0}^{(0,1,1)} + B_{1,1}^{(0,1,1)} + B_{0,1}^{(1,0,1)} + B_{1,0}^{(1,0,1)} + B_{1,1}^{(1,0,1)} + B_{0,1}^{(1,1,0)} + B_{1,0}^{(1,1,0)} + B_{1,1}^{(1,1,0)}\right] \\ & - \frac{1}{3}\left[B_{0,0}^{(0,0,1)} + B_{0,1}^{(0,0,1)} + B_{1,0}^{(0,0,1)} + B_{0,0}^{(0,1,0)} + B_{0,1}^{(0,1,0)} + B_{1,0}^{(0,1,0)} + B_{0,0}^{(1,0,0)} + B_{0,1}^{(1,0,0)} + B_{1,0}^{(1,0,0)}\right] \\ & + B_{0,0}^{(0,0,0)}. \end{aligned} \tag{4.3.8}$$

We see that this recurrence is organized in three blocks alternating in sign, each regrouping transition probabilities involving a same number of photons, which decreases by moving to the next block. In this equation, we notice that the vacuum term which was interpreted as a quantum interference suppression term in the two-mode case with a negative sign appears here with a positive sign. At first sight, destructive interferences seem to originate from the second block accounting for single-photon transitions, which is the only contribution having a negative sign.

To express the four-mode recurrence (4.3.6) in the case of transmitting single photons, we again set the particular situation:

$$i = j = k = l = n = m = p = q = 1, \tag{4.3.9}$$

and the recurrence is then:

$$\begin{aligned} B_{1,1,1}^{(1,1,1,1)} = & \frac{1}{4}\Big[B_{0,1,1}^{(0,1,1,1)} + B_{1,0,1}^{(0,1,1,1)} + B_{1,1,0}^{(0,1,1,1)} + B_{1,1,1}^{(0,1,1,1)} \\ & \quad + B_{0,1,1}^{(1,0,1,1)} + B_{1,0,1}^{(1,0,1,1)} + B_{1,1,0}^{(1,0,1,1)} + B_{1,1,1}^{(1,0,1,1)} \\ & \quad + B_{0,1,1}^{(1,1,0,1)} + B_{1,0,1}^{(1,1,0,1)} + B_{1,1,0}^{(1,1,0,1)} + B_{1,1,1}^{(1,1,0,1)} \\ & \quad + B_{0,1,1}^{(1,1,1,0)} + B_{1,0,1}^{(1,1,1,0)} + B_{1,1,0}^{(1,1,1,0)} + B_{1,1,1}^{(1,1,1,0)}\Big] \\ & - \frac{1}{8}\Big[B_{0,0,1}^{(0,0,1,1)} + 2.B_{0,1,0}^{(0,0,1,1)} + B_{0,1,1}^{(0,0,1,1)} + B_{1,0,0}^{(0,0,1,1)} + 2.B_{1,0,1}^{(0,0,1,1)} + B_{1,1,0}^{(0,0,1,1)} \\ & \quad + 2.B_{0,0,1}^{(0,1,0,1)} + 0.B_{0,1,0}^{(0,1,0,1)} + 2.B_{0,1,1}^{(0,1,0,1)} + 2.B_{1,0,0}^{(0,1,0,1)} + 0.B_{1,0,1}^{(0,1,0,1)} + 2.B_{1,1,0}^{(0,1,0,1)} \\ & \quad + B_{0,0,1}^{(0,1,1,0)} + 2.B_{0,1,0}^{(0,1,1,0)} + B_{0,1,1}^{(0,1,1,0)} + B_{1,0,0}^{(0,1,1,0)} + 2.B_{1,0,1}^{(0,1,1,0)} + B_{1,1,0}^{(0,1,1,0)} \\ & \quad + B_{0,0,1}^{(1,0,0,1)} + 2.B_{0,1,0}^{(1,0,0,1)} + B_{0,1,1}^{(1,0,0,1)} + B_{1,0,0}^{(1,0,0,1)} + 2.B_{1,0,1}^{(1,0,0,1)} + B_{1,1,0}^{(1,0,0,1)} \\ & \quad + 2.B_{0,0,1}^{(1,0,1,0)} + 0.B_{0,1,0}^{(1,0,1,0)} + 2.B_{0,1,1}^{(1,0,1,0)} + 2.B_{1,0,0}^{(1,0,1,0)} + 0.B_{1,0,1}^{(1,0,1,0)} + 2.B_{1,1,0}^{(1,0,1,0)} \\ & \quad + B_{0,0,1}^{(1,1,0,0)} + 2.B_{0,1,0}^{(1,1,0,0)} + B_{0,1,1}^{(1,1,0,0)} + B_{1,0,0}^{(1,1,0,0)} + 2.B_{1,0,1}^{(1,1,0,0)} + B_{1,1,0}^{(1,1,0,0)}\Big] \\ & + \frac{1}{4}\Big[B_{0,0,0}^{(0,0,0,1)} + B_{0,0,1}^{(0,0,0,1)} + B_{0,1,0}^{(0,0,0,1)} + B_{1,0,0}^{(0,0,0,1)} \\ & \quad + B_{0,0,0}^{(0,0,1,0)} + B_{0,0,1}^{(0,0,1,0)} + B_{0,1,0}^{(0,0,1,0)} + B_{1,0,0}^{(0,0,1,0)} \\ & \quad + B_{0,0,0}^{(0,1,0,0)} + B_{0,0,1}^{(0,1,0,0)} + B_{0,1,0}^{(0,1,0,0)} + B_{1,0,0}^{(0,1,0,0)} \\ & \quad + B_{0,0,0}^{(1,0,0,0)} + B_{0,0,1}^{(1,0,0,0)} + B_{0,1,0}^{(1,0,0,0)} + B_{1,0,0}^{(1,0,0,0)}\Big] \\ & - B_{0,0,0}^{(0,0,0,0)}. \end{aligned} \tag{4.3.10}$$

Now including four blocks, the structure of this recurrence is more complicated than the previous one. It accounts now for two negative contributions. Among the latter, the block containing the transition scenarios involving two photons reveals to be of a higher complexity due to the fact that its corresponding minors are not all equal, which was the case previously for any block, resulting in different appearing coefficients: $c_0 = 0$, $c_1 = 1$

and $c_2 = 2$ in front of the terms of this second block. As for the Hong-Ou-Mandel effect, we find back the vacuum term with a negative sign. We also see that those two last recurrences are organized following the structure represented on figure 4.3.

In previous chapter, we computed the transition probability thanks to the permanent of the interferometers matrices linking input modes to output modes. We propose next to realize those computations thanks to the recurrence equations, this in order to show that the framework presented in the second chapter of this thesis is consistent for any order N and to verify the results previously obtained with the permanent.

4.3.4 Probabilities for coincident events

By using the recurrence relations under their general form from equations (4.3.3) and (4.3.6), it is possible to evaluate any term coming from the recurrences particularized to the case of single photons in each port. As we are dealing with recurrence equations, we need to operate gradually. It means that in order to evaluate the probabilities of a given block, we first need to evaluate the probabilities from the following blocks, i.e. the blocks of probabilities involving less photons.

In order to begin the calculations, we first need an initial condition. Which will allow us to progressively evaluate every term of the recurrence. This initial condition is nothing other than the vacuum transition probability of order N:

$$B_{\mathbf{0}_N}^{(\mathbf{0}_N)} = 1, \tag{4.3.11}$$

where $\mathbf{0}_N$ is the null vector of dimension N. Starting from this initial condition, we can then gradually evaluate the probabilities involving a higher number of photons.

- **three modes**:

  First, we have as initial condition:

  $$B_{0,0}^{(0,0,0)} = 1. \tag{4.3.12}$$

  From this, we can evaluate single-photon probabilities from the second block of the recurrence (4.3.8), let us illustrate for the first term $B_{0,0}^{(0,0,1)}$. Using the values of its indices into recurrence (4.3.3):

  $$i = j = n = m = 0, \quad \text{and} \quad k = p = 1, \tag{4.3.13}$$

  and by dropping terms accounting for negative number of particles, i.e. having negative indices, we obtain:

  $$B_{0,0}^{(0,0,1)} = \frac{1}{3} B_{0,0}^{(0,0,0)} = \frac{1}{3}. \tag{4.3.14}$$

  Processing similarly for the other terms of the second block reveals that they are all equal. We can now evaluate the transition probabilities of the first block involving two photons, again let us use its first term $B_{0,1}^{(0,1,1)}$:

  $$\begin{aligned} B_{0,1}^{(0,1,1)} &= \frac{1}{3}\left[B_{0,0}^{(0,0,1)} + B_{0,1}^{(0,0,1)} + B_{0,0}^{(0,1,0)} + B_{0,1}^{(0,1,0)}\right] - \frac{1}{3} B_{0,0}^{(0,0,0)} \\ &= \frac{1}{3} \times \left[4 \times \frac{1}{3}\right] - \frac{1}{3} \\ &= \frac{1}{9}, \end{aligned} \tag{4.3.15}$$

here too, each probability from the first block has the same value. Finally, we can evaluate the transition probability for coincident events:

$$\begin{aligned} B_{1,1}^{(1,1,1)} &= \frac{1}{3} \times \left[9 \times \frac{1}{9}\right] - \frac{1}{3} \times \left[9 \times \frac{1}{3}\right] + \left[1\right] \\ &= \frac{1}{3} - 1 + 1 \\ &= \frac{1}{3}. \end{aligned} \tag{4.3.16}$$

Where we used brackets to show the value specific to each block. We find the same result as the one obtained in the previous chapter thanks to the permanent.

- **four modes**:

  The initial condition is here:

$$B_{0,0,0}^{(0,0,0,0)} = 1, \tag{4.3.17}$$

  from which we can evaluate single-photon probabilities from third block of recurrence (4.3.10). Again, We consider the first term and by injecting its indices into the recurrence we get:

$$B_{0,0,0}^{(0,0,0,1)} = \frac{1}{4} B_{0,0,0}^{(0,0,0,0)} = \frac{1}{4}, \tag{4.3.18}$$

  and as for the three-mode case, each probability involving one photon is equal. The evaluation of the second block represents a bit more difficulty as it contains different coefficients making that all its terms are not equal. We take successively an example of probabilities weighted by each of them. For coefficient $c_0 = 0$, we get:

$$B_{1,0,1}^{(1,0,1,0)} = \frac{1}{4}\left[B_{0,0,1}^{(0,0,1,0)} + B_{1,0,0}^{(0,0,1,0)} + B_{0,0,1}^{(1,0,0,0)} + B_{1,0,0}^{(1,0,0,0)}\right] = \frac{1}{4}, \tag{4.3.19}$$

  for $c_1 = 1$:

$$B_{0,1,1}^{(0,0,1,1)} = \frac{1}{4}\left[B_{0,0,1}^{(0,0,0,1)} + B_{0,1,0}^{(0,0,0,1)} + B_{0,0,1}^{(0,0,1,0)} + B_{0,1,0}^{(0,0,1,0)}\right] - \frac{1}{8} B_{0,0,0}^{(0,0,0,0)} = \frac{1}{8}, \tag{4.3.20}$$

  and for $c_2 = 2$:

$$B_{1,1,0}^{(1,0,1,0)} = \frac{1}{4}\left[B_{0,1,0}^{(0,0,1,0)} + B_{1,0,0}^{(0,0,1,0)} + B_{0,1,0}^{(1,0,0,0)} + B_{1,0,0}^{(1,0,0,0)}\right] - \frac{1}{4} B_{0,0,0}^{(0,0,0,0)} = 0. \tag{4.3.21}$$

  Terms with the same coefficient are equal. However, we notice that all transition scenarios involving only two photons in a balanced four-mode interferometer are not equiprobable. Especially some of them, with $c_2 = 2$, can not occur. Which would not happen in the classical case. Moreover, terms with $c_0 = 0$ do not contribute to the sum which makes that the second block then finally contains sixteen equal terms, the ones corresponding to $c_1 = 1$. Thanks to these results, we can then estimate the terms of the first block which are also all equal and are each valued:

$$B_{0,1,1}^{(0,1,1,1)} = \frac{1}{16}. \tag{4.3.22}$$

  Finally we obtain for the transition probability:

$$\begin{aligned} B_{1,1,1}^{(1,1,1,1)} &= \frac{1}{4} \times \left[16 \times \frac{1}{16}\right] - \frac{1}{8} \times \left[16 \times \frac{1}{8}\right] + \frac{1}{4} \times \left[16 \times \frac{1}{4}\right] - \left[1\right] \\ &= \frac{1}{4} - \frac{1}{4} + 1 - 1 \\ &= 0, \end{aligned} \tag{4.3.23}$$

  which is the result that we have obtained with the permanent.

This suggests that the formalism involving the generating function as well as the recurrence relation resulting from it allows to compute transition probabilities for any N. However, as the number of terms does increase sharply by passing from one order to the following, those calculations reveal quickly to become heavy to perform.

4.4 Structure of recurrences

We have presented the recurrence relations of the first interesting interferometric cases other than the Hong-Ou-Mandel effect. Each describing quantum interferences of a different nature. Before simplifying the obtained equations at previous section in order to be able to interpret them more easily, we propose to analyze the structure of such recurrences to see how it evolves according to N and to determine properties that would be valid for any order N.

Previously, we described the recurrences as being organized into blocks. As already shown by figure 4.3, each block contains transition probabilities involving a same number of photons. We now particularize this representation to the different orders we study in this thesis. Such recurrences are represented hereafter on figure 4.4 for the Hong-Ou-Mandel effect, the tritter and the four-mode interferometer where we also indicate the values of each block:

$$
\begin{aligned}
&N=2 \quad B_{1}^{(1,1)} = \boxed{1} - \boxed{1} = 0\\
&N=3 \quad B_{1,1}^{(1,1,1)} = \boxed{\tfrac{1}{3}} - \boxed{1} + \boxed{1} = \tfrac{1}{3}\\
&N=4 \quad B_{1,1,1}^{(1,1,1,1)} = \boxed{\tfrac{1}{4}} - \boxed{\tfrac{1}{4}} + \boxed{1} - \boxed{1} = 0
\end{aligned}
$$

Figure 4.4: Block structure of the cases studied. Red block: three photons, green block: two photons, blue block: one photon and grey block: vacuum.

The number of photons of each block decreases from left to right. On the far right represented by the grey block we find the vacuum term $B_{\mathbf{0}_N}^{(\mathbf{0}_N)}$ that interacts destructively for even orders and constructively for odd orders. The sign appearing in front of it is dictated by equation (2.3.23). The blue blocks account for single-photon scenarios, green blocks for two photons and red block for three photons.

From those three recurrences and observations made during calculations, we attempted to establish properties that could allow to know in advance the value of given blocks and that would be valid whatever the order N that is considered. This would allow to simplify the computations. These observations are the followings:

1. For any order N, the last block equals one.
2. For any order N, the penultimate block equals one.
3. Blocks cancel two-by-two from the right.

However, these previous observations could not all be rigorously proved. Indeed the first one is, while the second is only half-proved and the third is observed but could not be proved for all N.

Before describing these statements, we present some observed result about square submatrices of order $N-1$ of Fourier matrices, useful for their description. We observed

that the modulus of the determinants of such submatrices were all equal, valued $1/\sqrt{N}$, and that it also applies to the modulus of permanents, to which we were unable to associate an analytical form in N. We observed that by manipulating any submatrix of order $N-1$ we could express it in function of another submatrix multiplied by a power of the root ω. Although we can not provide an analytical proof to this observation that is valid for any submatrices, we however illustrate this result by an example linking submatrices $\mathrm{F}_{1,1}$ and $\mathrm{F}_{N,N}$, whose notations were introduced at equations (2.4.8). Starting from $\mathrm{F}_{1,1}$ we successively take out factors multiplying each row then each column to find another submatrix that is $\mathrm{F}_{N,N}$:

$$\begin{aligned}
\mathrm{F}_{1,1} &= \omega\omega^2\dots\omega^{N-1}\cdot\frac{1}{\sqrt{N}}\begin{pmatrix} 1 & \omega & \dots & \omega^{N-2} \\ 1 & \omega^2 & \dots & \omega^{2(N-2)} \\ \vdots & \vdots & \ddots & \vdots \\ 1 & \omega^{N-1} & \dots & \omega^{(N-1)(N-2)} \end{pmatrix} \\
&= \omega^{\sum_1^{N-1} j}.\omega^{\sum_1^{N-2} k}\cdot\frac{1}{\sqrt{N}}\begin{pmatrix} 1 & 1 & \dots & 1 \\ 1 & \omega & \dots & \omega^{N-2} \\ \vdots & \vdots & \ddots & \vdots \\ 1 & \omega^{N-2} & \dots & \omega^{(N-2)(N-2)} \end{pmatrix} \\
&= \omega^{(N-1)(N-1)}.\mathrm{F}_{N,N},
\end{aligned} \tag{4.4.1}$$

then,

$$|\det \mathrm{F}_{1,1}| = \left|\omega^{(N-1)(N-1)}\det \mathrm{F}_{N,N}\right| = |\det \mathrm{F}_{N,N}|\,, \tag{4.4.2}$$

due to the definition of ω. This also applies to the permanent. We now describe stated observations:

1. On the one hand, the minor associated to the last block corresponds to the determinant of the whole Fourier matrix. As it is a unitary matrix, the modulus of its determinant equals one. On the other hand, the only term from this block is the vacuum term, accounting for transition probability that equals one.

2. Each term from the penultimate block are associated to minors of order $N-1$ whose modulus as previously stated are all equal to $1/\sqrt{N}$. As this block contains scenarios that involve only one photon, there are N^2 possible transition scenarios. Since we consider balanced interferometers, a photon as a $1/N$ probability to go from a given input towards a given output. Finally, the last block therefore equals one as:

$$\frac{1}{N}\times\left[N^2\times\frac{1}{N}\right] = 1. \tag{4.4.3}$$

Following these two statements, the two last blocks of the recurrence equation cancel each other and this for any order N.

3. Such a cancellation scheme is noticeable by looking at figure 4.4. The vanishing transition probability for even orders then appears logical as all the blocks cancel in pairs while the probability for odd orders corresponds then to the value of the first block:

$$B_{\mathbf{1}_N}^{(\mathbf{1}_N)} = \frac{1}{N}\times\left[N^2\times|\mathrm{per}\,\mathrm{F}_{N,N}|^2\right]. \tag{4.4.4}$$

as minors correspond to matrix elements and we have N^2 terms whose permanent modulus is equal as previously stated. It is encountered for the tritter, we also checked this for the five and seven-mode cases:

$$B_{1,1,1,1,1}^{(1,1,1,1,1)} = \frac{1}{5}\times\left[25\times\frac{1}{625}\right] = \frac{1}{125}, \tag{4.4.5}$$

$$B_{1,1,1,1,1,1,1}^{(1,1,1,1,1,1,1)} = \frac{1}{7} \times \left[49 \times \frac{225}{117649} \right] = \frac{225}{16807}. \tag{4.4.6}$$

This last statement is more of an assumption than a true property as we could not prove its validity through an analytical reasoning. We did show that if some blocks could be determined with ease due to their simple structure, this is not the case for others.

We have approached here the recurrence equations under the perspective of their organization. Below, we simplify the recurrences previously obtained in order to facilitate their physical interpretation.

4.5 Simplifications

Let us remind the recurrence relation proper to the transition probability of one photon per input towards one photon per output for the three-mode Fourier interferometer:

$$\begin{aligned} B_{1,1}^{(1,1,1)} = \quad & \frac{1}{3}\left[B_{0,1}^{(0,1,1)} + B_{1,0}^{(0,1,1)} + B_{1,1}^{(0,1,1)} + B_{0,1}^{(1,0,1)} + B_{1,0}^{(1,0,1)} + B_{1,1}^{(1,0,1)} + B_{0,1}^{(1,1,0)} + B_{1,0}^{(1,1,0)} + B_{1,1}^{(1,1,0)}\right] \\ & - \frac{1}{3}\left[B_{0,0}^{(0,0,1)} + B_{0,1}^{(0,0,1)} + B_{1,0}^{(0,0,1)} + B_{0,0}^{(0,1,0)} + B_{0,1}^{(0,1,0)} + B_{1,0}^{(0,1,0)} + B_{0,0}^{(1,0,0)} + B_{0,1}^{(1,0,0)} + B_{1,0}^{(1,0,0)}\right] \\ & + B_{0,0}^{(0,0,0)}. \end{aligned} \tag{4.5.1}$$

Under this form, the interpretation of quantum interferences is not easily achievable. We then need to simplify this equation. We would like to obtain a relation with an equivalent simplicity that the equation (2.3.15) that was derived for the two-mode case and then highlighted the destructive interference effect that is the Hong-Ou-Mandel effect, for a balanced beam splitter.

For this purpose, we use the general recurrence relation from equation (4.3.3) in order to simplify the transition probabilities that involve more than one photon to express the recurrence relation only in terms of single-photon scenarios. Applied, for example to the first term $B_{0,1}^{(0,1,1)}$, it comes:

$$B_{0,1}^{(0,1,1)} = \frac{1}{3}\left[B_{0,0}^{(0,0,1)} + B_{0,1}^{(0,0,1)} + B_{0,0}^{(0,1,0)} + B_{0,1}^{(0,1,0)}\right] - \frac{1}{3}B_{0,0}^{(0,0,0)} \tag{4.5.2}$$

The representation of this decomposition equation in terms of physical transition scenarios involving only one photon is depicted hereafter in figure 4.5:

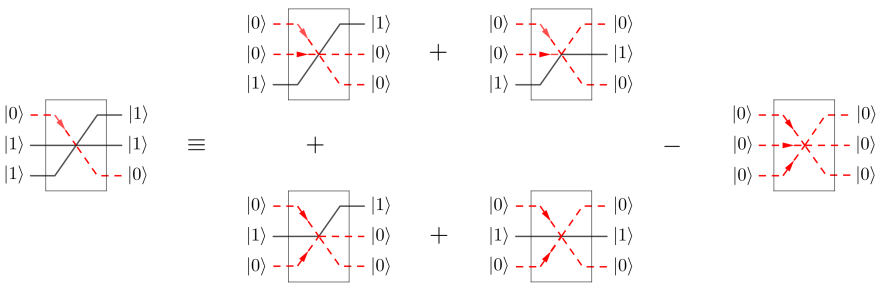

Figure 4.5: Decomposition of the transition probability $B_{0,1}^{(0,1,1)}$.

On this figure if we ignore the supplementary port occupied by vacuum at the input and the output of the interferometer, we retrieve the same decomposition scheme that in the two-mode case that was represented at figure 2.4. By substituting all of the two-photon scenarios present in the recurrence equation for coincident events by their own decomposition, we obtain an expression exclusively expressed in terms of single-photon

scenarios and vacuum terms. However, by reorganizing all the terms, it appears that the different contributions of the vacuum cancel each other to make this term vanish. Due to the heaviness of the obtained expression, we do not show it here nor the development to reorganize its terms. Finally, we end up with the following equation:

$$B_{1,1}^{(1,1,1)} = \frac{1}{9}\left[B_{1,0}^{(1,0,0)} + B_{0,1}^{(1,0,0)} + B_{0,0}^{(1,0,0)} + B_{1,0}^{(0,1,0)} + B_{0,1}^{(0,1,0)} + B_{0,0}^{(0,1,0)} + B_{1,0}^{(0,0,1)} + B_{0,1}^{(0,0,1)} + B_{0,0}^{(0,0,1)}\right]. \tag{4.5.3}$$

This equation is one the major results obtained in this thesis. The transition probability of an input pattern composed of one photon per port towards an output pattern of one photon per port is nothing but the arithmetic mean of the different transition probabilities involving only one photon. All these scenarios then interfere in a constructive way resulting in a non-vanishing transition probability. However, this last expression might appear to be surprising as we might wonder where the quantum character is hidden in such a simple sum, which however does not correspond to the classical case either. Furthermore, this expression does not allow to make any distinction between the coefficients in front of each of its terms.

In the case of the four-mode interferometer, the method is exactly similar. The difference is that in order to get rid of the terms involving three photons, we have to apply the recurrence twice. This leads to a very loaded equation that we do not explicit here. The final expression that is obtained for the four-mode case is:

$$\begin{aligned} B_{1,1,1,1}^{(1,1,1,1)} = \frac{1}{16}\Big[&B_{1,0,0,0}^{(1,0,0,0)} + B_{0,1,0,0}^{(1,0,0,0)} + B_{0,0,1,0}^{(1,0,0,0)} + B_{0,0,0,1}^{(1,0,0,0)} + B_{1,0,0,0}^{(0,1,0,0)} + B_{0,1,0,0}^{(0,1,0,0)} + B_{0,0,1,0}^{(0,1,0,0)} + B_{0,0,0,1}^{(0,1,0,0)} \\ &+ B_{1,0,0,0}^{(0,0,1,0)} + B_{0,1,0,0}^{(0,0,1,0)} + B_{0,0,1,0}^{(0,0,1,0)} + B_{0,0,0,1}^{(0,0,1,0)} + B_{1,0,0,0}^{(0,0,0,1)} + B_{0,1,0,0}^{(0,0,0,1)} + B_{0,0,1,0}^{(0,0,0,1)} + B_{0,0,0,1}^{(0,0,0,1)}\Big] \\ &- \frac{1}{4}B_{0,0,0,0}^{(0,0,0,0)}. \end{aligned} \tag{4.5.4}$$

We notice that we obtain the same scheme that in the case with three modes, indeed we find back the arithmetic mean of the scenarios involving the transition of one photon, but here we also have the vacuum term that did not vanish. This equation is then of a similar form to the case of the Hong-Ou-Mandel effect. Again, this vacuum term is responsible of destructive interferences and can then be interpreted as a quantum interference suppression term. Unfortunately, this simple reasoning does not extend beyond $N = 4$.

4.6 Conclusion

In this chapter, we started the study of the three-mode and four-mode Fourier interferometers. We have first derived their generating functions and then the recurrence equations resulting from it. We considered the latter for the particular case involving coincident events given one photon per input and verified thanks to these relations the numerical values of transition probabilities that were computed at previous chapter thanks to the permanent. The results were identical, supporting the consistence of such a formalism. We then analyzed the structure of the recurrence equations for the three cases under study and proposed conjectures that we assumed to be valid whatever the order N that is considered. Finally, in order to have a better comprehensive understanding of quantum interferences we managed, thanks to the recurrences themselves, to simplify the expressions to provide an interpretation of quantum interferences in a more convenient way. This has led to important results for this thesis where the three-mode case made appear the constructive nature of interferences by summing the probabilities of each single-photon scenarios while for four modes, we find a quantum suppression term as for the Hong-Ou-Mandel effect witnessing destructive interferences.

Chapter 5

Combining fermionic and bosonic statistics

5.1 Motivation

In the previous chapter, we have obtained the recurrence equations in a form that allowed to observe the constructive or destructive character of quantum interferences according to the number of modes in the interferometer. The three-mode case summed up all possible transition scenarios for one photon while when four-mode are considered appears again a quantum suppression term responsible of the impossibility to witness coincident events at the output of the setup. In this last chapter, we focus on the three-mode case interferometer whose recurrence did not allow to differentiate the origin of the coefficients in front of each term as they were all equal. We will see that by the introduction of new more practical notations as well as fermionic statistics which is related to the determinant, we will be able to rewrite the recurrence equation previously simplified in a more explicit form allowing to interpret the story of the photons in the interferometer. The key step in this progression will be to interpret the minors of the recurrence as fermionic transition probabilities. In the end we will obtain an equation entirely characterizing quantum interferences for a setup involving three modes and not specific to Fourier interferometers but that is valid for any passive unitary.

We start this chapter by briefly addressing the relation between the fermionic statistics and the determinant. We will then introduce a new notation by relating the determinants present in the minors to the fermionic statistics in order to express the recurrence relation in a more explicit way. We will then be able to interpret these minors used to derive the recurrence equation as fermionic transition probabilities. We will first introduce these new concepts in the case of the two-mode interferometer and show that we obtain the same result than previously. Finally, this will be applied to the third order recurrence derived in previous chapter.

In order to approach the subject of fermionic statistics, we refer to both [14] and [30].

5.2 Identical fermions statistics

5.2.1 Determinant

At the end of chapter 2, we introduced the permanent and more specifically we related it to quantum interferences involving bosons. We do the same here but this time for fermions.

While the quantum state of identical bosonic particles systems must be symmetric in regard to permutation of particles, this is not the case when fermions are considered. Indeed, due to Pauli exclusion principle, fermionic systems are anti-symmetric with respect to exchange of particles. In this case, the only completely anti-symmetric combination of single particle functions is the determinant of such functions [30]. The computations of probabilities linked to the transition of fermions will then be related to the determinant of the matrix linking input to output ports.

5.2.2 Fermionic transition probabilities

In order to further account for fermions when we will manipulate the third-order recurrence equation, we now introduce the transition probability concerning fermions. By analogy with the probabilities previously used for bosons we then denote this latter by now considering the determinant rather than the permanent:

$$F_{\mathbf{n}}^{(\mathbf{i})} = \frac{\left|\det \mathrm{M}[i_1, \ldots, i_N | n_1, \ldots, n_N]\right|^2}{i_1! \ldots i_N! n_1! \ldots n_N!}, \tag{5.2.1}$$

where we have considered the same notations as in the second chapter of this thesis for the N-dimensional input and output ports vectors $\mathbf{i}$ and $\mathbf{n}$ as well as the matrix $M[i_1, \ldots, i_N | n_1, \ldots, n_N]$ whose derivation is explained in section 2.4.3.

In the particular case of single-particles in each port, we consider the N-order Fourier matrix and this last expression simplifies:

$$F_{\mathbf{1}_N}^{(\mathbf{1}_N)} = \left|\det \mathrm{F}_N\right|^2, \tag{5.2.2}$$

as Fourier matrices are unitary matrices, we obtain from this equation:

$$F_{\mathbf{1}_N}^{(\mathbf{1}_N)} = 1. \tag{5.2.3}$$

We thus notice a significant difference between the behaviour of bosons and fermions inside a Fourier interferometer. While the former tend to bunch in the even cases, the latter always leave the setup separately ensuring thus coincident events for any order. This was already mentioned previously and is proven in detail in [14].

Thanks to this new writing, we can now express the minors of the recurrence equations in terms of transition probabilities of particles and more specifically in terms of fermionic transition probabilities. Indeed, the minors figuring in the global recurrence equation are the determinants of the different submatrices of the interferometer unitary. By taking the squared modulus, we find the definition of transition probabilities we have just introduced. To sum up and by using the notations from equation (2.3.23):

$$\left|\det \mathrm{U}(\beta, \alpha)\right|^2 = F_{\mathbf{1}_N^{(\beta)}}^{(\mathbf{1}_N^{(\alpha)})}, \tag{5.2.4}$$

which allows to rewrite this equation as:

$$B_{\mathbf{n}}^{(\mathbf{i})} = \sum_{m=1}^{N} (-1)^{m-1} \sum_{\substack{\alpha \in R_m^{(N)} \\ \mathbf{i}_s \neq 0, s \in \alpha}} \sum_{\substack{\beta \in R_m^{(N)} \\ \mathbf{n}_r \neq 0, r \in \beta}} F_{\mathbf{1}_N^{(\beta)}}^{(\mathbf{1}_N^{(\alpha)})} B_{\mathbf{n}-\mathbf{1}_N^{(\beta)}}^{\left(\mathbf{i}-\mathbf{1}_N^{(\alpha)}\right)}, \tag{5.2.5}$$

which now includes fermionic transition probabilities. In such an equation, we notice that the fermionic probabilities have input and output patterns with maximum one particle per port. Which is consistent given the fact that identical fermions can not occupy the same port.

5.3 Two modes

In order to illustrate the use of the fermionic transition probabilities, we propose to show it for the two-mode case. We remind that the corresponding recurrence equation we obtained was:

$$B_1^{(1,1)} = \frac{1}{2}B_0^{(0,1)} + \frac{1}{2}B_1^{(0,1)} + \frac{1}{2}B_1^{(1,0)} + \frac{1}{2}B_0^{(1,0)} - B_0^{(0,0)}, \tag{5.3.1}$$

where in this case, the minors reduced to the matrix elements of the second order Fourier matrix. We can then rewrite this expression by including fermionic probabilities, this gives:

$$B_1^{(1,1)} = F_1^{(1,0)}B_0^{(0,1)} + F_0^{(1,0)}B_1^{(0,1)} + F_0^{(0,1)}B_1^{(1,0)} + F_1^{(0,1)}B_0^{(1,0)} - F_1^{(1,1)}B_0^{(0,0)}, \tag{5.3.2}$$

note that strictly speaking we should write the left-hand side term as:

$$F_0^{(0,0)}B_1^{(1,1)} \tag{5.3.3}$$

but we do not for the sake of clarity as:

$$F_0^{(0,0)} = 1. \tag{5.3.4}$$

Let us also mention that in the case of single-particle transition probabilities, the bosonic or fermionic nature of the particle does not matter as the particle statistics plays no role.

By using the recurrence a second time we can further write:

$$B_1^{(1,1)} = F_1^{(1,0)}F_0^{(0,1)} + F_0^{(1,0)}F_1^{(0,1)} + F_0^{(0,1)}F_1^{(1,0)} + F_1^{(0,1)}F_0^{(1,0)} - F_1^{(1,1)}, \tag{5.3.5}$$

since the vacuum transition probability equals one, and this for both types of particles, as well as the fermionic probability for coincident events. The decomposition in terms of distinguishable fermions in this equation is schematized on figure 5.1.

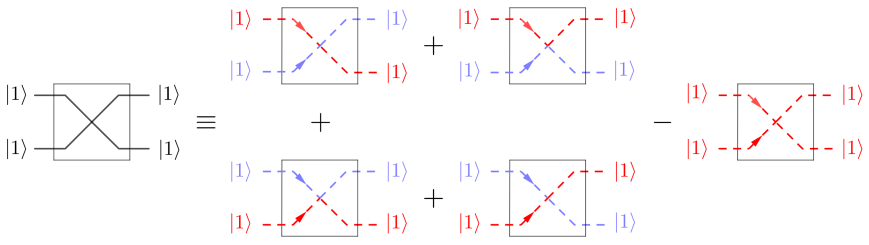

Figure 5.1: Decomposition of $B_1^{(1,1)}$ in terms of fermionic transition probabilities. (Red) paths of the first fermion and (blue) paths of the second fermion.

where red paths stand for the first fermion (left probability of each term) and blue paths for second one (right probability). Passing from one form to another is then equivalent to remove photons one by one and to replace them by fermions, except for the last term where particles are considered simultaneously. By checking numerically, as each fermion has equal probability to be reflected or transmitted:

$$B_1^{(1,1)} = \frac{1}{2}\times\frac{1}{2} + \frac{1}{2}\times\frac{1}{2} + \frac{1}{2}\times\frac{1}{2} + \frac{1}{2}\times\frac{1}{2} - 1 = 0. \tag{5.3.6}$$

Again, we directly work with probabilities rather than amplitudes and we retrieve the Hong-Ou-Mandel effect.

5.4 Three modes

Let us get back to the three-mode case. We are about to express the corresponding recurrence equation thanks to fermionic probabilities as we just did for the two-mode case. By comparison with the reduced recurrence obtained at equation (4.5.3) we will then be able to make the distinction between its multiplicative coefficients that were all equal thus allowing no distinction and to obtain them under an explicit form. Like what has just been illustrated for two modes, we obtain for three modes:

$$\begin{aligned} B_{1,1}^{(1,1,1)} = \quad & F_{1,0}^{(1,0,0)} B_{0,1}^{(0,1,1)} + F_{0,1}^{(1,0,0)} B_{1,0}^{(0,1,1)} + F_{0,0}^{(1,0,0)} B_{1,1}^{(0,1,1)} + F_{1,0}^{(0,1,0)} B_{0,1}^{(1,0,1)} + F_{0,1}^{(0,1,0)} B_{1,0}^{(1,0,1)} + F_{0,0}^{(0,1,0)} B_{1,1}^{(1,0,1)} \\ & + F_{1,0}^{(0,0,1)} B_{0,1}^{(1,1,0)} + F_{0,1}^{(0,0,1)} B_{1,0}^{(1,1,0)} + F_{0,0}^{(0,0,1)} B_{1,1}^{(1,1,0)} \\ & - F_{1,1}^{(1,1,0)} B_{0,0}^{(0,0,1)} - F_{1,0}^{(1,1,0)} B_{0,1}^{(0,0,1)} - F_{0,1}^{(1,1,0)} B_{1,0}^{(0,0,1)} - F_{1,1}^{(1,0,1)} B_{0,0}^{(0,1,0)} - F_{1,0}^{(1,0,1)} B_{0,1}^{(0,1,0)} - F_{0,1}^{(1,0,1)} B_{1,0}^{(0,1,0)} \\ & - F_{1,1}^{(0,1,1)} B_{0,0}^{(1,0,0)} - F_{1,0}^{(0,1,1)} B_{0,1}^{(1,0,0)} - F_{0,1}^{(0,1,1)} B_{1,0}^{(1,0,0)} \\ & + F_{1,1}^{(1,1,1)} B_{0,0}^{(0,0,0)}, \end{aligned} \tag{5.4.1}$$

as we see in this equation, there are still probabilities accounting for two photons. In order to have a comparison with the reduced recurrence, we need to express the previous equation in terms of single-photon transition probabilities. This can be achieved by using the recurrence one more time for each term involving two photons. Using the recurrence on the first term $B_{0,1}^{(0,1,1)}$ leads to:

$$B_{0,1}^{(0,1,1)} = F_{0,1}^{(0,1,0)} B_{0,0}^{(0,0,1)} + F_{0,0}^{(0,1,0)} B_{0,1}^{(0,0,1)} + F_{0,1}^{(0,0,1)} B_{0,0}^{(0,1,0)} + F_{0,0}^{(0,0,1)} B_{0,1}^{(0,1,0)} - F_{0,1}^{(0,1,1)}. \tag{5.4.2}$$

Such decomposition is represented on figure 5.2 where we kept into consideration the multiplication by $F_{1,0}^{(1,0,0)}$ for each term, as it appears in front of $B_{0,1}^{(0,1,1)}$ in equation (5.4.1).

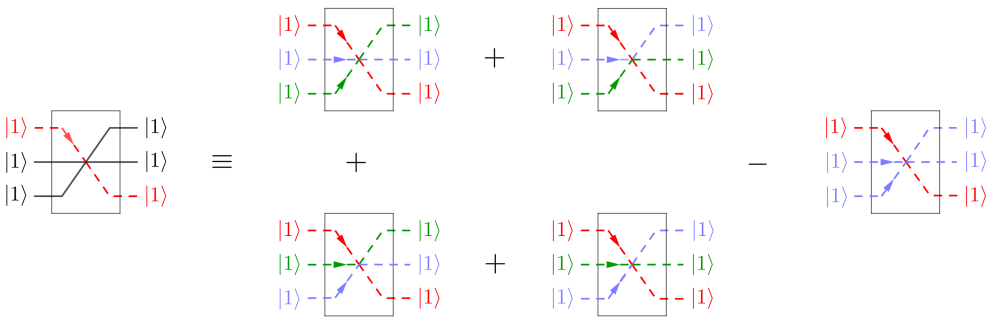

Figure 5.2: Decomposition of $B_{0,1}^{(0,1,1)}$ in terms of fermionic transition probabilities. (Red) paths of the first fermion, (blue) paths of the second fermion and (green) paths of the third fermion.

Where red paths stand for the first fermion, blue paths for second and green for third. We notice that as for the two-mode case, in such a decomposition still stands the last term where two particles were simultaneously considered. While the first four terms accounts for three different types of fermions, the last term accounts only for two.

By proceeding in the same way for these terms, we obtain an expression exclusively expressed in terms of single-photon transition probabilities multiplied by fermionic probabilities involving one or two particles. From this expression nothing cancels and the terms reorganization is not complicated as we only need to factorize in order to obtain each single-photon probability multiplied by a given factor. The final form we obtain for this recurrence equation is presented in appendix D. By comparing equation (D.0.1) to

equation (4.5.3) we see that the former contains more terms than the latter. Actually, this does not last as from a numerical point of view, these supplementary terms are equal and then cancel. Which allows us to write:

$$F_{1,1}^{(1,1,1)} = F_{1,0}^{(1,0,0)}F_{0,1}^{(0,1,1)} + F_{0,1}^{(1,0,0)}F_{1,0}^{(0,1,1)} + F_{0,0}^{(1,0,0)}F_{1,1}^{(0,1,1)} + F_{1,0}^{(0,1,0)}F_{0,1}^{(1,0,1)} + F_{0,1}^{(0,1,0)}F_{1,0}^{(1,0,1)} + F_{0,0}^{(0,1,0)}F_{1,1}^{(1,0,1)} + F_{1,0}^{(0,0,1)}F_{0,1}^{(1,1,0)} + F_{0,1}^{(0,0,1)}F_{0,1}^{(1,1,0)} + F_{0,0}^{(0,0,1)}F_{1,1}^{(1,1,0)}. \tag{5.4.3}$$

Indeed the single-fermion transition probabilities are evaluated by taking the squared modulus of the corresponding matrix elements of the third order DFT matrix and thus equal $1/N$ while the transition probabilities involving two fermions are the squared modulus of the corresponding minors of the DFT matrix. We stated in previous chapter that minors or order $N-1$ of an N-order DFT matrix are all equal and valued $1/\sqrt{N}$.

Finally, we obtain the following equation:

$$\begin{aligned}
B_{1,1}^{(1,1,1)} = \quad & \left(F_{0,1}^{(0,1,0)}F_{0,0}^{(0,0,1)} + F_{0,0}^{(0,1,0)}F_{0,1}^{(0,0,1)} + F_{0,1}^{(0,0,1)}F_{0,0}^{(0,1,0)} + F_{0,0}^{(0,0,1)}F_{0,1}^{(0,1,0)} - F_{0,1}^{(0,1,1)}\right) B_{1,0}^{(1,0,0)} \\
& + \left(F_{1,0}^{(0,1,0)}F_{0,0}^{(0,0,1)} + F_{0,0}^{(0,1,0)}F_{1,0}^{(0,0,1)} + F_{1,0}^{(0,0,1)}F_{0,0}^{(0,1,0)} + F_{0,0}^{(0,0,1)}F_{1,0}^{(0,1,0)} - F_{1,0}^{(0,1,1)}\right) B_{0,1}^{(1,0,0)} \\
& + \left(F_{1,0}^{(0,1,0)}F_{0,1}^{(0,0,1)} + F_{0,1}^{(0,1,0)}F_{1,0}^{(0,0,1)} + F_{1,0}^{(0,0,1)}F_{0,0}^{(0,1,0)} + F_{0,0}^{(0,0,1)}F_{1,0}^{(0,1,0)} - F_{1,1}^{(0,1,1)}\right) B_{0,0}^{(1,0,0)} \\
& + \left(F_{0,1}^{(1,0,0)}F_{0,0}^{(0,0,1)} + F_{0,0}^{(1,0,0)}F_{0,1}^{(0,0,1)} + F_{0,1}^{(0,0,1)}F_{0,0}^{(1,0,0)} + F_{0,0}^{(0,0,1)}F_{0,1}^{(1,0,0)} - F_{0,1}^{(1,0,1)}\right) B_{1,0}^{(0,1,0)} \\
& + \left(F_{1,0}^{(1,0,0)}F_{0,0}^{(0,0,1)} + F_{0,0}^{(1,0,0)}F_{1,0}^{(0,0,1)} + F_{1,0}^{(0,0,1)}F_{0,1}^{(1,0,0)} + F_{0,0}^{(0,0,1)}F_{1,0}^{(1,0,0)} - F_{1,0}^{(1,0,1)}\right) B_{0,1}^{(0,1,0)} \\
& + \left(F_{1,0}^{(1,0,0)}F_{0,1}^{(0,0,1)} + F_{0,1}^{(1,0,0)}F_{1,0}^{(0,0,1)} + F_{1,0}^{(0,0,1)}F_{0,1}^{(1,0,0)} + F_{0,1}^{(0,0,1)}F_{1,0}^{(1,0,0)} - F_{1,1}^{(1,0,1)}\right) B_{0,0}^{(0,1,0)} \\
& + \left(F_{0,1}^{(1,0,0)}F_{0,0}^{(0,1,0)} + F_{0,0}^{(1,0,0)}F_{0,1}^{(0,1,0)} + F_{0,1}^{(0,1,0)}F_{0,0}^{(1,0,0)} + F_{0,0}^{(0,1,0)}F_{0,1}^{(1,0,0)} - F_{0,1}^{(1,1,0)}\right) B_{1,0}^{(0,0,1)} \\
& + \left(F_{1,0}^{(1,0,0)}F_{0,0}^{(0,1,0)} + F_{0,0}^{(1,0,0)}F_{1,0}^{(0,1,0)} + F_{1,0}^{(0,1,0)}F_{0,1}^{(1,0,0)} + F_{0,0}^{(0,1,0)}F_{1,0}^{(1,0,0)} - F_{1,0}^{(1,1,0)}\right) B_{0,1}^{(0,0,1)} \\
& + \left(F_{1,0}^{(1,0,0)}F_{0,1}^{(0,1,0)} + F_{0,1}^{(1,0,0)}F_{1,0}^{(0,1,0)} + F_{1,0}^{(0,1,0)}F_{0,1}^{(1,0,0)} + F_{0,1}^{(0,1,0)}F_{1,0}^{(1,0,0)} - F_{1,1}^{(1,1,0)}\right) B_{0,0}^{(0,0,1)}.
\end{aligned} \tag{5.4.4}$$

This equation is another major result obtained in this work as it fully characterizes the three-mode interferometer quantum interferences. By comparing this last equation with the reduced recurrence from equation (4.5.3), we obtain the explicit form of each coefficient that can be then interpreted in terms of fermionic interferences. As we just reminded the values of fermionic probabilities involving one or two fermions, we can easily check the value of the factors between brackets. For each we have:

$$\frac{1}{3}\times\frac{1}{3} + \frac{1}{3}\times\frac{1}{3} + \frac{1}{3}\times\frac{1}{3} + \frac{1}{3}\times\frac{1}{3} - \frac{1}{3} = \frac{1}{9}, \tag{5.4.5}$$

which matches each coefficient from the reduced equation (4.5.3) derived at the end of the previous chapter.

Let us come back to equation (5.4.4). Under this form, the recurrence explicits again the quantum character of interferences through its fermionic coefficients as they exhibit a structure similar to the equation showing the Hong-Ou-Mandel effect. We draw attention on two important remarks. First, this recurrence is valid for any unitary. Indeed, as we started from the generalization formula of recurrence equations, we did not consider any particular unitary. However, we considered Fourier unitary to verify numerical results at equation (5.4.5). Secondly, the structure of each of these factors. By comparing it to the form of the two-mode recurrence obtained at equation (5.3.5), we notice the similarity between the two writings. In fact, each factor multiplying a single-photon probability has an identical form to the two-mode fermionic recurrence, excepting that fermionic

probabilities now contain a supplementary empty port located at input and output positions corresponding to those where the photon enters and leaves the interferometer. We then recover the structure proper to the two-mode case fermionic recurrence inside the equation for three modes, through its coefficients between brackets. This leads us to the assumption that this equation might then itself figure in the recurrence applied to the case involving four modes. However, we did not verify such an assumption.

5.5 Conclusion

In this last chapter, we went deeper in the recurrence equation for the three-mode interferometer. We started by addressing the subject of fermionic statistics especially by mentioning its relation with the determinant. We then introduced the transition probabilities of fermionic particles which allowed to interpret the minors of recurrence relations in terms of fermionic transition probabilities. This led to write the generalization formula of the recurrence equations for any N in terms of fermionic and bosonic transition probabilities. This was first illustrated with the two-mode case where we retrieved the Hong-Ou-Mandel effect and then it was applied to the tree-mode recurrence. Thanks to the introduction of fermionic statistics, we could rewrite this recurrence under a more explicit form bringing back the quantum character of interferences due to the fermionic interferometric coefficients. Moreover, the obtained equation is valid regardless of the three-mode passive unitary considered and seems to indicate that in each recurrence might appear the structure proper to the recurrence of the previous order.

Conclusion

In this Ms thesis, we have studied the extension of multi-photon quantum interferences to more than two photons sent in more than two modes. Estimating multi-photon multimode quantum interferences in linear interferometers revealed to be an interesting, yet very hard problem. We have been able to make a few progress, as exposed in the thesis, although the general problem remains largely open. We have in particular obtained original results allowing for a better understanding of quantum interferometric effects with three and four modes. Notably, the mathematical framework presented in the first part of the thesis and used to conduct this research revealed to be very convenient to manipulate and interpret multi-photon multimode quantum interferences.

By focusing on N-port Fourier interferometers, we first estimated the transition probabilities of coincident events within both the classical and quantum descriptions, which highlighted the absence of a regular pattern in the latter case (at least, for the range of values of N that we could access). However, we observed a difference in the nature of interferences as a function of the order N. Indeed, while the presence of a fully destructive interference had already been pointed out for even N, we could exhibit a constructive interference effect for some odd values of N(as well as a destructive interference effect for other odd values). Also, we connected the transition probabilities in a Fourier interferometer to the permanent of Fourier matrices, a mathematical object about which very little is known today. Unfortunately, our attempts to simplify the computation of this permanent revealed to be unsuccessful so far.

We then made use of the formalism of recurrence equations [10, 11] in order to investigate low-order quantum interferences in the simplest interesting cases, namely the three-mode and four-mode Fourier interferometers. This framework revealed to be convenient in the same way it had been shown for describing the Hong-Ou-Mandel effect in [10, 11]. From the derived recurrence relations applied to the specific situation of coincident events, we analyzed the structure of such expressions and proposed some conjectures in order to enable the computation of transition probabilities based on these recurrences. Especially, we conjectured that the transition probabilities for odd N could be computed through the value of the first block in their recurrences. Such a result still needs to be refined, but it could lead to a great simplification of the problem. We then manage to simplify the expressions of the recurrence relations in order to obtain a form enabling a precise interpretation of interferences. On the one hand, the constructive interference effect for three modes in a Fourier interferometer could be interpreted through a simple sum of the nine possible single-photon transition probabilities (corresponding to the nine classical classical paths). To our knowledge, this unexpected result is original to the present thesis. On the other hand, we observed that the destructive interference effect for four modes in a Fourier interferometer can be cast as a sum similarly as for the Hong-Ou-Mandel effect, which is responsible for the vanishing of the coincidence probability.

Finally, we revisited the recurrence relations [10, 11] by proposing a new approach, where the minors appearing in the formulas are ascribed to fermionic statistics. This combination of bosonic and fermionic interferometry allowed us to derive an original

expression of the three-mode recurrence relation, which explains the constructive interference in a Fourier interferometer and is universal as it applies to any passive three-mode interferometer.

The perspective of this Ms thesis is to open a new path towards expressing the constructive or destructive sums at the root of linear interferometers. Even though the evaluation of permanents in the context of Fourier interferometers remains an open problem for any N, some of our results will hopefully help gaining a better understanding of multi-photon multimode quantum interferences.

Bibliography

[1] Scott Aaronson and Alex Arkhipov, "The Computational Complexity of Linear Optics", *Theory of Computing* **9**, 143 (2013).

[2] Richard A. Brualdi and Dragoš Cvetković, *A Combinatorial Approach to Matrix Theory and Its Applications*, 1st Edition, Boca Raton: Chapman and Hall/CRC, 2008.

[3] Richard A. Campos, "Three-photon Hong-Ou-Mandel interference at a multiport mixer", *Phys. Rev. A* **62**, 013809 (2000).

[4] Nicolas J. Cerf, "Multiphoton interference in passive vs. active Gaussian unitaries - "spacelike" vs. "timelike" indistinguishability effects", Quantum Limits of Optical Communications II (Warsaw, Poland), 2018.

[5] Nicolas J. Cerf, Christoph Adami, and Paul G. Kwiat, "Optical simulation of quantum logic", *Phys. Rev. A* **57**, R1477 (1998).

[6] Levon Chakhmakhchyan, Nicolas J. Cerf, and Raul Garcia-Patron, "Quantum-inspired algorithm for estimating the permanent of positive semidefinite matrices", *Phys. Rev. A* **96**, 022329 (2017).

[7] Mark Fox, *Quantum Optics : An Introduction*, Oxford Master Series in Physics, Oxford: Oxford University Press, 2006.

[8] Philippe Grangier, "Single photons stick together", *Nature* **419**, 577 (2002).

[9] Chung Ki Hong, Zhe Yu Ou, and Leonard Mandel, "Measurement of subpicosecond time intervals between two photons by interference", *Phys. Rev. Lett.* **59,** 2044 (1987).

[10] Michael G. Jabbour, "Bosonic systems in quantum information theory Gaussian-dilatable channels, passive states, and beyond", PhD thesis, Ecole Polytechnique de Bruxelles - ULB, 2018.

[11] Michael G. Jabbour and Nicolas J. Cerf, "Multiphoton interference effects in passive and active Gaussian transformations", *arXiv:1803.10734* (2018).

[12] Emmanual Knill, Raymond Laflamme, and Gerard J. Milburn, "A scheme for efficient quantum computation with linear optics", *Nature* **409**, 46 (2001).

[13] Pieter Kok et al., "Linear optical quantum computing with photonic qubits", *Reviews of Modern Physics* **79**, 135 (2007).

[14] Yuan Liang Lim and Almut Beige, "Generalized Hong–Ou–Mandel experiments with bosons and fermions", *New Journal of Physics* **7**, 155 (2005).

[15] Rodney Loudon, *The Quantum Theory of Light*, Oxford: Oxford University Press, 1973.

[16] Marvin Marcus and Henryk Minc, "On the relation between the determinant and the permanent", *Illinois J. Math.* **5**, 376 (1961).

[17] Henryk Minc, "A note on an inequality of M. Marcus and M. Newman", *Proceedings of the American Mathematical Society* **14**, 890 (1963).

[18] Henryk Minc, *Permanents*, vol. 6, Encyclopedia of Mathematics and its Applications, Cambridge: Cambridge University Press, 1978.

[19] Mahdi Pourfath, "Numerical Study of Quantum Transport in Carbon Nanotube Based Transistors", PhD thesis, Vienna University, 2007, URL: http://www.iue.tuwien.ac.at/phd/pourfath/diss.html.

[20] George Póya, *Mathematics and plausible reasoning*, Princeton: Princeton University Press, 1954.

[21] John Preskill, "Quantum computing and the entanglement frontier", *arXiv:1203.5813* (2012).

[22] Michael Reck et al., "Experimental realization of any discrete unitary operator", *Phys. Rev. Lett.* **73**, 58 (1994).

[23] Stefan Scheel, "Permanents in linear optical networks", *arXiv:quant-ph/0406127v1* (2004).

[24] Franz Schwabl, *Advanced Quantum Mechanics*, Advanced texts in physics, Springer, 2005.

[25] Valery S. Shchesnovich, "Asymptotic evaluation of bosonic probability amplitudes in linear unitary networks in the case of large number of bosons", *arXiv:1304.6675* (2014).

[26] Nicolò Spagnolo et al., "Three-photon bosonic coalescence in an integrated tritter", *Nature Communications* **4**, 1606 (2013).

[27] Malte C. Tichy et al., "Zero-Transmission Law for Multiport Beam Splitters", *Phys. Rev. Lett.* **104**, 220405 (2010).

[28] Malte C. Tichy et al., "Stringent and Efficient Assessment of Boson-Sampling Devices", *Phys. Rev. Lett.* **113**, 020502 (2014).

[29] Päivi Törmä, Stig Stenholm, and Igor Jex, "Hamiltonian theory of symmetric optical network transforms", *Phys. Rev. A* **52**, 4853 (1995).

[30] Lidror Troyansky and Naftali Tishby, "Permanent Uncertainty: On the quantum evaluation of the determinant and the permanent of a matrix", *Proceedings of PhyComp96* (1996).

[31] Herbert S. Wilf, *Generatingfunctionology*, Philadelphia: Academic Press, 1994.

[32] Marek Zukowski, Anton Zeilinger, and Michael A. Horne, "Realizable higher-dimensional two-particle entanglements via multiport beam splitters", *Phys. Rev. A* **55**, 2564 (1997).

Appendix A

Numerical values

This annex contains the numerical results of classical and quantum transition probabilities in case of coincident events as well as quantum enhancement. Computed thanks to Mathematica and used at chapter 3 in graphs represented at figures 3.2 and 3.3.

N	P_{cl}	P_{qm}	$\mathcal{E}$
1	1	1	1
2	0.5	0	0
3	0.2222	0.3333	1.5
4	0.09375	0	0
5	0.0384	0.008	0.2083
6	0.0154	0	0
7	0.0061	0.0134	2.1875
8	0.0024	0	0
9	9.36e-04	1.69e-05	0.0181
10	3.63e-04	0	0
11	1.4e-04	1.6e-04	1.1465
12	5.37e-05	0	0
13	2.05e-05	1.01e-04	4.9602
14	7.84e-06	0	0
15	2.98e-06	2.1e-09	0.0007
16	1.13e-06	0	0
17	4.3e-07	7.69e-07	1.7882
18	1.62e-07	0	0
19	6.14e-08	1.03e-08	0.1679
20	2.32e-08	0	0
21	8.74e-09	3.54e-09	0.4049
22	3.29e-09	0	0
23	1.23e-09	4.65e-11	0.0375
24	4.65e-10	0	0

Table A.1: Dimension (N), classical transition probability (P_{cl}), quantum transition probability (P_{qm}) and quantum enhancement ($\mathcal{E}$) - approached values.

N	P_{cl}	P_{qm}	$\mathcal{E}$
1	1	1	1
2	$\frac{1}{2}$	0	0
3	$\frac{2}{9}$	$\frac{1}{3}$	$\frac{3}{2}$
4	$\frac{3}{32}$	0	0
5	$\frac{24}{625}$	$\frac{1}{125}$	$\frac{5}{24}$
6	$\frac{5}{324}$	0	0
7	$\frac{720}{117649}$	$\frac{225}{16807}$	$\frac{35}{16}$
8	$\frac{315}{131072}$	0	0
9	$\frac{4480}{4782969}$	$\frac{1}{59049}$	$\frac{81}{4480}$
10	$\frac{567}{1562500}$	0	0
11	$\frac{3628800}{25937424601}$	$\frac{378225}{2357947691}$	$\frac{18491}{16128}$
12	$\frac{1925}{35831808}$	0	0
13	$\frac{479001600}{23298085122481}$	$\frac{182763361}{1792160394037}$	$\frac{215993063}{43545600}$
14	$\frac{868725}{110730297608}$	0	0
15	$\frac{14350336}{4805419921875}$	$\frac{1}{474609375}$	$\frac{10125}{14350336}$
16	$\frac{638512875}{562949953421312}$	0	0
17	$\frac{20922789888000}{48661191875666868481}$	$\frac{2200834557441}{2862423051509815793}$	$\frac{319779380141}{178827264000}$
18	$\frac{14889875}{91507169819844}$	0	0
19	$\frac{6402373705728000}{104127350297911241532841}$	$\frac{56567110674321}{5480386857784802185939}$	$\frac{1020679109983}{6080126976000}0$
20	$\frac{14849255421}{640000000000000000}$	0	0
21	$\frac{7567605760000}{865405750887126927009}$	$\frac{4084441}{1153657446916149}$	$\frac{3063906656181}{7567605760000}$
22	$\frac{17717861581875}{5381999959460480073608}$	0	0
23	$\frac{1124000727777607680000}{907846434775996175406740561329}$	$\frac{1834570167359933025}{39471584120695485887249589623}$	$\frac{172207382304983}{4587289981747200}$
24	$\frac{2505147019375}{5385144351531158470656}$	0	0

Table A.2: Dimension (N), classical transition probability (P_{cl}), quantum transition probability (P_{qm}) and quantum enhancement ($\mathcal{E}$) - exact values.

Appendix B

Code for numerical computations

This annex contains the Mathematica code used to compute the permanent of the Fourier matrices thanks to Laplace expansion. It here returns results for $N = 5$.

```
(* Creation of the DFT matrix of size n *)

DFT[n_] := 1 / Sqrt[n] Table[Exp[I 2. Pi / n j k], {k, 0, n - 1}, {j, 0, n - 1}];
                racine c··· table   ex··· un··· nombre pi
(* A function receiving as input a matrix A and two numbers j and k,
and outpus the matrix without the jth rown and kth column *)

f[A_, j_, k_] := (n = Length[A];
                      longueur
  listj = Delete[Table[a, {a, 1, n}], j];
          supprime table
  listk = Delete[Table[b, {b, 1, n}], k];
          supprime table
  Table[A[[a, b]], {a, listj}, {b, listk}] )
  table
(* Parameters setting *)

n = 5; A = DFT[n]; l = 1; dim = Length[A];
                                longueur
(* This part calculates all the permanents of the submatrices that appear in
 the 1st step of the Laplace expansion on the lth row (with l chosen above). *)

res = Table[Permanent[f[A, l, k]], {k, 1, dim}] // Chop
      table  permanent                            remplace les petites valeurs par 0
```

Out[24]= {-0.04, -0.04, -0.04, -0.04, -0.04}

Appendix C

Limited expansion

We strongly recommend to read chapter 3 first before reading this appendix because it uses concepts presented in it. In this annex, we present an attempt to simplify the permanent of a Fourier matrix in the hope to facilitate its computation.

Given the complexity of calculating the permanent, the objective of this description is to facilitate its computation for a Fourier matrix. We will try to express the permanent of an order N matrix from the permanent of the matrix of lower order $N-1$. We remind the form of the DFT:

$$\mathrm{F}_N(\omega_N) = \frac{1}{\sqrt{N}} \begin{pmatrix} 1 & 1 & \dots & 1 \\ 1 & \omega_N & \dots & \omega_N^{N-1} \\ \vdots & \vdots & \ddots & \vdots \\ 1 & \omega_N^{N-1} & \dots & \omega_N^{(N-1)(N-1)} \end{pmatrix}, \quad \text{where } \omega_N = e^{-2\pi i/N}. \tag{C.0.1}$$

We first apply the Laplace expansion along the first column (2.4.8b) of previous matrix. As the expansion is performed along a column involving only ones, we know from section 3.3.2 that the N permanents of order $N-1$ matrices associated to expansion terms are all equal. Which allows us to write the permanent of the matrix from previous equation as:

$$\begin{aligned} \operatorname{per} \mathrm{F}_N(\omega_N) &= N \frac{1}{\sqrt{N}} . \operatorname{per} \frac{1}{\sqrt{N}} \begin{pmatrix} 1 & \dots & 1 \\ \omega_N & \dots & \omega_N^{N-1} \\ \vdots & \ddots & \vdots \\ \omega_N^{N-2} & \dots & \omega_N^{(N-1)(N-2)} \end{pmatrix} \\ &= \sqrt{N} . \omega_N \omega_N^2 \omega_N^3 \dots \omega_N^{N-2} . \operatorname{per} \frac{1}{\sqrt{N}} \begin{pmatrix} 1 & \dots & 1 \\ 1 & \dots & \omega_N^{N-2} \\ \vdots & \ddots & \vdots \\ 1 & \dots & \omega_N^{(N-2)(N-2)} \end{pmatrix} \\ &= \sqrt{N} . \omega_N^{(N-2)(N-1)/2} . \sqrt{\frac{(N-1)^{N-1}}{N^{N-1}}} . \operatorname{per} \mathrm{F}_{N-1}(\omega_N). \end{aligned} \tag{C.0.2}$$

Thanks to property 5 from section 2.4.2, we obtain second equality by taking out the factors multiplying each line. The third equality is then obtained by use of property 3 as we wrote the square root which is the scaling factor allowing us to express the permanent of the $N-1$ order DFT matrix.

Note that from the start of this reasoning, we considered N to be odd as the left-handed side would vanish for even N. Also, the right-handed side does not vanish as the

even order $(N-1)\times(N-1)$ matrix is still evaluated with root ω_N. The result would be zero if it was evaluated with ω_{N-1} though.

The next step of this development resides in the use of the Taylor expansion:

$$f(x) = \sum_{n=0} \frac{f^{(n)}(x_0)}{n!}(x-x_0)^n, \tag{C.0.3}$$

that we apply to the permanent appearing in the last line of equation (C.0.2) and that we truncate at first order which gives:

$$\operatorname{per} \mathrm{F}_{N-1}(\omega_N) = \underbrace{\operatorname{per} \mathrm{F}_{N-1}(\omega_{N-1})}_{=0} + c.\left[\operatorname{per} \mathrm{F}_{N-1}(\omega)\right]'\Big|_{\omega_{N-1}}, \tag{C.0.4}$$

with coefficient c:

$$c = \omega_N - \omega_{N-1}. \tag{C.0.5}$$

Let us specify that this approximation is only verified when $(x-x_0)\to 0$, i.e. when x and x_0 are very close from each other. In our case this comes down to consider N to be large, implying that ω_{N-1} and ω_N are very close to one. This is illustrated in figure C.1 where N becomes larger by passing from left to right, note that this figure is not scaled:

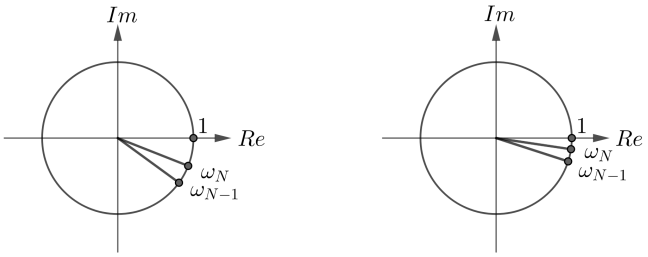

Figure C.1: Roots ω_N and ω_{N-1} getting closer from one for large N.

Knowing this, we can calculate the coefficient:

$$\begin{aligned}\omega_N - \omega_{N-1} &= e^{-2\pi i/N} - e^{-2\pi i/N-1} \\ &\approx \left(1-\frac{2\pi i}{N}\right) - \left(1-\frac{2\pi i}{N-1}\right) \\ &= \frac{2\pi i}{N(N-1)} << 1, \quad \text{for } N \text{ large},\end{aligned} \tag{C.0.6}$$

thanks to the first order truncated development of the exponential function. With this last result and by means of the definition of ω_N, equation (C.0.4) then writes:

$$\operatorname{per} \mathrm{F}_{N-1}(\omega_N) \approx \frac{2\pi i}{N(N-1)}\left(\frac{d}{d\omega}\left[\operatorname{per} \mathrm{F}_{N-1}(\omega)\right]\right)\Big|_{\omega_{N-1}}. \tag{C.0.7}$$

Finally we can write:

$$\operatorname{per} \mathrm{F}_N(\omega_N) \approx \sqrt{N}.\omega_N^{(N-2)(N-1)/2}.\sqrt{\frac{(N-1)^{N-1}}{N^{N-1}}}\cdot\frac{2\pi i}{N(N-1)}\left(\frac{d}{d\omega}\left[\operatorname{per} \mathrm{F}_{N-1}(\omega)\right]\right)\Big|_{\omega_{N-1}}. \tag{C.0.8}$$

The computation of the permanent of the DFT for N being odd can then be expressed in terms of the derivative of the permanent of the lower order matrix. Such a result should

be real considering what has been sais in chapter 3. However, we notice from this last expression that the coefficient is complex, we should then expect the derivative to be also complex. By processing this way, we reduce the order of computation by one unity. The difficulty is then to find a way of processing the derivative of the permanent. We have reduced the initial problem to another one that is computing the derivative of the permanent.

This method has been used for computing numerical results at low orders that unfortunately do not match with the results previously calculated. This could be expected as this development is based on the assumption of considering large orders. However, we are not able to evaluate the derivative of permanent at such orders.

Appendix D

Three-mode recurrence

In this annex, we write the complete form of the recurrence equation obtained for three modes after reorganizing the terms:

$$
\begin{aligned}
B_{1,1}^{(1,1,1)} = \quad & \left(F_{0,1}^{(0,1,0)}F_{0,0}^{(0,0,1)} + F_{0,0}^{(0,1,0)}F_{0,1}^{(0,0,1)} + F_{0,1}^{(0,0,1)}F_{0,0}^{(0,1,0)} + F_{0,0}^{(0,0,1)}F_{0,1}^{(0,1,0)} - F_{0,1}^{(0,1,1)}\right) B_{1,0}^{(1,0,0)} \\
& + \left(F_{1,0}^{(0,1,0)}F_{0,0}^{(0,0,1)} + F_{0,0}^{(0,1,0)}F_{1,0}^{(0,0,1)} + F_{1,0}^{(0,0,1)}F_{0,0}^{(0,1,0)} + F_{0,0}^{(0,0,1)}F_{1,0}^{(0,1,0)} - F_{1,0}^{(0,1,1)}\right) B_{0,1}^{(1,0,0)} \\
& + \left(F_{1,0}^{(0,1,0)}F_{0,1}^{(0,0,1)} + F_{0,1}^{(0,1,0)}F_{1,0}^{(0,0,1)} + F_{1,0}^{(0,0,1)}F_{0,0}^{(0,1,0)} + F_{0,0}^{(0,0,1)}F_{1,0}^{(0,1,0)} - F_{1,1}^{(0,1,1)}\right) B_{0,0}^{(1,0,0)} \\
& + \left(F_{0,1}^{(1,0,0)}F_{0,0}^{(0,0,1)} + F_{0,0}^{(1,0,0)}F_{0,1}^{(0,0,1)} + F_{0,1}^{(0,0,1)}F_{0,0}^{(1,0,0)} + F_{0,0}^{(0,0,1)}F_{0,1}^{(1,0,0)} - F_{0,1}^{(1,0,1)}\right) B_{1,0}^{(0,1,0)} \\
& + \left(F_{1,0}^{(1,0,0)}F_{0,0}^{(0,0,1)} + F_{0,0}^{(1,0,0)}F_{1,0}^{(0,0,1)} + F_{1,0}^{(0,0,1)}F_{0,1}^{(1,0,0)} + F_{0,0}^{(0,0,1)}F_{1,0}^{(1,0,0)} - F_{1,0}^{(1,0,1)}\right) B_{0,1}^{(0,1,0)} \\
& + \left(F_{1,0}^{(1,0,0)}F_{0,1}^{(0,0,1)} + F_{0,1}^{(1,0,0)}F_{1,0}^{(0,0,1)} + F_{1,0}^{(0,0,1)}F_{0,1}^{(1,0,0)} + F_{0,1}^{(0,0,1)}F_{1,0}^{(1,0,0)} - F_{1,1}^{(1,0,1)}\right) B_{0,0}^{(0,1,0)} \\
& + \left(F_{0,1}^{(1,0,0)}F_{0,0}^{(0,1,0)} + F_{0,0}^{(1,0,0)}F_{0,1}^{(0,1,0)} + F_{0,1}^{(0,1,0)}F_{0,0}^{(1,0,0)} + F_{0,0}^{(0,1,0)}F_{0,1}^{(1,0,0)} - F_{0,1}^{(1,1,0)}\right) B_{1,0}^{(0,0,1)} \\
& + \left(F_{1,0}^{(1,0,0)}F_{0,0}^{(0,1,0)} + F_{0,0}^{(1,0,0)}F_{1,0}^{(0,1,0)} + F_{1,0}^{(0,1,0)}F_{0,1}^{(1,0,0)} + F_{0,0}^{(0,1,0)}F_{1,0}^{(1,0,0)} - F_{1,0}^{(1,1,0)}\right) B_{0,1}^{(0,0,1)} \\
& + \left(F_{1,0}^{(1,0,0)}F_{0,1}^{(0,1,0)} + F_{0,1}^{(1,0,0)}F_{1,0}^{(0,1,0)} + F_{1,0}^{(0,1,0)}F_{0,1}^{(1,0,0)} + F_{0,1}^{(0,1,0)}F_{1,0}^{(1,0,0)} - F_{1,1}^{(1,1,0)}\right) B_{0,0}^{(0,0,1)} \\
& - \Big[F_{1,0}^{(1,0,0)}F_{0,1}^{(0,1,1)} - F_{0,1}^{(1,0,0)}F_{1,0}^{(0,1,1)} - F_{0,0}^{(1,0,0)}F_{1,1}^{(0,1,1)} - F_{1,0}^{(0,1,0)}F_{0,1}^{(1,0,1)} - F_{0,1}^{(0,1,0)}F_{1,0}^{(1,0,1)} \\
& \qquad + F_{0,0}^{(0,1,0)}F_{1,1}^{(1,0,1)} + F_{1,0}^{(0,0,1)}F_{0,1}^{(1,1,0)} + F_{0,1}^{(0,0,1)}F_{1,0}^{(1,1,0)} + F_{0,0}^{(0,0,1)}F_{1,1}^{(1,1,0)}\Big] \\
& + F_{1,1}^{(1,1,1)}F_{0,0}^{(0,0,0)}.
\end{aligned}
\tag{D.0.1}
$$